Interference Mitigation in Cognitive Femtocell Networks

Harold Orduen Kpojime

Interference Mitigation in Cognitive Femtocell Networks

Harold Orduen Kpojime

Department of Computer Science and Technology

University of Bedfordshire

A thesis submitted for the degree of

Doctor of Philosophy

September 10, 2015

Abstract

Femtocells have been introduced as a solution to poor indoor coverage in cellular communication which has hugely attracted network operators and stakeholders. However, femtocells are designed to co-exist alongside macrocells providing improved spatial frequency reuse and higher spectrum efficiency to name a few. Therefore, when deployed in the two-tier architecture with macrocells, it is necessary to mitigate the inherent co-tier and cross-tier interference. The integration of cognitive radio (CR) in femtocells introduces the ability of femtocells to dynamically adapt to varying network conditions through learning and reasoning. This research work focuses on the exploitation of cognitive radio in femtocells to mitigate the mutual interference caused in the two-tier architecture. The research work presents original contributions in mitigating interference in femtocells by introducing practical approaches which comprises a power control scheme where femtocells adaptively controls its transmit power levels to reduce the interference it causes in a network. This is especially useful since femtocells are user deployed as this seeks to mitigate interference based on their blind placement in an indoor environment. Hybrid interference mitigation schemes which combine power control and resource/scheduling are also implemented. In a joint threshold power based admittance and contention free resource allocation scheme, the mutual interference between a Femtocell Access Point (FAP) and close-by User Equipments (UE) is mitigated based on admittance. Also, a hybrid scheme where FAPs opportunistically use Resource Blocks (RB) of Macrocell User Equipments (MUE) based on its traffic load use is also employed. Simulation analysis present improvements when these schemes are applied with emphasis in Long Term Evolution (LTE) networks especially in terms of Signal to Interference plus Noise Ratio (SINR).

Declaration

I, Harold O. Kpojime, declare that this thesis is my own unaided work. It is being submitted for the degree of (*Doctor of Philosophy*) at the University of Bedfordshire.

It has not been submitted before for any degree or examination in any other University.

Name of candidate: Signature:

Date:

Dedication

This thesis is dedicated to the memory of my father, Hon. Victor F. Kpojime, who would have been proud to see what his little son 'Or Turan' achieved and to my mother Justice Elizabeth N. Kpojime whose love and support has no boundaries.

I will always love you.

Acknowledgement

I would like to express my sincere gratitude to my Director of Studies, Dr. Ghazanfar A. Safdar, first of all, for the opportunity he gave to me to work with him and the confidence and extreme patience he had during all these years. I still remember when I walked into his office for the first time to request his supervision of my master's thesis and the rest is history. I tremendously benefitted from the unique professional vision and technical insight he had right from the beginning to the end. It was like he had written the script before we started. I appreciate the time he invested and the motivation he ensued in me but most especially the undying commitment he had towards this research which was immeasurable. I appreciate him as a person, his discipline and the helping hand he extended to me outside our research which I have to admit has made me a better person today. I feel very fortunate to have worked with him and the things we achieved together which seemed impossible but for his hunger for success. I will forever remain indebted to him.

I would like to thank my family for all the undying love. My queen, Elfreeda, for always being there, my prince, Terkator, who always lightens up my day, my mother, Justice Elizabeth Kpojime, for her selfless struggle and financial support to make me a better person every day, my brother Denen, my sisters, Deve and Dem and my uncle Tivfa Addingi, for all the prayers and making my dream come true. I love you all.

Finally, I would also like to thank my colleagues and friends, Julius, Chijioke, Elias, Tochukwu and Kapil for the continuous friendship and support all through the years. I wish you all success in your research and future endeavours.

List of publications

Published

Harold O. Kpojime and Ghazanfar A. Safdar. Interference Mitigation in Cognitive Radio based Femtocells. Published in *IEEE Communications Surveys & Tutorials*, 17(3):1511-1534, 2015.

Harold O. Kpojime and Ghazanfar A. Safdar. Efficacy of coverage radius-based power control scheme for interference mitigation in femtocells. Published in *IET Electronics Letters*, 50(8):639-641, April 2014.

Harold O. Kpojime and Ghazanfar A. Safdar. Coverage Radius Bounds and Impact on SINR in Blindly Placed LTE Femtocells. Published in Springer *International Journal of Wireless Information Networks.*22(3):262-271, September 2015.

Harold O. Kpojime, Ghazanfar A. Safdar and Mehmet E. Aydin. ITU-R and WINNER II Path Loss Modelling of Femtocells. Published in the *7th International Working Conference of HET-NETs*, 11-13 November 2013.

Under Review

Harold O. Kpojime and Ghazanfar A. Safdar. Joint UEs Admittance and Contention free resource allocation for Interference Mitigation in Cognitive Femtocells. Submitted in *IET Communications*. March, 2015

Harold O. Kpojime and Ghazanfar A. Safdar. Traffic aware matching policy based Resource Allocation for Interference mitigation in Cognitive Femtocells. Submitted in *Elsevier Computer Networks*. July, 2015.

Acronyms

3GPP	3rd Generation Partnership Project
AMR-WB	Adaptive Multi-Rate Wideband
ATM	Asynchronous Transfer Mode
BLER	Block Error Ratio
BS	Base Station
CAPEX	Capital Expenditure
CF	Cognitive Femtocell
CFBS	Cognitive Femtocell Base Station
CM-RM	Cognitive Manager for Resource Management
CM-SM	Cognitive Manager for Spectrum Management
CP	Cyclic Prefix
CR	Cognitive Radio
CRC	Cyclic Redundancy Check
CSG	Close Subscriber Group
CQI	Channel Quality Indicator
DAS	Distributed Antenna Systems
DL	Downlink
DMUE	Desired MUE
DOA	Direction of Arrival
DSA	Dynamic Spectrum Access

DSL	Digital Subscriber Line
ETSI	European Telecommunications Standards Institute
FAPs	Femtocell Access Points
FCC	Federal Communications Commission
FDD	Fractional Frequency Donation
FTP	File Transfer Protocol
FUE	Femtocell User Equipment
FPC	Fractional Power Control
GRACE	Game-based Resource Allocation in Cognitive Environments
HARQ	Hybrid Automatic Repeat Request
HeNB	Home eNodeB
HNB	Home NodeB
HO	Handover
HSDPA	High-Speed Downlink Packet Access
HSUPA	High-Speed Uplink Packet Access
HTTP	Hypertext Transfer protocol
IEEE	Institute of Electrical and Electronics Engineers
IP	Internet Protocol
ISM	Industrial, Scientific and Medical
LCR-TDD	Low Chip Rate Time Division Duplex
LE	Logit Equilibrium
LTE	Long term Evolution
MBS	Macrocell Base Station
MIESM	Mutual Information based Exponential SNR Mapping
MIMO	Multi-Input and Multi-Output
MMS	Multimedia Messaging Service
MS	Mobile Station

MUE	Macrocell User Equipment
OPEX	Operational Expenditure
OFDM	Orthogonal Frequency Division Multiplexing
OFDMA	Orthogonal Frequency Division Multiplexing Access
PC	Physical Cluster
PHY	Physical Layer
PKI	Performance Key Indicator
PF	Proportional Fair
PU	Primary User
QAM	Quadrature Amplitude Modulation
QoS	Quality of Service
QPSK	Quadrature Phase Shift Keying
RAU	Remote Antenna Units
RBs	Resource Blocks
RF	Radio Frequency
RSS	Received Signal Strength
RSSI	Received Signal Strength Indication
SAE	System Architecture Evolution
SINR	Signal to Interference plus Noise Ratio
SC-FDMA	Single Carrier Frequency Division Multiple Access
SCFN	Smart Cognitive-Femto Network
SFA	Selfish Frequency Access
SRS	Sounding Reference Signal
SU	Secondary User
TTI	Transmission Time Interval
TVWS	Television White Space
UEs	User equipments

UMUE	Undesired MUE
UL	Uplink
VC	Virtual Cluster
VOIP	Voice over Internet Protocol
WiFi	Wireless Fidelity
WIMAX	Worldwide Interoperability for Microwave Access

List of figures

Contents

Chapter 1

Introduction

1.1 Evolution of wireless and cellular communication

Wireless communication has involved relentless years of research and design and comprises cellular telephony, broadcast and satellite television, wireless networking to today's 3rd Generation Partnership Project's (3GPP) and Long Term Evolution (LTE) technology. However, cellular telephony networks surpass the others in terms of usage [1]. Although cellular networks were designed to provide mobile voice services and low rate mobile data services, data services have excelled voice and findings show that global data traffic has grown by 280% since 2008 and is expected to double annually in the next five years [2]. Importantly, it has already exceeded those expectations in 2010 by nearly tripling and it is further predicted that by 2015 nearly one billion people will access the internet using a wireless mobile device [3].

The limited and in some cases under-utilised spectrum cannot accommodate this continuous increase in traffic therefore network operators have to come up with ways of increasing spectrum efficiency.

The introduction of new or the upgrade of existing wireless standards such as the Institute of Electrical and Electronics Engineers (IEEE) Worldwide Interoperability for Microwave Access (WiMAX) and 3GPP's LTE have been developed to meet traffic and high data rates. Most of the methods to increase spectrum capacity in practice today are aligned towards, a) improving the macro layer by upgrading the radio access, b) densifying the macro layer by reducing the inter-site distances and c) the use of low power nodes to complement the macro layer [4].

The macro layer deployment is the typical approach of deploying Base Stations (BS) in proximity to each other covering large distances with reduced handover frequency. Although it is the backbone of most wireless networks, it has proven to be inefficient as it does not guarantee a high quality link in situations where the BS and Mobile Station (MS) are relatively far away. Moreover, a BS serving hundreds of contentious users all vying for resources is old fashioned [5]. Researchers indicate that 50% of all voice calls and most of the data traffic, more than 70%, originate indoors [6].

However, indoor users may suffer from a reduced Received Signal Strength (RSS) due to low signal penetration through the walls or attenuation leading to total loss of signal in situations where the distance between transmitter and receiver is large. There is a need to provide solutions for poor indoor coverage to satisfy consumers. According to [5] the solutions to poor indoor coverage can be classified into two types, Distributed Antenna Systems (DAS) and Distributed Radios.

Distributed Antenna Systems comprise a group of Remote Antenna Units (RAU) spaced apart, providing not only enhanced indoor signal quality by significantly reducing transmission distance but also reducing transmit power (power of the reference signal) [7]. Some of the challenges involved in deploying DAS are the choice of antennas and selecting a suitable location [8], [9].

Distributed Radios involve the introduction of smaller cells to complement the deficiencies of the larger macrocell and the gains include an efficient spatial reuse of spectrum [10]. These small cells which include picocells and microcells are overlaid in the macrocell to provide voice and data service. Due to the two-tier nature of its architecture, it is prone to interference which may result to a low Signal to Interference plus Noise Ratio (SINR) and throughput and in some cases a total disruption of service. As a result, there is a need to provide interference avoidance and mitigation schemes.

Recently, a new distributed radio known as femtocells has emerged that promises to be a viable solution to indoor cellular communication.

1.2 Femtocells: a solution to indoor network coverage

Femtocell provides the solution to poor indoor coverage in cellular communication which has hugely attracted network operators and stakeholders. Femtocells are low powered, low cost and subscriber controlled units which provide a dedicated BS to indoor subscribers. The concept of femtocells, also known as home base stations, Home NodeB (HNB) or Home eNodeB (HeNB) [11] and residential small cells [12] was first studied in 1999 by Bell Laboratory of Alcatel-Lucent but it was in 2002 that Motorola announced the first 3G based home base station product [13].

Femtocell units, known as Femtocell Access Points (FAPs), connect standard mobile devices also known as Femtocell User Equipment (FUE) to the network of a mobile operator through residential Digital Subscriber Line (DSL), optical fibres, cable broadband connections or wireless last-mile technologies as shown in Figure 1.1 [13]-[16]. By installing FAPs indoors, the cell sites are reduced thereby bringing the transmitter and receiver closer to each other. The use of the subscriber's broadband network to backhaul data offer improved indoor mobile phone coverage for both voice and data because of improved connectivity compared to the

Macrocell Base Station (MBS). Femtocells are similar to WiFi as both are connected to a wired backhaul but unlike WiFi, femtocells make use of an existing cellular standard for their operation [15], [17].

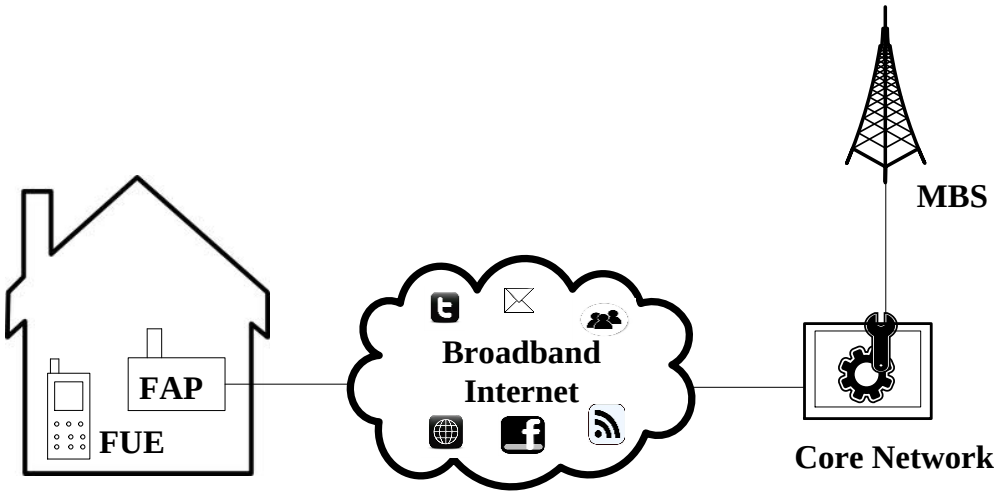

Figure 1.1: Femtocell deployment.

The benefits of femtocells now and in the long term cannot be overemphasised as it has advantages for both network operators and subscribers. As far as network operators are concerned, the reduction in macrocells due to the deployment of femtocells will result in a huge saving in CAPEX (Capital Expenditure) of network operators and the reduction in traffic will also yield a saving in the OPEX (Operational Expenditure) through advanced self-management and optimisation techniques. The subscribers also benefit as the close proximity of the transmitter and receiver offered by femtocells enables subscribers to have high speed services such as voice, video and multimedia.

The close proximity greatly lowers transmission power and increases the battery life of mobile devices. With a dedicated FAP in their homes, it offers subscribers a single billing address for mobile phone, broadband and land line as they are all channelled through the same backhaul [13], [18]. Femtocells also act as a solution towards convergence of landline and mobile [19].

1.2.1 Femtocells and the inherent interference problems

Due to the two-tier architecture of femtocells and macrocells, interference is imminent. The cell sites covered by a number of FAPs (in some cases overlapping each other) is overlaid in the larger cell site of the macro base stations as shown in Figure 1.2. Interference here denotes the transmitted signals from the FAPs or MBS and their serving User Equipments (UEs) that appear as unwanted signals to each other.

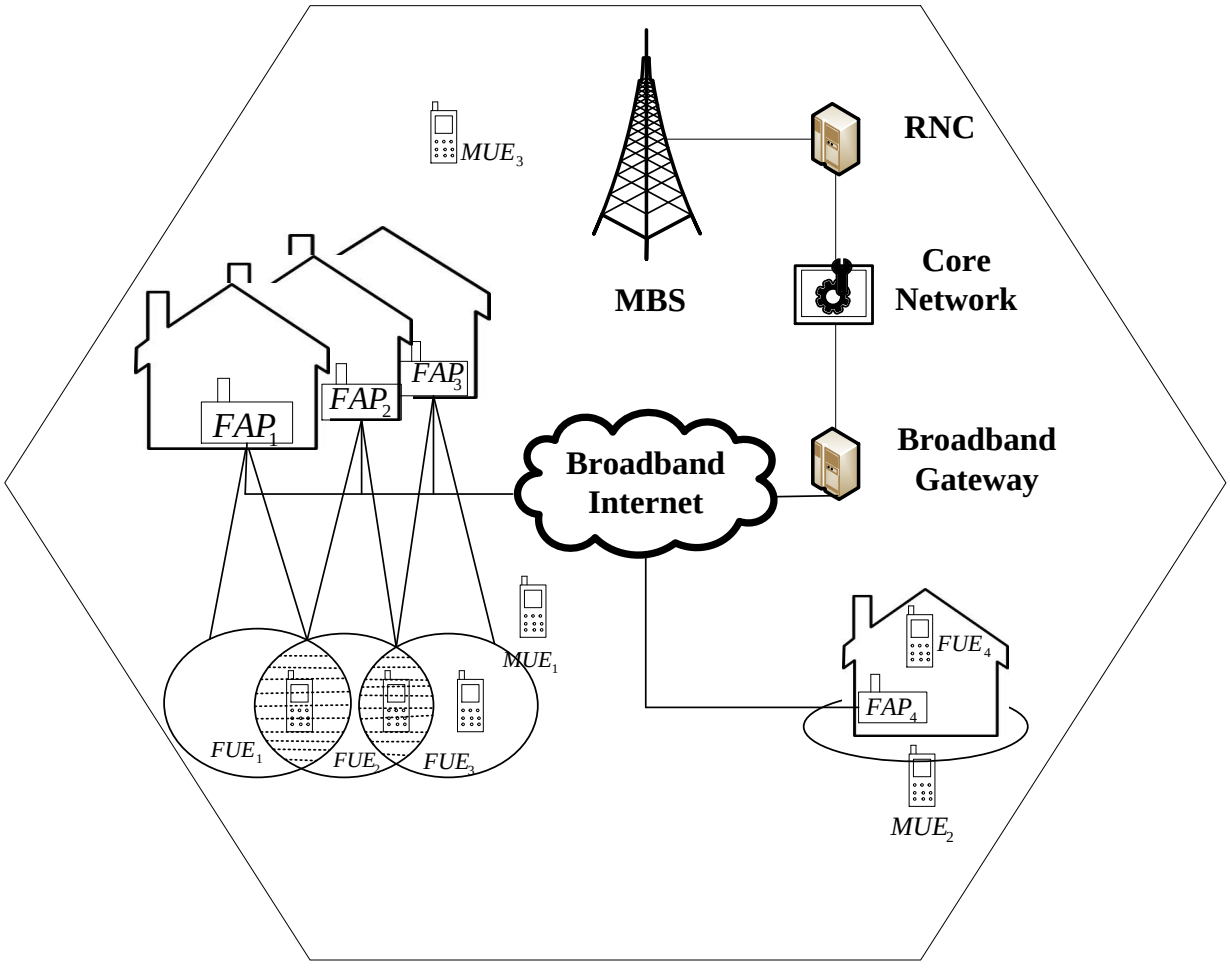

Figure 1.2: Femtocell scenario with co-tier and cross-tier interference

Interference could be between femtocell and macrocell which is known as cross-tier or between neighbouring femtocells known as co-tier [20]. Interference can be further classified as Uplink (UL) or Downlink (DL) based on the sources, which besides the FAP and MBS, also includes

the Femtocell User Equipments (FUEs - a UE served by a FAP) and Macrocell User Equipments (MUEs - a UE served by a MBS).

Uplink interference is caused by;

a) FUE interfering with the signals of a neighbouring FAP or the MBS

b) MUE interfering with the signals of FAPs (while MUE is communicating with MBS)

While downlink interference is caused by;

a) A FAP interfering with the signals of UEs from a neighbouring FAP or MBS

b) A MBS interfering with the signals of UEs (sent from FAP to UEs).

A femtocell scenario with four FAPs denoting four cell sites overlaid in a macrocell is shown in Figure 1.2 to describe co-tier and cross-tier interference. The cell sites covered by FAPs 1, 2 and 3 overlap each other thereby causing co-tier inference but they also suffer cross-tier interference as they are overlaid in the macrocell. FAP 4 on the other hand is a standalone FAP therefore the only interference experienced is cross-tier from the MBS.

1.2.2 Femtocells - Interference versus Deployment

It is important to note that the scale at which interference affects a femtocell network is largely dependent on the deployment scenario. The 3GPP's technical specification of the scenarios for deployment of femtocells are summarised in [18] and described as follows;

a) Spectrum Usage - Dedicated channel or Co-channel deployment.
b) Access Methods - Open access or Close Subscriber Group (CSG).
c) Transmit Power - Fixed Downlink (DL) transmit power or Adaptive DL transmit power.

Figure 1.3 summarises different femtocell deployment scenarios followed by explanation of interference versus deployment.

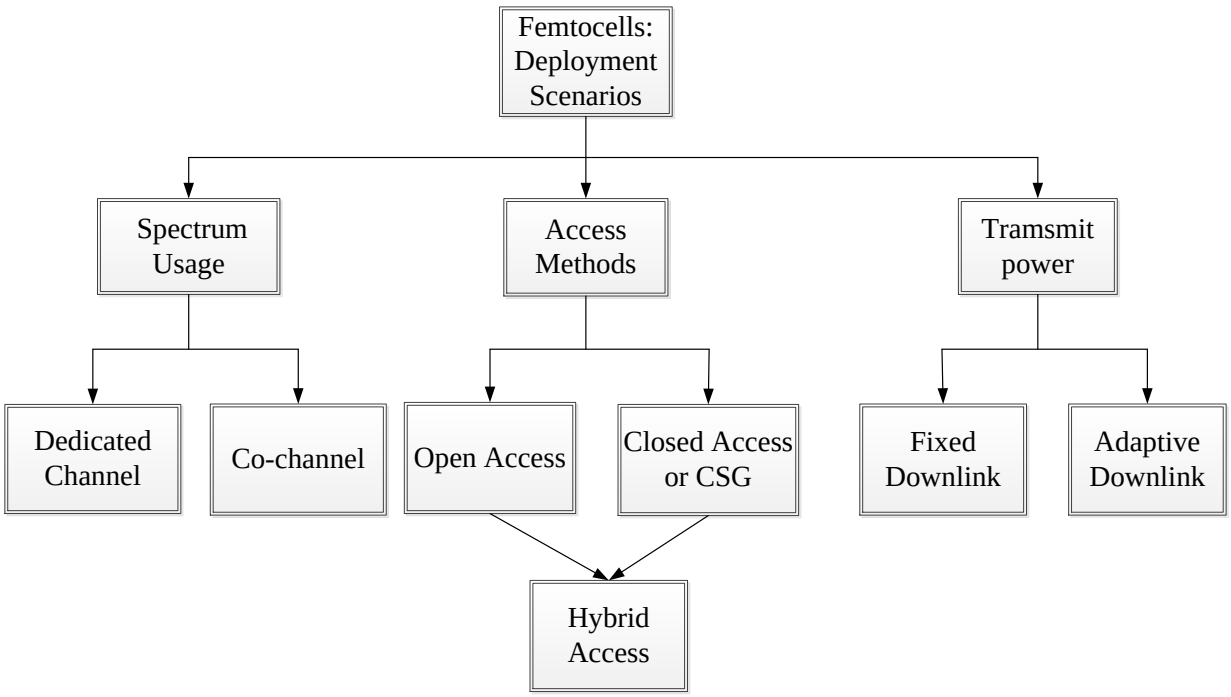

Figure 1.3: Femtocell deployment scenarios

In a dedicated channel deployment, the licensed spectrum is split into different portions for each tiered network to operate in a dedicated manner whereas both tiers share the same licensed spectrum in co-channel deployment [21]. The choice of deploying any of the two requires a trade-off between spectrum availability and interference. In dedicated channel, spectrum availability is limited as each portion is assigned a specific bandwidth to utilize. It still leads to a low cross tier interference. On the other hand, spectrum is available for all users in a co-channel deployment but this result to high cross tier interference. Network operators prefer a co-channel deployment due to the limited available bandwidth but will have to deal with the interference issues [22]-[25].

FAPs deployed in an open access allow connection for all users whereas in a CSG mode only the subscribed owners of the FAP have access. Cross tier interference in open access is reduced due to the fact that users can connect to the nearest FAP with the strongest signal. In CSG,

users experience strong UL and DL cross tier interference. In UL, MUEs close to the FAP and far away from their BSs will have to increase their transmit power to gain a better throughput and SINR causing interference to the FAP**.** In DL, FAP interferes with the communication between an MUE and its serving BS. However, in CSG, higher SINR values are guaranteed for the served FUEs in contrast to an open access mode as FAP resources are restricted to subscribed users only. A new access deployment is the hybrid access which combines the open access and the CSG by allowing full resource access to its subscribed FUEs and limiting the amount of resource access to other FUEs [26].

In fixed mode, the DL transmit power is set to a predefined value while in an adaptive mode, the transmit power is controlled to avoid perceived interference in the environment which implies reducing its power depending on its location to a BS such as at the cell edge and cell centre **[**27**].** A very high transmit power will cause interference to neighbouring FAPs and MBSs while a very low transmit power on the other hand will limit the FAP coverage and in turn limit the quality of service provided [28]. An adaptive transmit power is preferred over a fixed transmit power because of the inability of the FAP in a fixed mode to alter its transmit power when necessary to avoid interference [19].

1.3 Cognitive radio networks

The Federal Communications Commission (FCC) and the European Telecommunications Standards Institute (ETSI) acknowledged the scarcity of available spectrum thus the idea of Cognitive Radio (CR) came as a solution to the limited wireless spectrum where most of the frequency bands are already assigned or in some cases under-utilized [29]. CR is the ability of Radio Frequency (RF) to sense its environment and automatically alter its characteristics such as frequency, modulation, power and other operating parameters to dynamically reuse whatever spectrum is available [30]. Unlicensed spectrum bands such as the Industrial, Scientific and

Medical (ISM) [1], which is set aside to encourage innovation, is either too congested or heavily underutilised. The FCC released a 'notice of proposed rule-making' for the use of technological capabilities in the exploration of unused bands such as television broadcast bands [31].

CR has been regarded as a technology capable of achieving this with its opportunistic ability of spectrum sensing, management and mobility [28, 32-35]. Through spectrum sensing and management CR can detect the availability of an unused licensed spectrum also known as spectrum hole or white space, vacated by the user who is the licensed or primary user (PU) and assign it to an unlicensed secondary user (SU). Also, CR detects and vacates the spectrum into another spectrum hole as soon as a PU re-emerges while maintaining its seamless connection – which defines its mobility capability. A three dimensional view of white spaces and spectrum occupancy is shown in Figure 1.4 below**.**

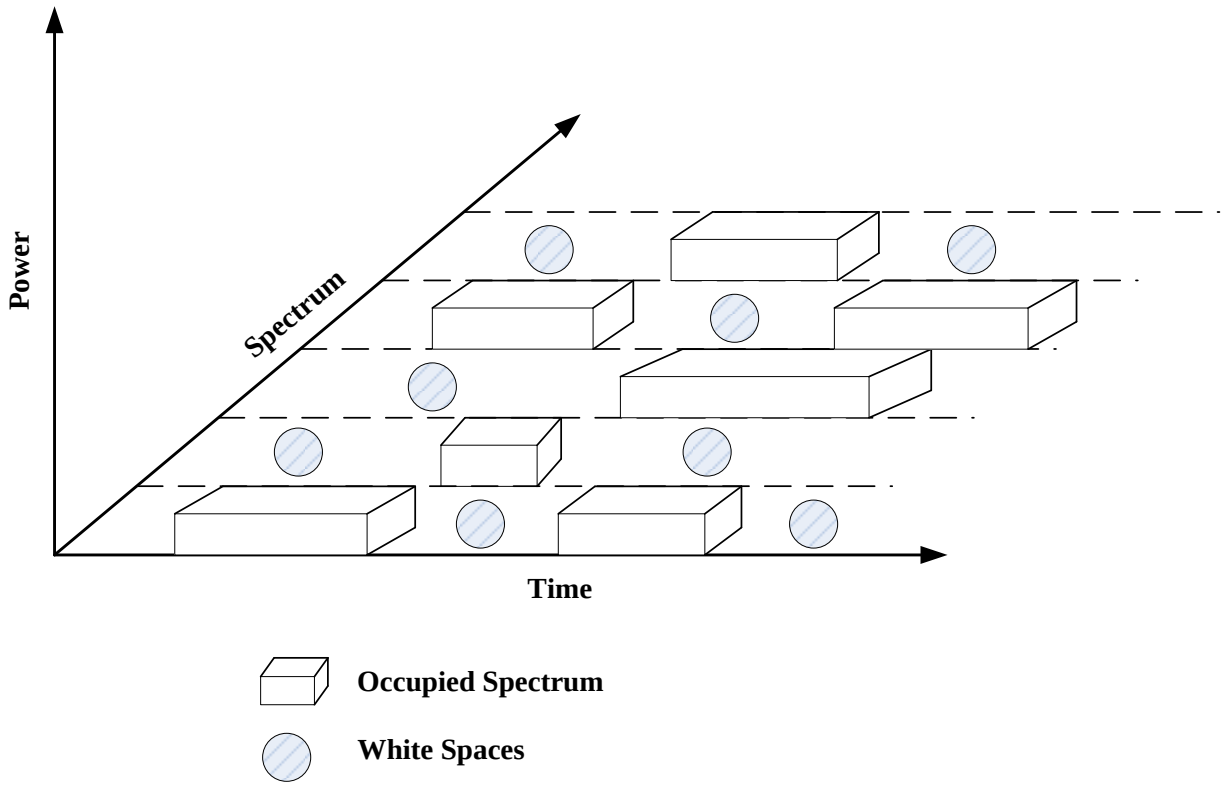

Figure 1.4: White spaces denoting availability of spectrum

CR, through its ability to manage the spectrum and handoff when appropriate, allows a SU to choose the best frequency band among the available to support Quality of service (QoS) requirements [36]. There are mainly three spectrum sharing concepts in CR named underlay, overlay and interweave, which can be applied to mitigate interference while also ensuring that maximum capacity is maintained [37].

1.4 Cognitive Femtocell networks

The integration of CR in femtocells is known as Cognitive Femtocells (CF) [38], or Cognitive Femtocell Base Station (CFBS) [39], which signifies a femtocell with CR capabilities. Femtocells having the spectrum sensing capabilities of a CR can avoid co-tier and cross tier interference by sensing the spectrum and allocating resources on a different spectrum to avoid interference. In this regard, The FUEs are able to sense the environment for white spaces and opportunistically occupy them in the absence of a PU and also vacate them for another possibly available white space as soon as the PU reclaims it.

In situations where the FAPs overlap each other as in Figure 1.2, a dynamic spectrum access technique (DSA) is required to allow SUs (i.e. FUEs) share spectrum resources between themselves and the PUs while avoiding interference. The self-optimization capabilities of cognitive femtocells allow the radio environment to be sensed in a dispersed manner to salvage operational parameters in order to manage interference.

1.5 Principal objectives of research

The principal objectives of this research can be summarized as follows:

1. To present an overview of indoor mobile coverage deficiencies and present various solutions that has been implemented so far to arrest this problem. This will introduce the need for a feasible and optimized solution from the list of available options.

2. To highlight interference in cellular systems with simulations depicting real deployment scenarios and the ability of femtocells to mitigate the inherent interference as well as improve indoor network coverage. Femtocell is presented in terms of its standardization, connectivity and scalability. Drawbacks such as security concerns are also highlighted.
3. To highlight the advantages of incorporating cognitive radio with femtocells in mitigating interference.
4. To propose algorithms for mitigating both co-tier and cross-tier interference in cognitive femtocells to enhance the network performance due to the mutual interference between femtocells and macrocells.
5. To implement and compare the algorithms with existing approaches using a network simulation tool.

1.6 Main contributions of research

The main contributions of this thesis are summarized below in terms of the chapters:

- **Chapter 2**

  This chapter introduces the typical approaches in mitigating interference in femtocells and subsequently presents an overview of the state-of-the-art interference mitigation schemes specific to cognitive femtocells in literature today. The advantages and disadvantages of these schemes are provided as well. This chapter is published in [40] and the contribution of this chapter is a **literature review**.

- **Chapter 3**

  In this chapter an overview of LTE as a candidate for cellular radio access technology (RAT) is presented to aid deployment of femtocells by the 3GPP standards body. This femtocell network architecture enables a variety of femtocells from different

manufacturers to work in the networks of different operators. This chapter will also provide the foundation for femtocell interference analysis in LTE with novel algorithms as solutions in mitigating interference in cognitive based LTE femtocells presented in the proceeding Chapters. The contribution of this chapter is the significance of **LTE as a platform for femtocell deployment and the need for development of mitigation algorithms for the inherent interference.**

- **Chapter 4**

  In chapter 4, a novel coverage radius based downlink power control scheme to mitigate interference in densely deployed femtocells is proposed. This schemes operates with a FAP self-update algorithm determines the coverage radius of the femtocell with respect to its farthest served FUE. Based on varying coverage radius, a max/min function is used to adjust the downlink transmit power value of an FAP. Furthermore, the scheme is applied to circumvent the problems caused by blind placement of FAPs. This chapter is published in [41] and [42]. The contribution of this chapter is **a novel power control algorithm for femtocells and its efficacy in mitigating interference.**

- **Chapter 5**

  In chapter 5, a joint threshold power based admittance and matching policy algorithm based on a contention free resource allocation for interference mitigation in cognitive femtocells. In this scheme, a FAP calculates the mutual interference between itself and a close by MUE and admits the closest MUEs as one of its UEs to mitigate cross tier interference. Further scheme employs a scheduling engine which engages a matching policy that orthogonally assigns the resource blocks (RBs) of MUEs resulting into significantly reduced co-tier interference. The contribution of this chapter is a **hybrid algorithm for Interference Mitigation in Cognitive Femtocells.**

- **Chapter 6**

  Chapter 6 proposes a scheduling algorithm known as service associated (SA) where CFs assign the RBs of MUEs with a low data traffic load which experience a low interference temperature to its FUEs based on the interweave concept in spectrum sensing. This is based on the realistic premise that MUEs transmit with different traffic loads and it is highly likely for its assigned resource units or resource blocks (RBs) being either empty or with a low interference. The contribution of this chapter is a **service associated (SA) scheduling algorithm for cognitive femtocells.**

- **Chapter 7**

  In chapter 7, the conclusions are drawn with Lessons Learnt provided. Open issues and future work is also discussed. The contributions of this chapter are the **guidelines for future research**.

Chapter 2

Interference mitigation in cognitive radio based femtocells: an overview

2.1 Femtocells – typical interference mitigation techniques

Interference management can be classified under ways of avoiding, cancelling or distributed (randomised) approaches [20], the typical schemes to mitigate interference are aligned towards spectrum access/frequency assignment, power control and antenna schemes. Joint schemes consist of a combination of two or more schemes. A brief overview of mentioned schemes is given in the following sections.

2.1.1 Spectrum Access / Frequency Assignment Schemes

Spectrum access schemes require methods where a FAP assigns its UE a spectrum with limited or no interference with neighbouring FAPs, FUEs, MUEs or the MBS [43]-[53]. The choice between a dedicated or co-channel deployment is implemented with considerations such as the amount of spectrum available and density of femtocells in a specified region. Hybrid spectrum access schemes combine both deployment modes where the spectrum is split into the two access modes with priority given to the MBS.

In a hybrid scheme for example, a portion of the spectrum is assigned for a dedicated channel mode specific to the MBS and its MUEs, whereas the remaining spectrum is accessed in co-channel fashion both by MBS, FAPs and their UEs [43]. Figure 2.1 illustrates an example of such an implementation with inner and outer regions denoting areas of dedicated and co-channel deployments respectively. As shown in Figure 2.1, FAP1 overlaps in both inner and outer regions. This means FUEs falling into the region of intersection will have to access the spectrum based on that mode, whereas FAP2 and its UEs on the other hand access the spectrum only in a co-channel mode. The problem with hybrid schemes such as this is that it requires the FAP to ascertain which region it falls into which introduces additional computation and complexity.

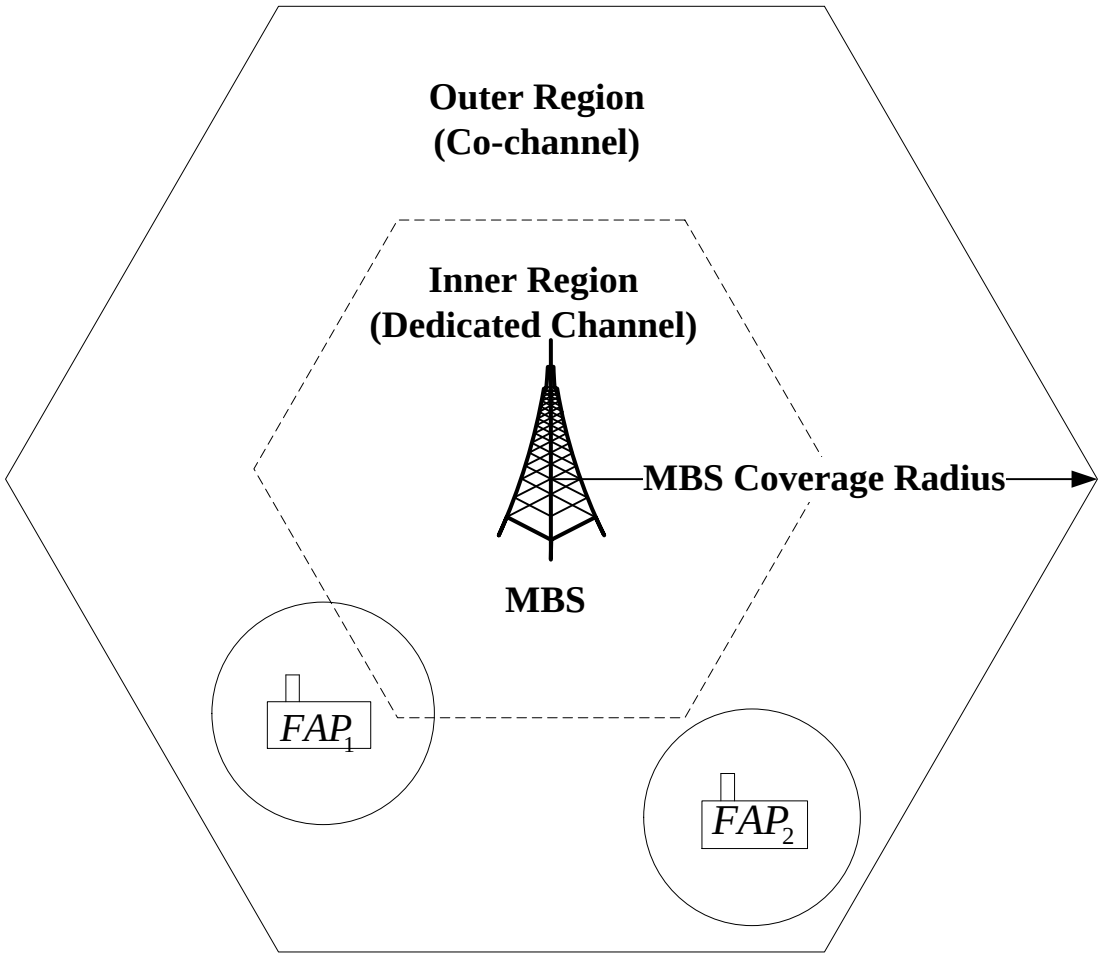

Figure 2.1: Interference Mitigation - Hybrid Spectrum Allocation.

Frequency assignment schemes mitigate interference by exploiting the knowledge of the resources as well as the direct coordination between FAPs and MBS. These schemes thus prevent the use of Resource Blocks (RBs) of neighbouring FAPs and MBS such as in LTE systems [19].

2.1.2 Power Control (PC) Schemes

The radiated power transmitted by FAPs comprises of the FAPs pilot power, which determines the cell coverage area and traffic power (consists of the signalling and data) [54]. The effect of interference on other FAPs and the macrocell is dependent on these two power levels. A high pilot power will result into a large cell coverage area, which consequently has higher chances of causing interference. There is a need to optimize the transmit power in femtocells to avoid interference while maintaining certain Quality of Service (QoS).

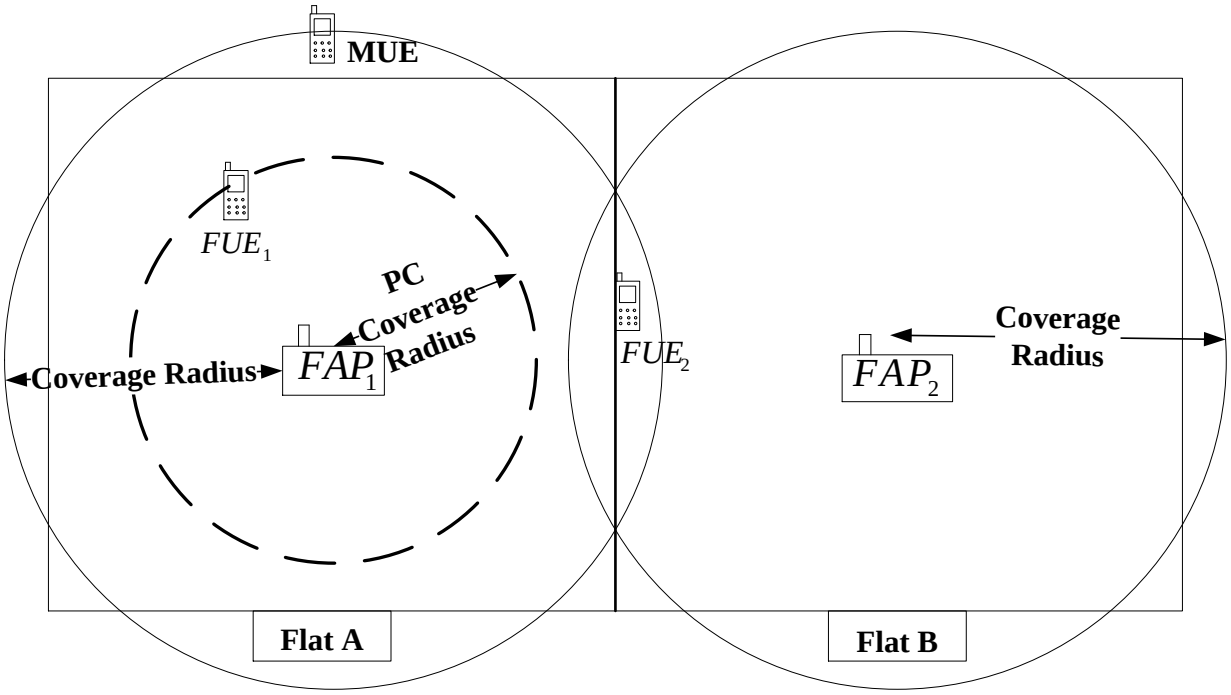

Figure 2.2: Interference Mitigation - Power Control

Figure 2.2 illustrates a scenario where FAP_1 and FAP_2 are deployed in two flats, Flat A and Flat B, serving FUE1 and FUE2 respectively with their pilot power levels overlapping each

other (solid circles in Figure 2.2). In this scenario, FAP1 employs a power control mechanism which reduces its pilot power, i.e. coverage area (dotted region in Figure 2.2) thus preventing co-tier interference to FUE2 and FAP2 and cross-tier interference with the MUE. Power control however is not only restricted to the FAPs as UEs can also optimise their power levels or assist their FAPs to reduce interference to neighbouring FAPs and other UEs. Some of the typical power control schemes employed by femtocells are described in [54]-[70].

2.1.3 Antenna Schemes

Beam directivity of the antennas, both in FAP and FUEs, can be exploited to avoid interference in femtocell networks [71]-[78]. Typical antenna schemes are implemented which allow the FAP to direct their beams to specific UEs while creating a null in other zones, thus cancelling the interference to a greater extent. The scenario represented earlier in Figure 2.2 is replicated in Figure 2.3 to highlight how antenna schemes can generally be used to mitigate interference in femtocells.

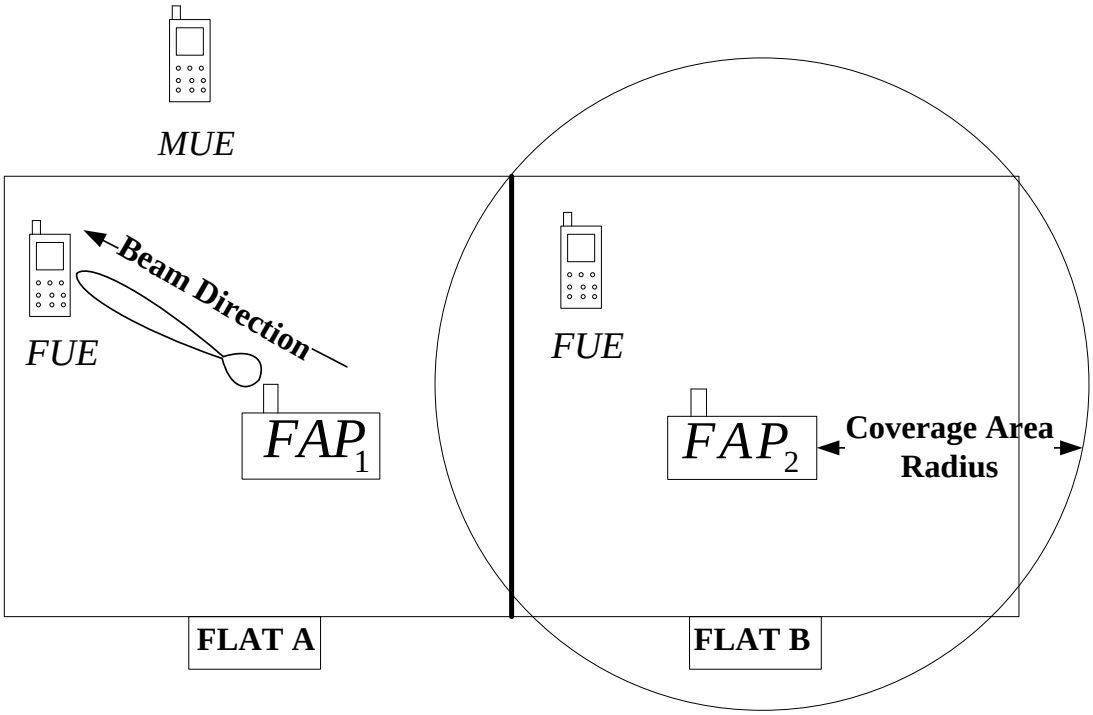

Figure 2.3: Interference Mitigation - Antenna Schemes

To sum up, the problems associated with mitigating interference in femtocells are largely dependent on its tiered architecture and random deployment where there is no central coordination between its neighbouring femtocells and the macrocell network. Importantly, information about the radio environment, such as characteristics of all the interfering signals, if known, can be controlled to help mitigate interference in femtocells. An ideal femtocell interference mitigation technique is the one which is aware of the interfering signals and takes into consideration the best deployment criteria to suit subscribers' needs while efficiently utilising the network operators' resources. One example is the use of a co-channel deployment in a scarce spectrum environment and the use of CSG for subscribers who consider security a priority.

2.2 Cognitive Interference Mitigation schemes overview

Figure 2.4 provides an overview of the cognitive interference mitigation schemes discussed in this section. Presented schemes are classified based on their functionality and conferred in greater detail before salient features offered by each scheme are highlighted.

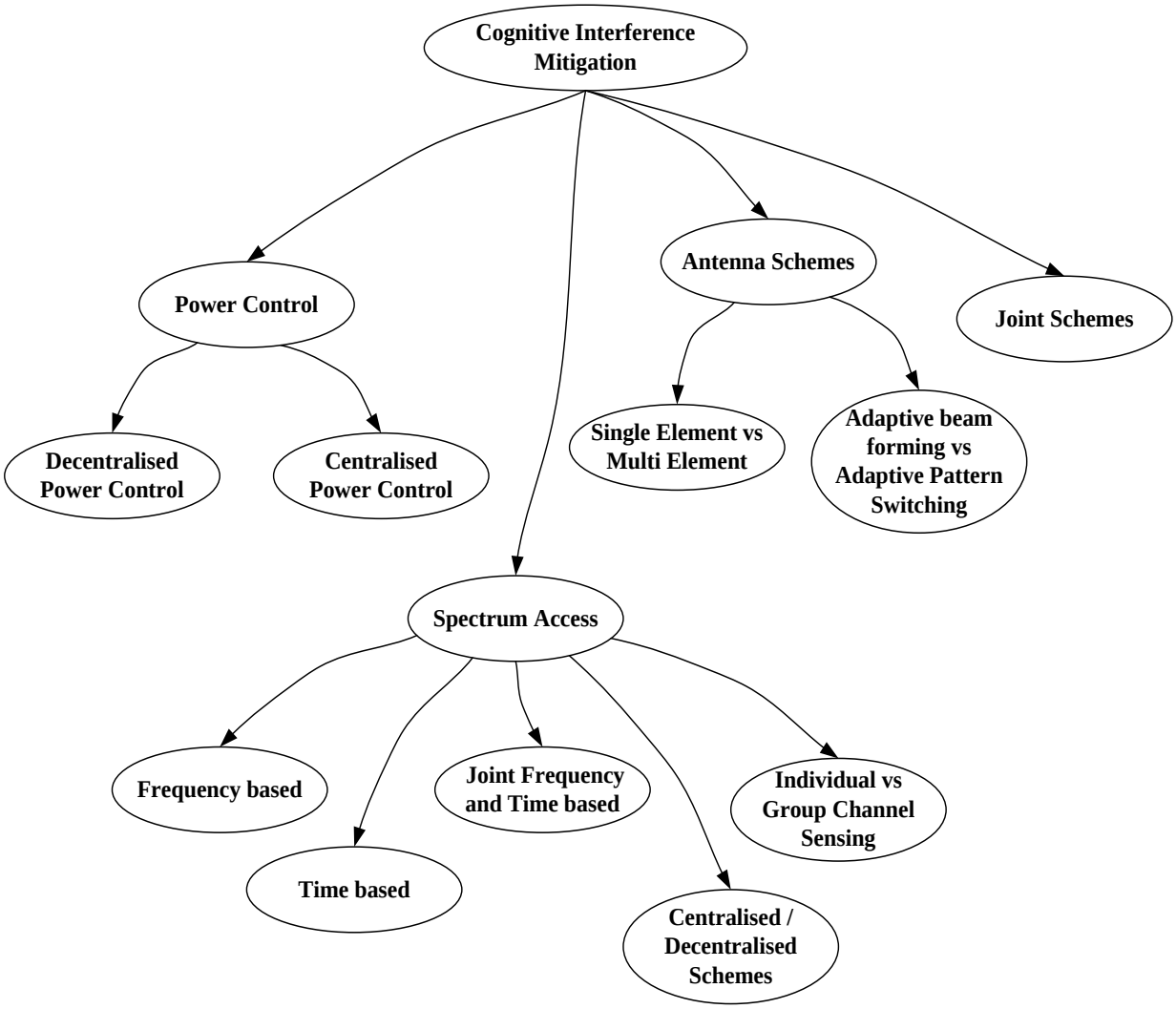

Figure 2.4: Cognitive Interference Mitigation Schemes.

2.2.1 Cognitive Interference Mitigation - Power Control

Power control schemes can either be decentralised or centralised as presented in the following subsections.

2.2.1.1 Decentralised Power Control

A scheme which requires the exploitation of a MBS control channel by an FAP and FUEs in a network to mitigate interference is presented in [79]. By using CR, a FAP and its UEs are able to decode control information such as number, location and power of each active MUE in a spectrum in order to adjust their transmit power. Two rules are implemented after the

acquisition of the necessary control information to mitigate interference. As a first rule, the MBS and MUEs are given top transmission priorities in what is known as forbidden radius which is the area of an active MUE or a MBS. FAPs within the range of this forbidden radius are restricted to transmit. In the second rule, FAPs and FUEs are tasked with controlling their transmit power such that the interference received at the MBS or MUE does not exceed a set value. A MUE assisted power control scheme is adopted in [80] where MUE measures the received power from its serving MBS and forwards the information to all FAPs in its vicinity. Each FAP subsequently calculates its path loss from the MUE utilising CR to optimize its power level to avoid interference with the MUE.

2.2.1.2 Centralised Power Control

As mentioned earlier, FAPs can be deployed in an open, closed and hybrid access which largely depend on the subscriber's choice. A novel approach with the ability of FAPs to switch between these access modes based on cognitive sensing and power control is presented in [81]. This self-configurability approach requires each FAP to sense the radio environment and identify white spaces or slots with less interference. For each slot identified, a SINR threshold is set based on channel conditions and a power control algorithm updates the transmit power to define its coverage range.

This predefined SINR threshold determines the change in access mode. For example, if a received SINR for a particular slot is less than this threshold it means it can accommodate unregistered UEs in its vicinity and therefore switches to open/hybrid access as long as it does not affect the FUEs being served by the FAP otherwise it switches to a closed/hybrid access to limit the UEs. This scheme highlights the dynamic capabilities of the femtocell. However, in reality, most subscribers would prefer a single CSG mode as added security becomes a factor in open or hybrid modes. Moreover, femtocells are paid for by the subscribers who would not want to share resources with unknown users.

A power control scheme using Q-learning which enables FAPs to allocate power optimally in a cognitive underlay approach is proposed in [82**]** to mitigate cross-tier interference in the downlink. A FAP carries out a distributed learning technique by sensing the radio environment to observe its state and takes an action to determine its consequences which can be assessed as a reward (low interference and high MUE capacity) or penalty (high interference and low MUE capacity). By repeating this process, it analyses the entire radio environment and is able to find an optimal power allocation policy to mitigate interference while maintaining MUE capacity. The problem with this scheme is that by trying to determine a suitable policy to mitigate interference, it accumulates a lot of signalling overhead which also leads to delay.

Another power control scheme utilizing communication in the uplink (UL) and composed of three phases (channel sensing, channel training and data transmission) is described in [83]. During channel/spectrum sensing, a FAP senses the radio environment by employing any of the well known techniques to find unoccupied spectrum. A hypothesis test is conducted to make a decision as to whether a spectrum is occupied (MUE(s) present) or Null (absent). The channel coefficient between the FAP and the FUE is estimated in channel training by the FUE sending a signal known as training signal to its FAP. The cognitive FAP thus optimises the rate at which power is transmitted by allowing its FUE transmit at a reduced or maximum power when a MUE is present or absent respectively to avoid interference during data transmission.

The technique proposed in [84] is based on the overlay approach where each FAP in the network periodically senses and deduces the macrocell path loss denoted as *PLM*, between itself and the MBS. Spectrum sensing in this case is divided into two stages, the uplink and downlink sensing. In the uplink stage, FAP deduces the *PLM* of MUE by measuring a parameter such as Reference Signal Received Power (RSRP). In downlink sensing, based on the *PLM*, the spectrum sensing threshold denoted as γ is calculated. Using this information, a FAP is able to identify a channel as unoccupied if the received signal power, denoted as *PMC*,

on that channel does not exceed γ. On each sensed channel, FAP is able to allocate a lagrangian based transmit power function on its FUE for data transmission to mitigate interference.

In a nutshell, most power control schemes utilize an adaptive power control mode where the pilot power levels of an FAP is controlled effectively not only to mitigate interference but to reduce the need for handover of close by UEs in open access mode. Although UEs can also employ power control techniques, distributed power control schemes assisted by UEs of a FAP or MBS may have a detrimental effect on the UEs as it increases their overhead which may result to increased battery drain. On the other hand, a centralised power control scheme will require a continuous update of the information about all its UEs in real time which makes it computationally complex. In our opinion, since most UEs are mobile devices it is better to leave the optimisation of power to FAPs and MBS (centralised) who have a dedicated power supply and make the computation of the algorithms less complex.

2.2.2 Cognitive Interference Mitigation - Spectrum Access

Most spectrum allocation schemes involve the MUE as the PU and the cognitive FAP and its FUE as SUs. This paradigm differentiates and defines how spectrum is allocated in a co-channel mode with top priorities to the MBS and MUEs. Cognitive spectrum access schemes are largely based on the opportunities that exist in various domains such as frequency and time. In the following subsections, the spectrum access schemes are grouped based on these opportunities as well as how they are implemented (distributed/centralised) and how the channels are sensed (individual/group sensing).

2.2.1.1 Frequency based

Unlike the conventional PU and SU analogy, a scheme which recognises a femtocell in the same regard as macrocell is proposed in [85] with the argument that FAPs could be densely populated with large amount of data and traffic requiring high priorities like MBS. The scheme

employed in LTE-A Macro-Femto Orthogonal Frequency Division Multiple Access (OFDMA) systems utilizes the concept of cross cognition and graph colouring to mitigate cross tier and co-tier interference respectively. In cross cognition, all the parties perform cognition in the system (FAPs FUEs, MBSs and MUEs) and the spectrum is divided into licensed and unlicensed parts with the MBSs and FAPs having access to both parts. FUEs and MUEs utilize the licensed spectrum offered by the corresponding serving FAP and MBS but opportunistically utilize the unlicensed spectrum when the licensed spectrum is exhausted.

A scheme to reduce the macro uplink interference (interference from a MUE to a FAP) in heterogeneous networks combining channel sensing and resource scheduling is proposed in [86]. FAPs sense channel occupation by analysing the energy in the sub-channels and subsequently assign those with the lowest interference to its users. The scheme employs the concept of Fractional Frequency Reuse (FFR) where the spectrum is divided into Frequency Assignments (FA) comprising various sub-channels. Since the FAP cannot effectively sense the weak DL from the MBS, it capitalises on the strong UL transmit power of the macro user as it tries to reach its MBS to find out available FAs. It subsequently employs a hypothesis which determines the presence and absence of a macro user signal [87].

If a macro user is present it immediately vacates the FA to protect the macro users UL and DL signal transmission. Under this hypothesis, the number of sub channels for each FA, false alarm and detection probability are deduced which helps the FAP determine a FA not occupied (idle) by a macro user. It identifies this FA as the operating FA and in a situation where there is no idle FA, identifies the one with the lowest signal energy as the operating FA. To allocate resources, the FAP estimates the DL interference signature of the sub channels in the operating FA using an algorithm and allocates it to its users for signal transmission.

However, a DL approach is preferred in [88] for WiMAX femtocells by capitalising on the downlink activity of MUEs by arguing that spectrum sensing accuracy is more achievable since there is more activity of MUEs in the DL and less activity in the UL as proposed in [84]. The scheme which utilises cyclostationary feature detection for spectrum sensing allocates resources to FUEs only if the activity of MUEs is not significant.

A scheme based on the interweave paradigm with Gale-Shapely spectrum sharing (GSOIA) is presented in [89] where cognitive femtocells opportunistically and orthogonally assign PU channels based on a one-to-one matching policy to avoid interference. In GSOIA, the utility of each channel is calculated by each FAP and subsequently sets a back-off timer for each channel. A channel is deemed available for communication if an FAP detects no busy tone at the expiration of the timer, otherwise it abandons it and waits for the expiration of the next back off timer until each FAP is able to communicate on an available channel.

To limit the downlink cross tier interference of a FAP to a nearby MUE, a novel spectrum access scheme is proposed in [90]. In this scheme an MUE joins a nearby open access FAP while freeing up its allocated sub-channel. A FAP capitalises and takes control of this available sub-channel from the MBS while adding the MUE on the list of its UEs. Utilizing CR, the FAP assigns its FUEs and the MUE sub-channels from its list of available spectrum including the freed up channel. Although open access schemes appear to conveniently tackle cross tier interference, some issues need to be addressed such as the criteria for joining a FAP. Such a choice is suggested for an FAP with the strongest interference which although is feasible in standalone FAPs, will prove to be difficult in a highly populated FAP scenario. This is because close-by MUEs will opt for the same FAP while ignoring other FAPs which prompt for coordination between FAPs in closed access.

A cognitive empowered FUE method is proposed in [91] to assist the FAP in allocating resources. FAP continuously senses the radio environment for available spectrum in what is regarded as the proactive sensing phase. It shares the channel statistics with each of its FUEs who in turn perform a stand-alone spectrum sensing to verify if the sub-channel are actually 'available'. This is because the 'available' sub-channel may have been concurrently sensed with a neighbouring FAP who might have occupied it. The FUE subsequently sends an acknowledgement (ACK) message to its FAP to confirm if the sub-channel is still available or otherwise to enable the FAP update its list of available sub-channels. This serves as a measure to tackle co-tier interference. By exploiting the delivered and undelivered packets through the Automatic Repeat request (ARQ) feedback between MBS and MUE, a cognitive FAP is able to mitigate interference as proposed in [92**]**. A FAP senses the initial DL transmission to decode information about the (re)reception and (re)transmission sub-channels. In the event of an unsuccessful packet the FAP capitalises on the time between retransmissions to communicate with its FUE thereby avoiding interference.

Cognitive Radio Resource Management (CRRM) and a Strategic Game-based Radio Resource Management (SGRRM) are combined in [31] to manage cross-tier and co-tier interference respectively. In CRRM, each FAP cognitively senses the spectrum periodically to identify which RBs are unoccupied. A FAP senses the received interference power for each of the RBs in a frame and compares it against a threshold thereby identifying a RB as occupied if it exceeds this threshold and vice versa. Resultantly, the RBs found unoccupied are assigned to the UEs. SGRRM is developed to avoid co-tier interference due to the selfish nature of FAPs as they view the same resources as unoccupied after cognition and try to assign their UEs to the available spectrum. In SGRRM, overlapped (collocated) FAPs coordinate to autonomously ascertain the total number of RBs that is available and randomise its use to avoid co-tier interference.

2.2.1.2 Time based

The exploitation of available bands in Global System for Mobile communications (GSM) networks can also be used for efficient spectrum access as proposed in [93]. To mitigate interference, it requires FAPs and FUEs to sense a spectrum based on per-time slots rather than the conventional method of continuous sensing of all the available bands. This scheme is based on the possibility of analysing the channels of GSM bands in consecutive frames using per-time-slots of a common sequence number. First, each FUE carries out a fast stand-alone cognitive sensing. It uses the current status of the bands where FUE senses an individual spectrum and identifies idle slots for transmission as illustrated in Figure 2.5**.** An FUE performs a fast sensing for a time T_s which is a fraction of the time slot T_{slot}.. A request message is then sent to the FAP if any idle slot is identified and FAP assigns one or more channels to a FUE for transmission from the available time slots.

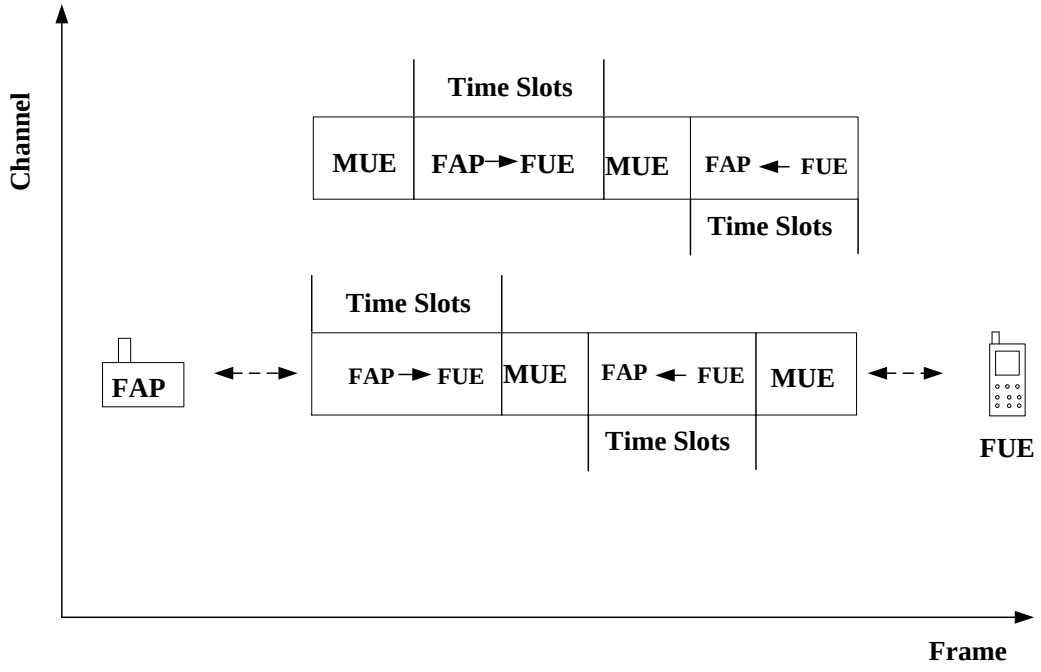

Figure 2.5: Interference mitigation on per-time slot basis

To tackle the problem of coordination of Cognitive Femtocells (CFs) in CF networks (CFNs), the use of dedicated signalling channels in LTE networks is proposed in [94]. In the network,

each FAP analyses its radio environment as well as the activity of other FAPs and capitalises on the uplink (UL) communication between a MUE and the MBS (Time Division Duplex mode) to measure the level of interference it has on a MUE. This information is shared between the femtocell nodes through the signalling channel and a dynamic spectrum allocation method is implemented to mitigate interference with the macrocell.

2.2.1.3 Joint frequency and time based

A cognitive spectrum selection scheme for LTE-A femtocells based on a distributed carrier selection process is presented in [95]. This scheme employs carrier aggregation in LTE-A systems where spectrum is made available by combining component carriers (CC) on to the physical layer allowing UE to be assigned single or multiple CCs for transmission. To mitigate interference, each FAP must transmit on a different CC and select an anchor CC known as Primary CC (PCC) which acts as a control for the other CCs as illustrated in Figure 2.6. To select a PCC, a FAP senses its environment and randomly picks a CC if no other FAPs are on site. In a situation where other FAPs are detected, it analyses which CCs are occupied by its neighbours and then chooses the farthest CC as its PCC. A secondary CC (SCC) selection is conducted if a PCC fails to satisfy the requirements of a FUE by cognitively measuring the path loss between FUE and neighbouring FAPs.

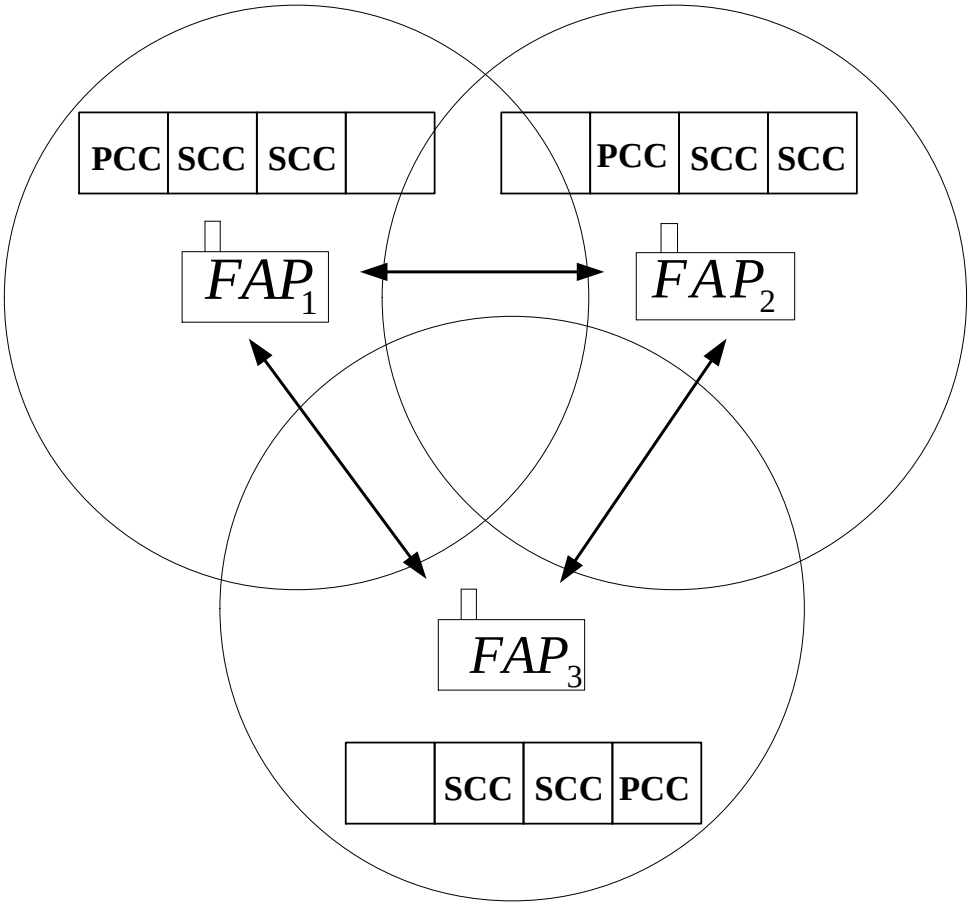

Figure 2.6: Distributed Carrier Selection Process - PCC and SCC.

A co-tier and cross-tier downlink cognitive interference management scheme for heterogeneous femto/macro cell networks in CSG mode is proposed in [96]. This scheme allocates resources both in time and frequency in terms of transmission opportunities and resource blocks (RBs). It requires feedback from UEs and coordination between neighbouring FAPs and MBSs to ascertain the level of interference caused to each other's UEs. The scheme involves identifying the victims of interference by each UE in the network measuring the RSRP of other FAPs and MBS and reporting it back to its serving FAP/MBS. Each FAP and MBS in turn classifies the UEs in a safe/victim table which it shares with its neighbours similar to a routing table scenario (Figure 2.7, Table 2.1). A UE is considered to be safe if it is free from a FAP or MBS interference and likewise considered a victim if it experiences a significant level of interference from a FAP or MBS. In Figure 2.7, MUE_2 who is served by the MBS (safe) is within the

coverage radius of FAP_2 and FAP_3 making it a victim of both FAPs. On the other hand, it is safe from FAP_1 since it is not in its coverage radius as highlighted in Table 2.1.

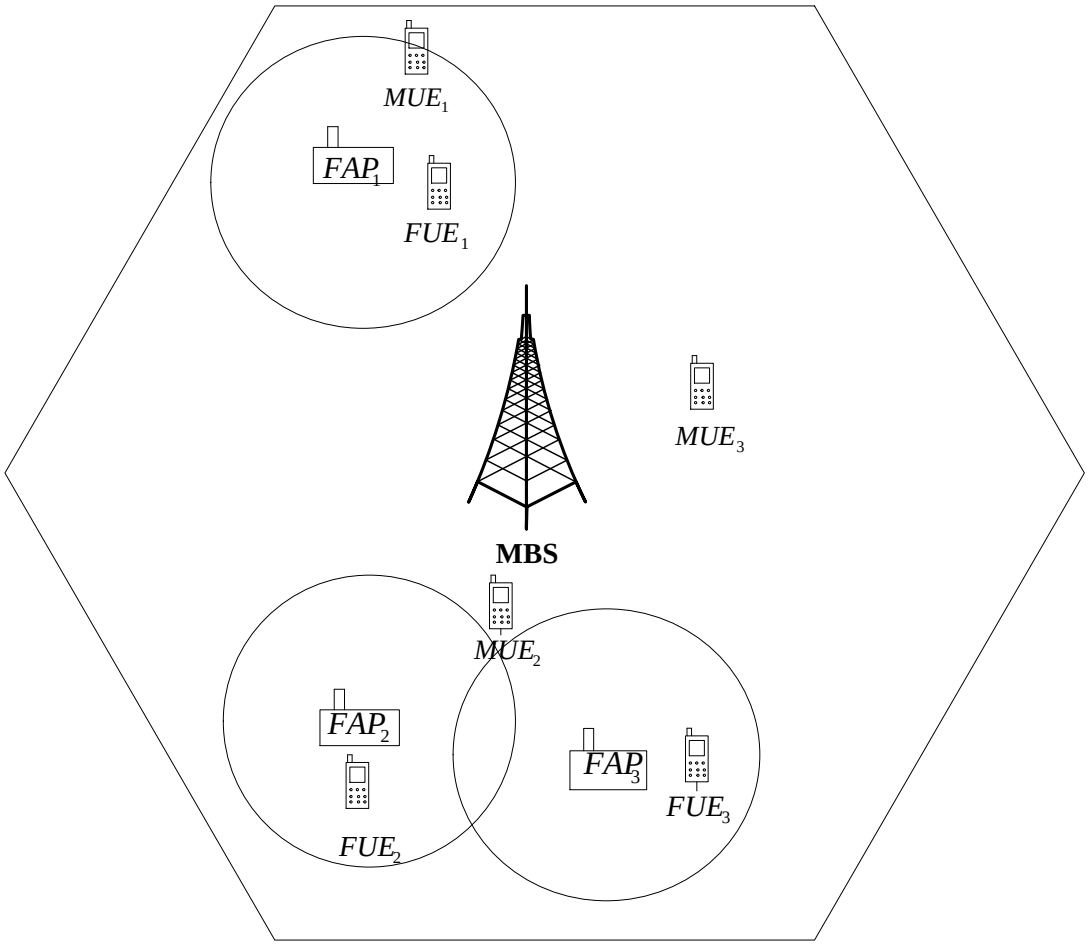

Figure 2.7: Interference Mitigation Scenario to illustrate Safe / Victim UE

Table 2.1: Classification of Safe/Victim UE

MUE/FUE	**Safe / Victim**			
	MBS	FAP1	FAP2	FAP3
MUE1	Safe	Victim	Safe	Safe
MUE2	Safe	Safe	Victim	Victim
MUE3	Safe	Safe	Safe	Safe
FUE1	Victim	Safe	Safe	Safe
FUE2	Victim	Safe	Safe	Victim
FUE3	Victim	Safe	Safe	Safe

Four different spectrum access schemes, Slotted Aloha, Opportunistic Aloha, Distance Sense Multiple Access (DSMA) and Opportunistic DSMA are proposed in [97]. In Slotted Aloha, each FAP can only access a random subset of the spectrum sub-channels with equal probability, if it gets a head in a coin toss thereby preventing co-tier interference. In opportunistic Aloha a predefined threshold is set and a FAP is only allocated a sub-channel if its channel gain exceeds threshold. In DSMA, each FAP creates a guard zone which is given a radius to protect itself from interference. It notifies interferers of its guard zone by generating and exchanging real numbers between (0, 1) with the smallest number identifying its location. Lastly, Opportunistic DSMA combines Opportunistic Aloha and DSMA, the FAP with the highest gain in the guard zone is given preference in this scheme. A cognitive hybrid division duplex (CHDD) suitable for heterogeneous networks is proposed in [98] where both frequency division duplex (FDD) and time division duplex (TDD) are simultaneously performed by cognitive femtocells underlaid in the macrocell. In this scheme, FDD is implemented at the macrocell tier to prevent cross tier interference whereas TDD is implemented at the femtocell tier to prevent co-tier interference.

2.2.1.4 Centralised/Decentralised Schemes

A group of CFs can form a CFN based on some criteria such as location to enhance the sensing capabilities and share channel conditions to effectively mitigate interference. Group sensing in CFNs greatly improves the capabilities of sensing and the power levels of each node can be maintained or reduced accordingly based on the shared information. A scheme built around this concept can be implemented in a centralised or decentralised approach to assign spectrum in a CFN [99]. However, coordination on information gathering and spectrum allocation besides specification of the roles of each sensing node is a major issue in these schemes.

A game theory approach presented in [100] makes use of correlated equilibrium policy [101] to mitigate co-tier interference among cognitive FAPs for the downlink OFDMA LTE networks. Correlated equilibrium is used in preference to the traditional Nash equilibrium policy as it is a decentralised and adaptive algorithm which allows the agents to directly coordinate their strategies achieving better performance. In this case, the decision to allocate spectrum is assisted by the global and local FAP utility functions. The global utility function is an analysis of the entire network and provides fairness by giving spectrum access priority to all FAPs and it is dependent on factors such as the demand levels of each FAP. On the other hand, the local FAP utility function is dependent on each FAP to make the relevant decision to maximise its estimate of the global utility function.

The Logit Equilibrium (LE) which is another decentralised scheme presented in [102] where FAPs experiment all the available options after a distributed learning algorithm to mitigate interference. The interference scheme which incorporates game and learning theory with a stochastic approximation relies on sensing of the SINR of MUEs acquired through communication with its serving MBS. FAP utilises the constant SINR information to dynamically configure the probability distribution of the spectrum which includes information

about the spectrum and transmit power. Interference is mitigated by guaranteeing a minimum time-average SINR for the MUEs in the network at the equilibrium.

An adaptive spectrum access scheme is proposed in [103] which involve a central FAP with a two-fold CR management. The two-fold management comprises the Cognitive Manager for Spectrum Management (CM-SM) which is tasked with providing the spectrum opportunities by sensing the radio environment and accessing all the necessary information such as geo-location databases, whereas Cognitive Manager for Resource Management (CM-RM) manages the allocation of spectrum to all FUEs. The combination of the two processes provides the information for active channels (used by MUEs), operating channels (used by the allocated FUEs) and the reserve channels which are the channels that are reserved for FUEs to relocate in case PU returns. In this scheme, the FUE also have CR capabilities which make it possible for them to report to the FAP for any interference. Upon receiving feedback from FUEs, the FAPs also request for interference measurements from neighbouring FAPs and subsequently tabulates two tables, A and B, based on all the statistics with table A containing a list of interference free resources and B containing resources that are restricted or shared. The level of allowable transmit power for resources in both tables varies with table A allowed a maximum transmit power and table B a dedicated transmit power. Accordingly based on this information, FAP allocates resources for FUEs to avoid interference.

A sensing and scheduling information based scheme to avoid cross tier interference, both UL /DL, for OFDMA femtocell and macrocell wireless networks is introduced in [104]. It encompasses a FAP which assigns RBs to its FUEs that are not in use by a MUE or in a spectrum reuse approach the RBs of far-away MUEs to avoid the interference of closely located MUEs. To accomplish this, a FAP obtains the scheduling information of MUEs from the MBS using two methods: the first method includes the backhaul connection and the second method involves the air interface. The second approach which makes use of air interface

implies the FAP connecting to the MBS as a MUE and retrieving the information. The FAP then senses the spectrum to find the occupied RBs of nearby MUE through methods such as energy detection and compares it with the received scheduling algorithm and assigns a RB to an FUE from the available opportunities (Figure 2.8).

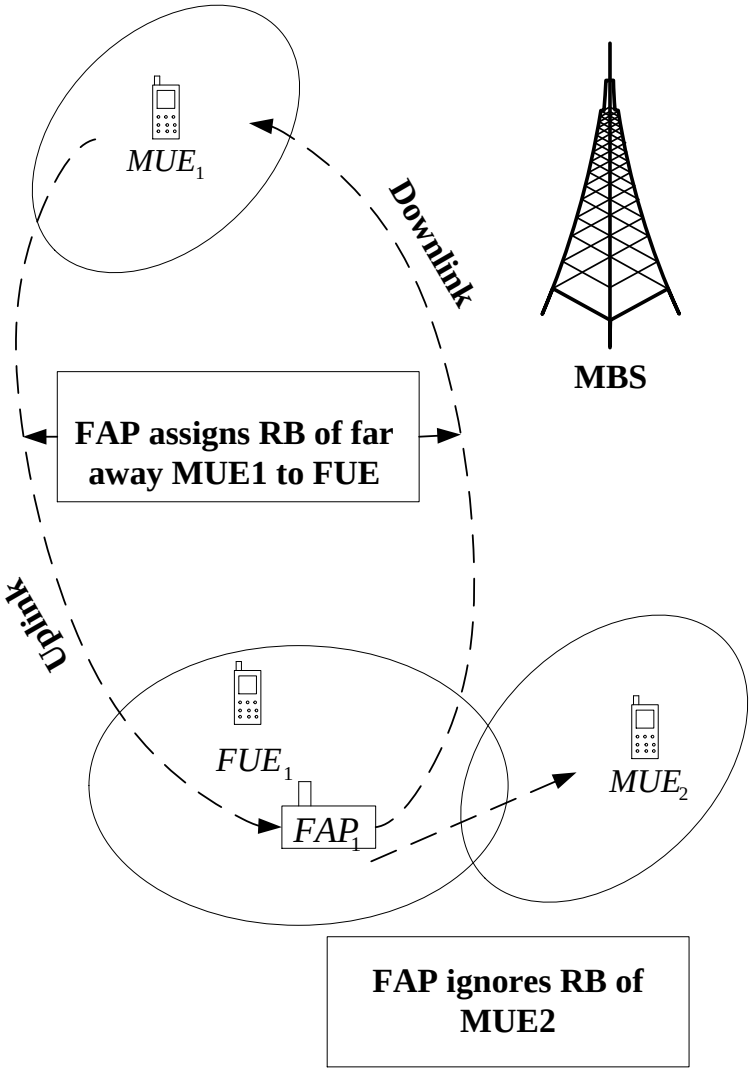

Figure 2.8: Spectrum Reuse- FAP assigns RBs of a far-away MUE to FUE.

2.2.1.5 Individual vs Group Channel Sensing

Some schemes prefer individual channel sensing compared to group channel sensing. A FAP retrieves the SINR and received power of each individual channel of the spectrum utilizing the UL communication of nearby MUEs. By sensing individual channels the femtocell is not only

able to calculate the level of interference but also the style of interference [105]. In such a scheme, each femtocell is classified into three categories of channels:

a) MUE occupied channels (*Mc*) – MUEs the source of interference to FAPs and FUEs
b) FAP interfered channels (*Fc*) – FAPs the source of interference to neighbouring FAPs and FUEs
c) Qualified Channels (*Qc*) – Channels that are free from both FAP and MUE Interference

Both co-tier and cross-tier interference can be mitigated by using mentioned channel classification. To mitigate cross tier interference, FUEs are allocated orthogonal resources with *Mc* while an algorithm which consists of a predefined threshold, γ, with SINR $\geq \gamma =$ *Qc* or SINR $< \gamma =$ *Fc* to distinguish *Qc* from *Fc* is implemented to mitigate co-tier interference. Individual spectrum sensing can decrease the probability of false detection but it introduces sensing overhead and the idea of group of FAPs sensing an individual channel concurrently may degrade the whole process of sensing. Co-operative sensing performed over the entire range of available channels help to improve probability of misdetection and solve hidden node problem. A hybrid channel sensing is proposed in [106] where cooperative sensing of the available channels is conducted by all the cognitive femtocells to mitigate cross and co-tier interference.

Most spectrum access schemes are based on the analogy of two-tier system, where the MUE is considered as PU and cognitive FAP and its FUEs are considered as SUs. Spectrum access in Cognitive enabled femtocells is not only restricted to licensed resources but spectrum in TV white spaces (TVWS) can also be utilised. Spectrum access schemes mostly employ channel sensing and since spectrum access approaches could also be either centralised or distributed, a distributed spectrum access approach which requires no or little coordination is more feasible

due to the fact that FAPs are usually randomly and densely deployed. Since there is more MUEs activity in the downlink, spectrum access schemes which involve spectrum sensing in the downlink are more promising compared to the uplink schemes. An ideal cognitive spectrum access scheme is the one which overlays, underlays, or interweaves its signal into the licensed spectrum undetected without causing any harm to PU or satisfying all the PU constraints.

2.2.3 Cognitive Interference Mitigation – Antenna Schemes

The CR-enabled antenna schemes are sub-divided in single vs multi-element antenna schemes and adaptive beam-forming vs adaptive pattern switching schemes as described below.

2.2.3.1 Single-element vs Multi-element

A low cost multi-element antenna and UE assisted cognition has been employed in [107] to optimise coverage and to mitigate interference. In this scheme, FUEs are employed to sense and retrieve pilot power signals from the MBS and report to their serving FAP at places described as ‘crucial places’ (CP), where power leaks are prone to occur such as windows and doors. This involves a subscriber walking around CPs and sending signals to its FAP by pressing a specific button on their device which has guided operator software. The sensed information is processed using the conventional Direction of Arrival (DoA) estimation algorithm on a 6-element antenna which adjusts the antenna gains; this method thus optimizes the coverage area of the FAP thereby mitigating interference. However, the problem with this scheme is that it would require special and compatible software installed on each handset. Also, FAPs are required to accommodate multi-antenna elements for all antenna patterns and this is difficult as FAPs are size constrained.

To tackle the problem of a multi-antenna system, cognitive FAPs equipped with omni-directional antennas form a network known as Smart Cognitive-Femto Network (SCFN) [108].

In this scheme, the cooperation of a group of cognitive FAPs who operate like a BS with multiple antennas dispersed in a large network is exploited. Although each of the cognitive FAPs is equipped with omni-directional antennas, the SCFN acts like a multi-antenna network system. Each FAP can sense the environment to mitigate interference by directing the main beam only towards a desired FUE and creating a null towards others that may be causing interference (Figure 2.9).

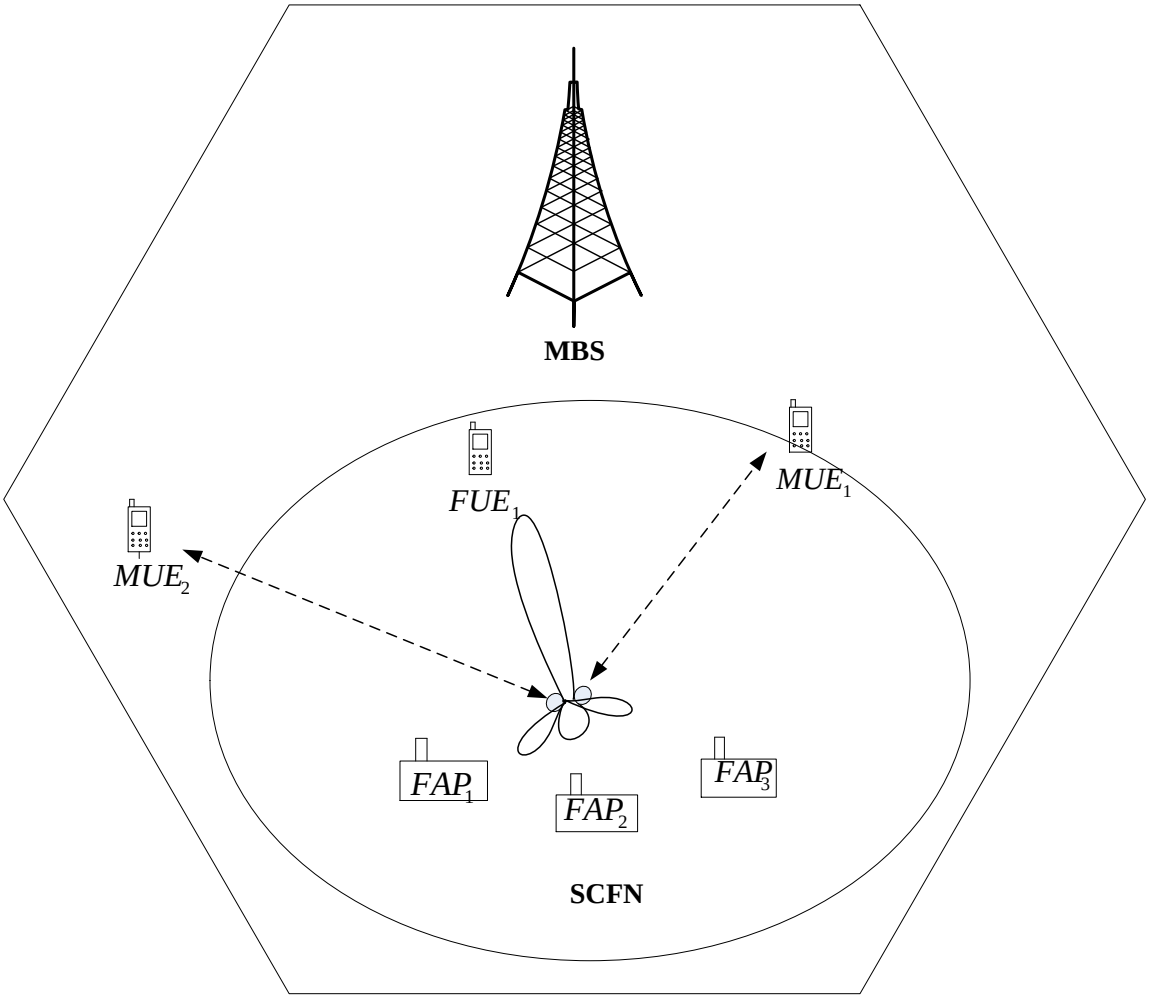

Figure 2.9: SCFN: Interference mitigation with main beam direction.

2.2.3.2 Adaptive beam-forming vs Adaptive pattern-switching

Two antenna schemes, an adaptive pattern switching and adaptive beam-forming antennas, are designed and independently employed in [109] for cognitive LTE femtocells to exploit the available white spaces in TV White Space (TVWS). In the adaptive pattern switching, 4 patch antennas in a single FAP is proposed with each element at an angle of 0º, 90º, 180º and 270º respectively. The FAP measures the Received Signal Strength Indication (RSSI) and the uplink Sounding Reference Signal (SRS) which is a parameter to analyse the quality of the uplink channel in what is known as the training process. One or more of the elements in the antenna can be switched ON or OFF based on this information to a specific target to mitigate interference. The adaptive beam-forming antenna scheme is similar to the adaptive pattern switching with an antenna array consisting of four elements in each FAP, whereas the difference lies in the fact that it is able to perform the Eigen-based beam-forming introduced in [106].

2.2.4 Cognitive Interference Mitigation – Joint Schemes

Joint or hybrid schemes introduce the combination of two more schemes with the aim of complementing and improving the overall performance of a single scheme. Some hybrid schemes are presented in this section.

A Joint power control and cognitive spectrum access is proposed in [39] to mitigate the downlink cross tier interference. The scheme comprises of FAPs with cognitive capabilities (CFBS) in cognitive femtocell network architecture. However, in this scheme, cognition is not restricted only to the CFBS, but with the femtocell and macrocell Ues having cognitive abilities too, accordingly known as cognitive femtocell users (CFUs) and cognitive macrocell users (CoMUs) respectively. The common macrocell users (CMUs) are defined to represent macrocell users with no cognitive capabilities. The CFBS which are randomly deployed in the

MBS periodically senses the radio environment within its defined range known as cognition range (although it may increase its transmission power to exceed this range) to gather statistics such as SINR, unoccupied spectrum bands and mobility information from all the cognitive users in the environment.

To mitigate downlink interference in the network, based on the received statistics, the CFBS controls its power or enhances its coverage area for nearby CoMUs and CMUs. In this case it lowers its transmission power to avoid its interference to a closely located CMU, whereas for the CoMUs it may apply either of the two. For instance, it will increase its cognition area to provide coverage for CoMUs whose SINR fall below a defined threshold or reduce its power to avoid interference on a CoMU with a high SINR from its serving MBS.

A novel spectrum allocation scheme to mitigate interference in LTE femtocell networks is proposed in [110] which involves the sensing of available unlicensed TVWS. In this scheme, all MUEs in the network sense the transmission power of nearby femtocells and compare it with a predefined threshold and tabulate 2 lists:

a. Interfering Femtocell List – FAPs with transmission power above threshold
b. Non-Interfering Femtocell List – FAPs with transmission power below threshold

The interfering femtocell list is sent back to the MBS and based on this feedback it allocates RBs and TVWS to MUEs and FAPs respectively in the non-interfering and interfering femtocell lists respectively.

Another similar scheme called Fractional Frequency Donation (FFD) mitigates cross-tier interference in co-channel deployment by utilising TVWS and cellular bands [111]. In this scheme, each FAP with a good throughput is required to donate bands to poor ones and this is achieved by the FAP first finding suitable donors and subsequently bands to donate. To find a

suitable donor a FAP measures a FUE's noise power plus interference power and estimates its average channel gain. After spectrum sensing, a band is regarded as a polluted or polluting if the donor FAP receives strong interference from, or if it causes strong interference to other frequency bands respectively. As a result, FAP donors perform what is known as Selfish Frequency Access (SFA) without utilising the polluted or polluting bands. Poor FAPs mitigate cross tier interference by allocating more power on the donor bands and less on the un-donated bands.

A power control algorithm which merges the concept of DSA with Fractional Power Control (FPC) is described in [112]. FPC is used to define the SNR targets of both cell centre and edge users based on a Game-based Resource Allocation in Cognitive Environments (GRACE). GRACE is a fully distributed algorithm which evaluates a marginal utility function that trades off capacity and outgoing interference between CFs and neighbouring CFs and macrocells respectively. Importantly, cell centre and cell edge are terms used to describe the proximity of a UE to its serving BS. Cell centre users experience a better SNR as they are well within the coverage range of the BS whereas cell edge users are prone to poor SNR due to their increased distance from the serving BS. FPC allows the transmission of high data rate of both cell centre and edge users by allocating power to each channel defining the transmission power and path loss, L, in dB. The path loss in UL is specific for user equipments (Ues) but FPC capitalises on the advantages of keeping a constant power spectral density in DL which includes an efficient spectrum sensing by other CFs. It achieves this by setting the DL path loss, L, to its highest among all the Ues served by the FAP which subsequently provides enough transmit power even to the weakest link.

In GRACE, which performs a cognitive cycle of sensing, analysis, decision and action, a CF makes decisions to update its channel allocation so as to coordinate the inter-cell interference

without a need for inter-cell communication. Figure 2.10 illustrates functioning of FPC scheme with cell centre user FUE_1 and cell edge users FUE_2 and FUE_3 respectively.

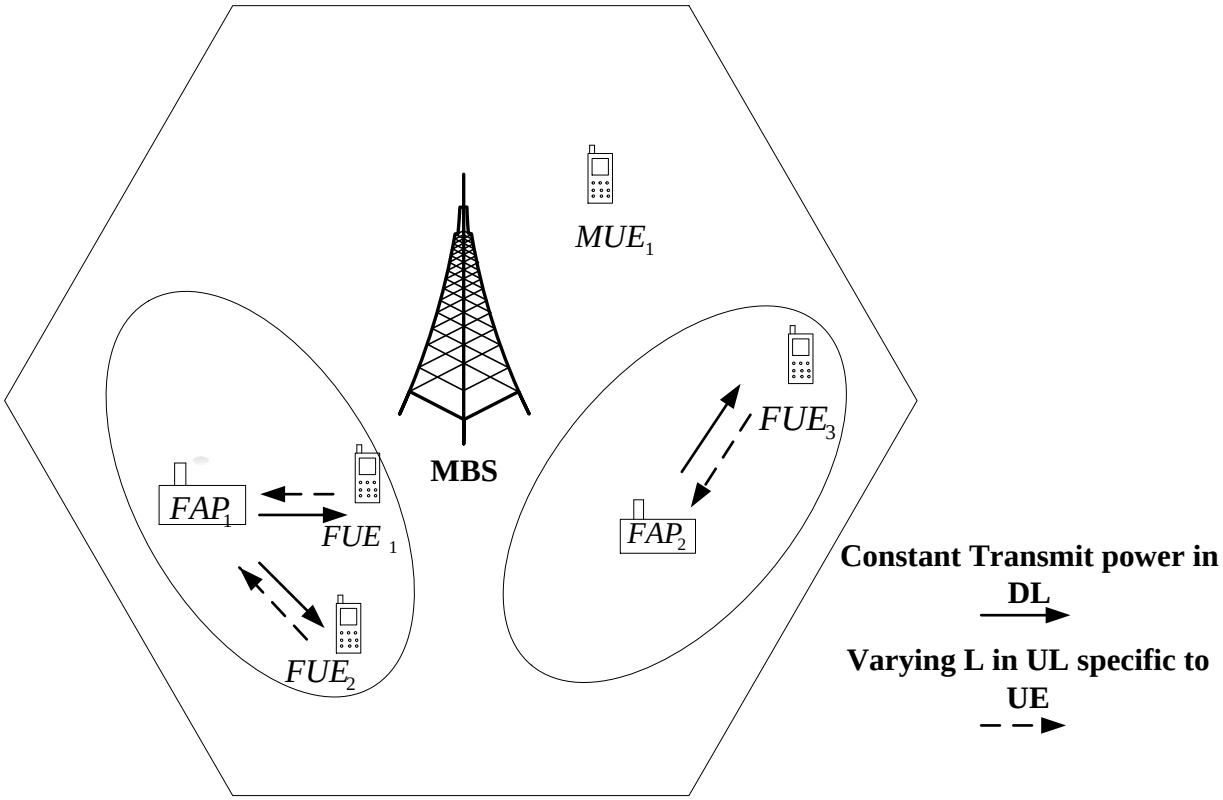

Figure 2.10: Interference mitigation through FPC

A cognitive spectrum reuse and power allocation scheme for 3G femtocells is introduced in [113**]** where a FAP recognizes the interference signature from its environment and avoids interference in the network by cognitively allocating spectrum to its UE with emphasis on reusing the spectrum in a proper way. In this scheme, FAP periodically senses the network environment to retrieve the interference signatures of its neighbours. Upon acquiring the interference signatures, an opportunistic channel scheduler is invoked which allocates the best spectrum for reuse, where the best spectrum in this context is the spectrum which causes the lowest interference. The FAP then allocates power to FUE to reuse the spectrum only if the spectrum is found to satisfy Quality of Service (QoS), otherwise a handoff is triggered to

allocate another spectrum. The same scheme is further studied in [114] and proposed with some improvements to mitigate uplink interference in 4G cellular femtocells.

A channel assignment and power allocation scheme is proposed in [115] for cognitive LTE-femtocell network to minimize downlink co-tier and cross-tier interference. Cognitive femtocells utilise available licensed spectrum of the macrocell network as well as TV broadcast systems and avoid co-tier interference based on some safety distance achieved through clustering. Neighbouring femtocells are grouped into Physical Clusters (PCs) based on their physical location and the number of available finite channel so that each femtocell in the cluster uses a different channel to avoid interfering with each other. Femtocells in different PCs but sharing same channel are grouped in Virtual Clusters (VCs). A spatial correlation however is defined to avoid the interference that may occur between two PCs which are closely located. A downlink subcarrier and power allocation scheme is implemented to reduce the imminent aggregate interference due on the subcarriers. In line with the scheme presented in [90], an uplink subcarrier and power allocation scheme which uses disruptive solutions against optimal solutions is implemented for OFDMA femtocells in [116] to help mitigate interference.

2.3 Cognitive interference mitigation vs conventional interference mitigation

The effect of CR on conventional interference mitigation schemes cannot be overemphasized as it offers the advantages of CR with regards to spectrum management in a coordinated and interference void manner. The cognitive femtocells have the capability to operate as normal femtocell as well but can also use opportunistic spectrum access when a user requires higher QoS for certain services. As mentioned earlier, one of the ways to mitigate interference in a two-tier network will be in a dedicated manner where each UE is assigned a dedicated spectrum but that introduces a trade-off between interference and available spectrum, thus co-

channel is preferred at the detriment of interference. However, CR enabled femtocells in a two-tier network are able to opportunistically allocate both licensed and unlicensed spectrum bands to UEs unlike the conventional schemes which are restricted to licensed band only. The random user deployment of FAPs is also a major problem as coordination between FAPs and MBSs is required to mitigate interference. Conventional or traditional schemes in most cases employ a direct coordination between FAPs and MBS through the backhaul which introduces overhead and delay.

The self-optimization capabilities of cognitive enabled FAPs and FUEs allow the radio environment to be sensed in a distributed manner to retrieve operating parameters in order to mitigate interference. The operating parameters retrieved are specific to the radio technology but offers a wide range of options to include transmit power, channel statistics (channel gain and path loss), available spectrum (white spaces), SINR, RSSI, SRS, noise, etc. By continuous sensing of the parameters, current as well as future intentions of interfering sources can be deduced, and in our opinion thus CR brings improved interference mitigation over the conventional schemes as illustrated in Figure 2.11. Highlights of the pros and cons of cognitive interference mitigation schemes are listed in Table 2.2.

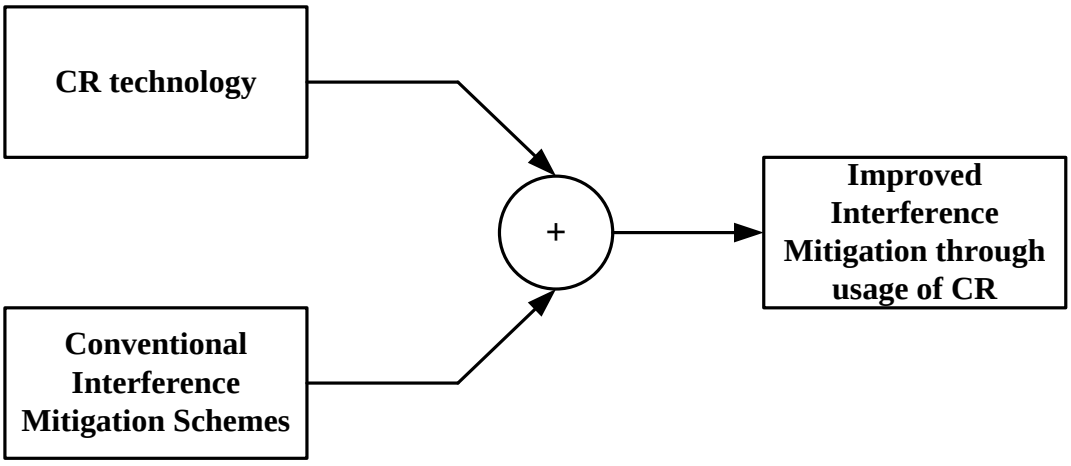

Figure 2.11: CR enabled interference mitigation

Table 2.2: Pros and Cons of Cognitive Interference mitigation schemes

Scheme	***Pros***	***Cons***
Power Control	• Power can be optimised in an adaptive manner to mitigate interference • Flexible power control reduces the need for handover in open access as it restricts its coverage area	• UE assisted power optimisation schemes introduce signalling overhead which results in battery drain • Power control schemes based on the pilot power of a FAP which determines its coverage area becomes less significant if a FUE is located close to a neighbouring FAP
Spectrum Access	• Distributed access to spectrum with more spectrum opportunities for femtocells • Access to licensed systems not restricted to MBS but also TVWS • Universal frequency reuse can be achieved in co-channel deployment	• Spectrum inefficiently utilised in dedicated channel deployment. • Added security concern introduced in open/hybrid access modes • MUE is given more priority over FUE even when FUE incurs more voice and data traffic
Antenna	• FAP targets a specific FUE while creating a null towards other users • Complex beam-forming schemes can be replaced with antenna switching systems which reduce signalling overhead	• Multi antenna elements may be required to accommodate antenna patterns in a FAP which is size constrained • Diversified-antenna elements incur costs which will increase the unit price of a FAP
Joint/Hybrid	• Combines the advantages of two or more schemes	• Introduces complexity and signalling overhead

2.4 Cost of using CR in Femtocells

Most of the cognitive interference mitigation schemes are aligned towards spectrum access compared to other schemes. One of the compelling factors for higher percentage of spectrum access schemes compared to other schemes might be the fact that unlike other schemes, such as antenna schemes which require provision of customised hardware and software etc., most spectrum access schemes do not have any such requirements and can be implemented by incorporation of intelligence and cognition in femtocells. Cognition can range from spectrum sensing, spectrum decision to spectrum mobility and importantly it may include extra overhead in terms of increased computations and communications. Joint or hybrid schemes introduce the combination of two or more schemes with the aim of complementing and improving the overall performance of a single scheme but still they suffer from increased coordination and signalling overhead. Further insight about these tradeoffs and cost of using CR in femtocells is presented in Table 2.3.

Table 2.3: Tradeoffs / Cost of using CR in femtocells

Tradeoffs/ Cost	***Description of Tradeoffs/ Cost***
Incorporation of Cognition in FAPs/FUEs	CR enabled interference mitigation schemes require some sort of cognition in FAPs/FUEs. Cognition can range from spectrum sensing, spectrum decision, spectrum mobility to intelligent learning techniques etc.
Increased Communicational and Computational Overhead	Cognition can incur increased communicational and computational overhead for FAPs/FUEs. FUEs may suffer from augmented losses such as delay and energy consumption.
Roles Specification for Cognitive enabled femtocells	Cognitive radio enabled nodes necessitate role specification such as to perform spectrum sensing, spectrum sharing, spectrum decision making etc. This obliges to have either a centralised or distributed coordination.
Feedback/Information gathering	Cognitive enabled femtocells stay in need of coordination on information gathering, exchange and maintenance of channel lists and subsequent spectrum allocation through sophisticated communication mechanisms and feedback.
Intelligent Scheduling	Cognitive FAPs need to adopt intelligent mechanisms to retrieve scheduling information of MUEs from the MBS, either using backhaul connection or air interface.
Signalling overhead	Information gathering and subsequent exchange require dedicated or some other signalling channels leading to signalling overhead. This overhead can further point to increased delays, energy consumption and loss of bandwidth etc.
Device Customisation/Operator Software	Some CR enabled interference mitigation schemes necessitate femtocells to employ customisation with the provision of guided operator software and hardware such as multi antenna elements etc. This will result in increased unit cost.
Lack of Security	Irrespective of the chosen deployment scenario, there will be some tradeoffs of security in retrieval and sensing processes. In OSG for example, Denial of Service (DoS) when unsubscribed users connect to the link between the FAP and core network causing an overload on the capacity of the network thereby preventing the subscribed user access to their FAP or the cognitive FAP sensing accurately.
Timing	PUs can claim their frequency bands anytime while a cognitive FAP is operating on their bands. Hence, sensing methods should be able to identify the presence of PUs within certain duration. This requirement creates a limit on the performance of sensing algorithms and poses a challenge for cognitive FAPs. The sensing of parameters introduces a trade-off between sensing time and reliability. Sensing frequency is a design parameter that needs to be chosen carefully.

In the next chapter, an overview of LTE as a candidate for cellular RAT is presented to aid deployment of femtocells. The effect of femtocell interference in the two-tier architecture with a macrocell is also laid bare in form of network performance analysis.

Chapter 3

Fundamentals of LTE femtocells

In this chapter an overview of LTE is presented as a candidate for cellular radio access technology (RAT) to aid deployment of femtocells by the 3GPP standards body. In order to enable femtocells operate within a variety of networks, a standard femtocell network architecture is required. This architecture enables a variety of femtocells from different manufacturers to work in the networks of different operators. This introduction will cover the physical-layer details of LTE which will comprise, time slot structures and available data rates. This chapter will also provide the foundation for femtocell interference analysis with novel algorithms as solutions in mitigating interference in cognitive based LTE femtocells presented in the proceeding chapters.

3.1 Fundamentals of LTE femtocells

An evolutionary step in the 3GPP roadmap for future wireless cellular systems was introduced in 3GPP Release 8 in December 2008 with minor improvements in Release 9 and Release 10 [117].

This release is commonly known as the Long Term Evolution (LTE) and it introduces enhancements to previous specifications to achieve higher throughput spectral bandwidth and more flexible spectrum management. The design of the LTE is heavily influenced by the need for high peak transmission rate (100 Mbps for DL and 50 Mbps for UL), efficiency and multiple channel bandwidths. To achieve these requirements, the PHY layer was modelled using orthogonal frequency division multiplexing (OFDM). LTE also implements multiple-antenna techniques such as multiple input multiple output (MIMO) in addition to OFDM which can either enhance signal robustness or increase channel capacity. Both OFDM and MIMO are two key attributes in LTE and contribute to the major difference over 3G systems which are code division multiple access (CDMA) based. The advantages to using OFDM in a cellular system with femtocells comprises but not limited to the following:

- Flexible use of frequency spectrum.
- Increase in robustness to multipath and limits inter-symbol interference due to its long symbol time and guard interval
- Optimization of data rates for all users in a cell by transmitting on the best (i.e. non-faded) subcarriers for each user.
- Increase in spectral efficiency due to orthogonality between sub-carriers.

. The LTE specifications introduce a wide range of support for femtocells.

Table 3.1: 3GPP standard release functionality roadmap

Release 99	Release 4	Release 5	Release 6	Release 7	Release8
WCDMA	LCR TDD	HSDPA	HSDPA	Higher-order modulation • 64-QAM HSDPA • 16-QAM HSUPA	**Home NodeB (FAP)**
R99 radio bearers	Repeaters	WB-AMR	WB-AMR	HSDPA MIMO	**LTE**
ATM transport layer	Multimedia Messaging Service (MMS)	IP transport layer	Advanced receivers	Interference cancellation (Type 3i)	SAE
	ROHC	MMS enhancement	Voice over IMS	Enhanced FACH	64-QAM + MIMO
	ATM transport layer			Dynamically reconfigurable receiver	Dual-cell HSDPA

The data rates achieved by LTE are higher than those provided by most network interfaces, which increases the advantages of femtocells based on this release. Table 3.1 presents the roadmap up to Release 8 which features LTE and femtocells. In the following sections, an overview of the main transmission schemes of the LTE radio interface is provided.

3.1.1 LTE architecture Overview

The radio frame of LTE is defined as having a length of 10 ms as illustrated in Figure 3.1. It is divided equally into 10 sub-frames of duration $T_{FS} = 1\ ms$ per sub-frame. Each sub-frame is further divided into $N_{FS} = 2$ slots of length $T_S = \frac{T_{FS}}{2} = 0.5\ ms$. Each sub-frame contains $N_{sym} = 6$ or $N_{sym} = 7$ OFDM symbols on the length of the selected cyclic prefix. An extended cyclic prefix of 16.7 μs is allowed in LTE which might be suitable in accommodating delay.

However, in femtcoells a normal length cyclic prefix (T_{CP} = 5.2 μs) might be enough due to its limited coverage area and short delay periods as compared with a MBS. More information about the frame structures can be found in [118].

3.1.2 LTE downlink transmission

In LTE, the radio transmission in the downlink is Orthogonal Frequency Division Multiplexing Access (OFDMA) and it is defined by a sub-carrier spacing of $\Delta f = 7.5$ kHz and $\Delta f = 15$ kHz for multicast and all other cases respectively. An RB in OFDMA is equivalent to $N_{sc} = 12$ adjacent SC. Therefore, the total number of SCs contained in 1 RB during a single time slot is $N_{sc}^{rb} = N_{sc} \times N_{sym} = 12.7 = 84$. LTE allows between 6 and 110 RBs based on the frequency which is between 1-20 MHz. In LTE, reference symbols (which are transmitted between the first and fifth OFDM symbols) are responsible for the modulation of certain sub-carriers in the OFDM grid. Also, the reference symbols are used for cell identification as well for channel sounding. LTE supports QPSK (Quadrature Phase Shift Keying), 16QAM and 64QAM (Quadrature Amplitude Modulation) as modulation schemes. Therefore, the minimum usable data rate of a resource block with normal cyclic prefix occurs for the case of QPSK ($N_{bit} = 2$ bits per symbol). Furthermore, LTE supports MIMO schemes which can accommodate up to four transmitting antennas [119].

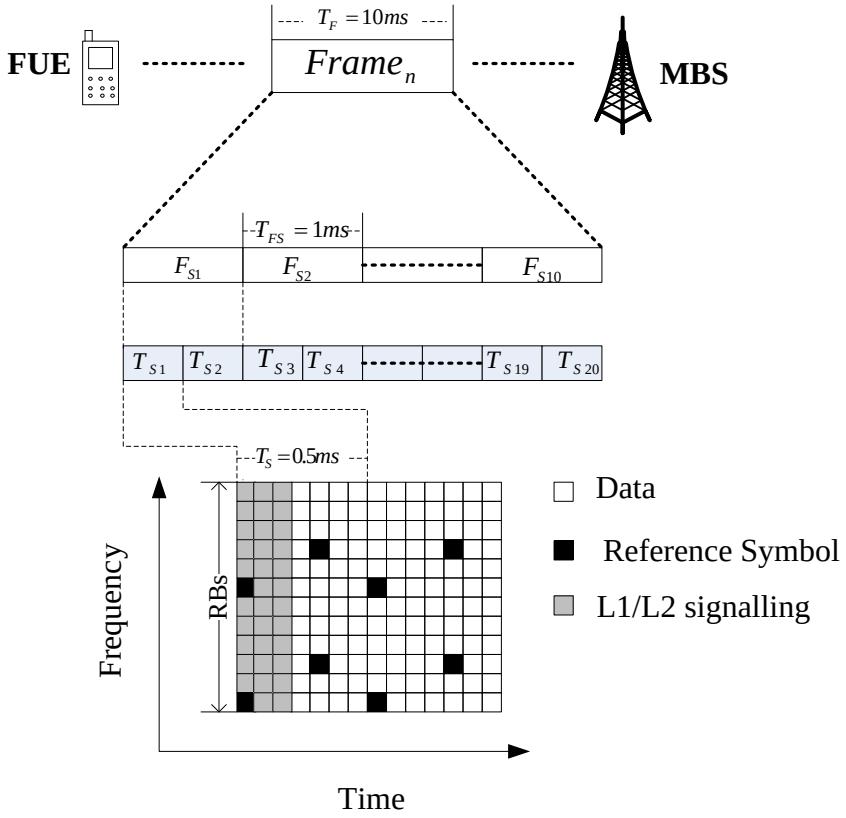

Figure 3.1. Downlink resource block and sub-frame structure in downlink LTE

3.1.3 LTE uplink transmission

In LTE, the radio transmission technology in the UL is known as Single Carrier FDMA (SC-FDMA). SC-FDMA is a modified version of OFDM with similar complexity and throughput performance. Thus, SC-FDMA inherits all the advantages of OFDM over well-known techniques such as Code Division Multiple Access (CDMA) and Time Division Multiple Access (TDMA). The main advantage of SC-FDMA is its robustness against multipath signal propagation, which makes it suitable for broadband systems. SC-FDMA brings additional benefit of low peak-to-average power ratio (PAPR) compared to OFDM making it suitable for uplink transmission by UEs.

Reference signals differ in the UL but are also important as it allows the implementation of co-herent demodulation in FAPs. Also, it provides useful insight into channel conditions.

Reference signals are also transmitted in LTE for the purpose of channel sounding which facilitates scheduling in the UL based on accurate channel knowledge. In LTE, for each OFDM symbol, different RBs can be allocated to UEs. Most of the PHY layer functionality in UL which includes but not restricted to channel coding, Hybrid Automatic Repeat Request (HARQ), Cyclic Redundancy Check (CRC) insertion, inter leaving, scrambling and data modulation is similar to DL.

3.2 Interference modelling in LTE femtocells

This section provides interference modelling of LTE femtocells adopted from [13] which will also be used in the proceeding chapters except stated otherwise.

3.2.1 Interference in the downlink

In downlink, where the users suffer from interference, it can be said that a certain user *UEx*, whose connected server (best server) is C_i, suffers from the interference of cell C_j, based on the following condition; If C_i and C_j are using the same sub-channel for DL transmission at the same OFDM symbol. It is important to note that UE_x could be a FUE or MUE and C_i could be a FAP or MBS. Therefore the total interference suffered in DL by UE_x at slot $slot_{i,k,t}$ is the summation of the interferences coming from all neighbouring cells C_j.

$$I_{x,k,t}^{DL} = \sum_{j=0,j\neq i}^{N-1} \sum_{t=0}^{T-1} \left(P_{j,k} \cdot G_j \cdot L_j \cdot L_{pj,x} \cdot G_x \cdot L_x \right) \quad (3.1)$$

where,

x is the interfered UE, UE_x; k is the kth sub channel and t is the tth symbol; i is the best server, $C_{i,j}$ is an interfering cell, C_j; $P_{j,k}$ is the transmit power of cell C_j in a SC of the kth sub-channel; $Lp_{j,x}$ is the channel gain or path loss (PL) between C_j and UE_x; G_j and G_{xs} are the

antenna gains in Cj and UE_x. Also, L_j and L_x stands for the equipment losses in cells, C_j and UE_x.

3.2.2 Interference in the uplink

On the other hand, in UL, interference is suffered by the cells (MBS or FAPs in our scenario). The conditions are that if a certain cell C_i, serving user is UE_x, suffers from the interference of another UE UE_y, if UE_x and UE_y are using the same sub channel for UL transmission at same OFDM symbol. Therefore the total interference suffered in UL by cell C_i at slot $slot_{i,k,t}$ will be the summation of all the interferences emanating from all neighbouring UEs, UE_y.

$$I_{i,k,t}^{UL} = \sum_{y=1,y\neq x}^{M-1} \sum_{t=0}^{T-1} \left(P_{y,k} \cdot G_y \cdot L_y \cdot L_{py,i} \cdot G_i \cdot L_i \right) \quad (3.2)$$

where, i indicates cell suffering from interference, C_i; k is the kth sub channel and t is the tth symbol; x is the user being served, UE_x; y is the user causing interference, UE_y; $P_{y,k}$ is the applied transmit power of UE_x in a sub-carrier of the kth sub channel; $Lp_{y,i}$ is the PL between user UE_y and cell C_i; G_y and G_i stands for the antenna gains for UE_y and C_i, respectively while L_y and L_i stands for the equipment losses in UE_y and C_i. Shadowing effects and multi-path fading should be taken into account computing L_p. L_p can be deduced as:

$$L_p = L_{att} \cdot L_s \cdot L_{ff} \quad (3.3)$$

Where L_{att} is the attenuation, L_s is the shadow fading and L_{ff} is multi-path fading. Therefore the SINR of each slot, $slot_{i,k,t}$ can be expressed as follows:

$$SINR = \frac{C}{I+\sigma} \quad (3.4)$$

where, C is the received power of the carrier and I the interfering signals. σ denotes the background noise. The received signal power C can be expressed as:

$$C_{x,k}^{DL} = P_{i,k} \cdot G_i \cdot L_i \cdot L_{pi,x} \cdot G_x \cdot L_x \quad (3.5)$$

$$C_{i,k}^{uL} = P_{x,k} \cdot G_x \cdot L_x \cdot L_{px,i} \cdot G_i \cdot L_i \quad (3.6)$$

The background noise, σ, on the other hand, can be deduced by:

$$\sigma_n = n_o + nf_{eq} \quad (3.7)$$

$$n_o = -174 \frac{dBm}{Hz} \cdot 10\log\left(F_{sam} \cdot \frac{SC_{used}}{SC_{total}}\right) \quad (3.8)$$

where, n_o is noise, and nf_{eq} for the noise figure of the UE. Also, F_{sam} represents the sampling frequency, while SC_{used} and SC_{total} are the number of used and total sub-carriers respectively. Once the SINR of all slots allocated to a user are known, the effective SINR of the user is computed using the Mutual Information based Exponential SNR Mapping (MIESM) average [120]-[122].

3.3 LTE femtocell interference analysis

In this section, a brief analysis of the advantages and disadvantages of femtocells in a two-tier interference scenario is provided. Consider an OFDMA system as described in section 3.1.2 where the femtocell and macrocell are deployed in a co-channel fashion. A tri-sector MBS is in the centre of the network and serves the randomly distributed MUEs within its coverage area. Since there is more activity of MUEs in the downlink (DL) and less activity in the UL, the analysis is conducted on downlink interference in the system model (see section 3.2.1). FUEs are randomly located within the coverage area of the MBS and the number of MUEs

within the coverage area of the femtocells. The simulation parameters are based on 3GPP LTE specifications [123]. 4 FUEs are attached to each FAP. The Performance Key Indicator (PKI) used in the following analysis is SINR as presented in Equation 3.4.

3.3.1 Importance of femtocells in a network

In this analysis, the importance of using femtocells on the system network is laid bare as shown in Figure 3.2 and as discussed in Section 1.2. This plot is a simulation of indoor users when they are served by the MBS (i.e MUEs) and when the same indoor users are served by a FAP (i.e when the MUEs become FUEs). The results show a significant increase in SINR values with the average value of 22dB for UEs. The indoor MUEs with an average SINR value of 11dB could even suffer more depending on the conditions of the environment.

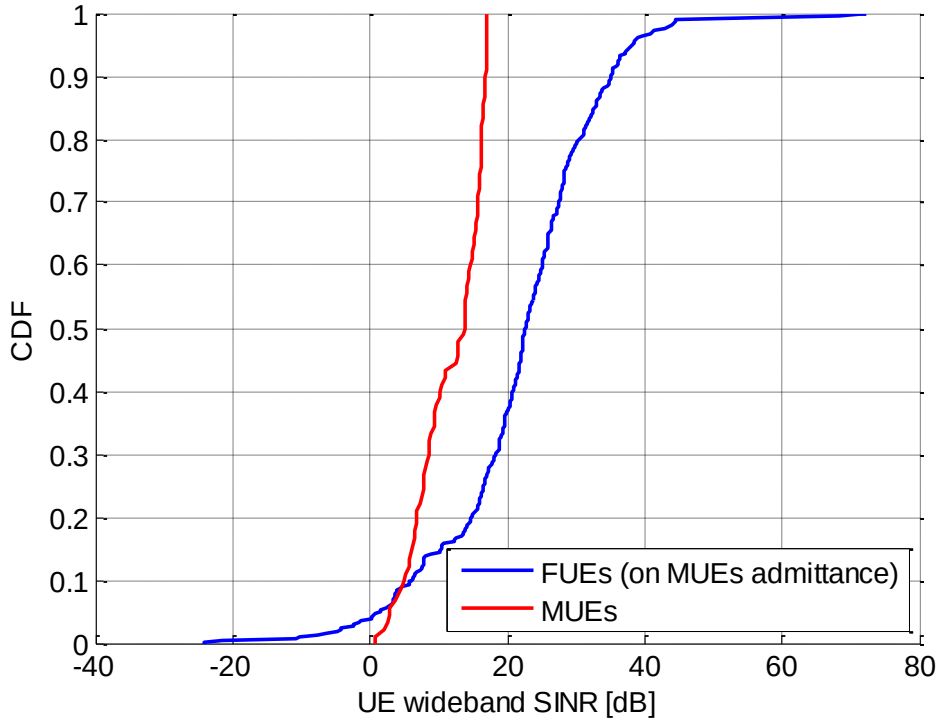

Figure 3.2. Femtocell as a solution for indoor MUEs

3.3.2 Effect of femtocell deployment

In Section 1.2.2, the possible access modes of femtocells were discussed to be either OSG or CSG. In Figure 3.3, the network simulation shows the effects of the OSG and CSG deployment on MUEs. In CSG, the MUEs suffer a degradation of around 8dB (SINR) as compared to when OSG access in incorprated. This is due to the fact that OSG allows admittance of MUEs (to become FUEs) contrary to CSG which inhibits admittance.

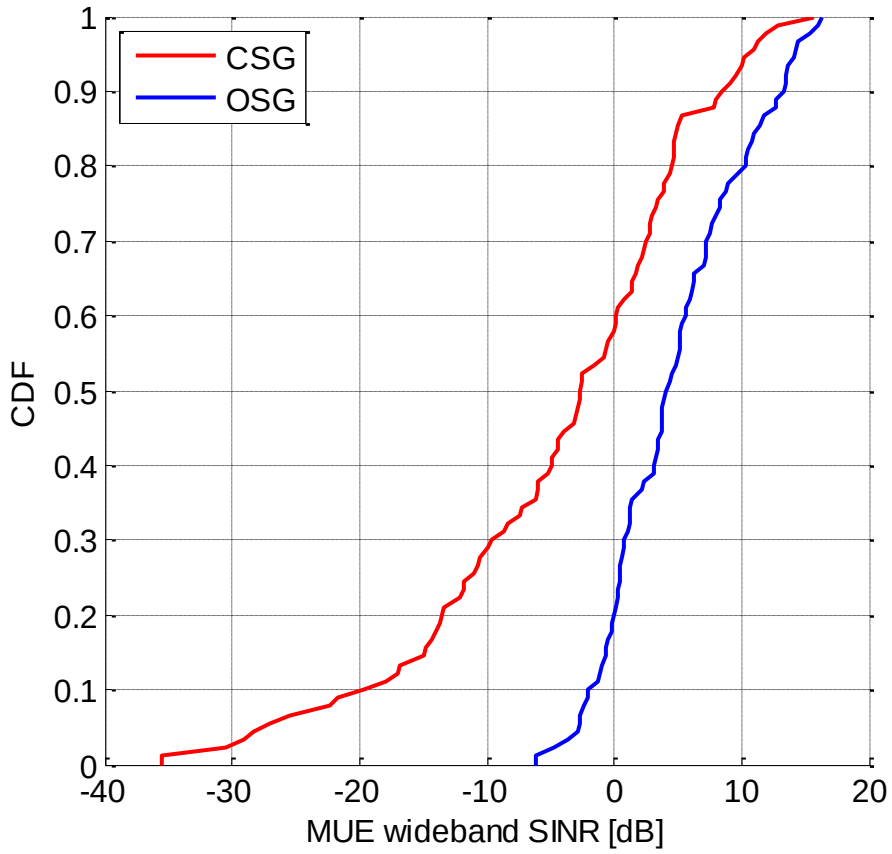

Figure 3.3: Effect of Femtocell access mode on MUEs

3.3.3 Cross-tier Interference analysis

The effect of femtocells on MUEs is presented in the cross-tier interference analysis plot in Figure 3.4. The plot reflects a scenario where MUEs suffer a degradation of around 11dB (SINR) in the presence of close by femtocells (with femtocells) as compared to its absence (without femtocell) and served by the MBS. The femtocells operate in a CSG mode and as a result of no admittance, the MUEs have to contend with the inherent interference as reflected.

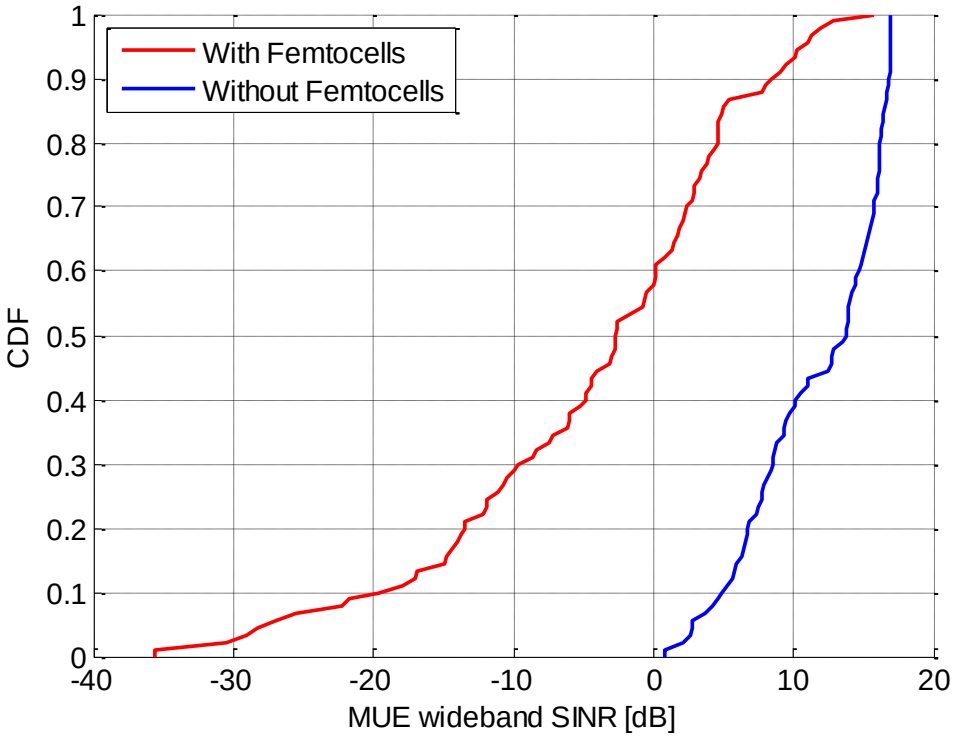

Figure 3.4: Cross-tier interference on MUEs

3.3.4 Co-tier Interference analysis

When the network coverage of femtocells is overlaid on each other, it is known as a collocated scenario as discussed in Section 1.2.1 (see Figure 1.2). Figure 3.4 is a plot of two femtocell scenarios to include a standalone femtocell (STA femtocells) and two collocated

femtocells (COL femtocells). Four FUEs are attached to each FAP and the SINR values show that FUEs in standalone femtocells can reach average values of 29dB whereas in a collocated scenario, FUEs can suffer an average SINR loss of 17dB.

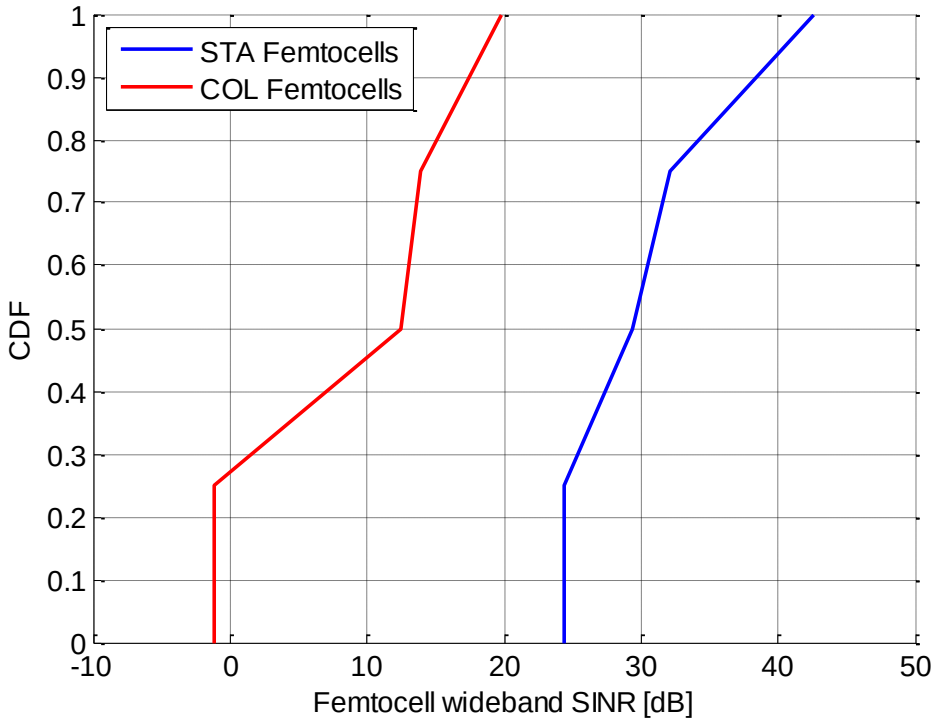

Figure 3.5: Co-tier interference in femtocells

3.3.5 Effect of varying FAP transmit power levels on UEs

It is fair to say that an adaptive power control level for FAPs presents a more viable solution to interference management than a fixed power control scheme as discussed in Section 2.1.2. In Figure 3.6, a plot of 3 power control levels (0dBm, 10dBm, 20dBm) of a FAP is presented illustrating its effect on a MUE in a CSG femtocell. At 20dBm and 10dBm, MUEs attain average values of -2dB and 3dB respectively. However, an improved average SINR of 5dB is experienced by MUEs when a FAP transmit power is 0dbm. In the next chapter, the research

is focussed on an adaptive transmit power control for femtocells in order to reduce power control levels to minimize interference on close by UEs.

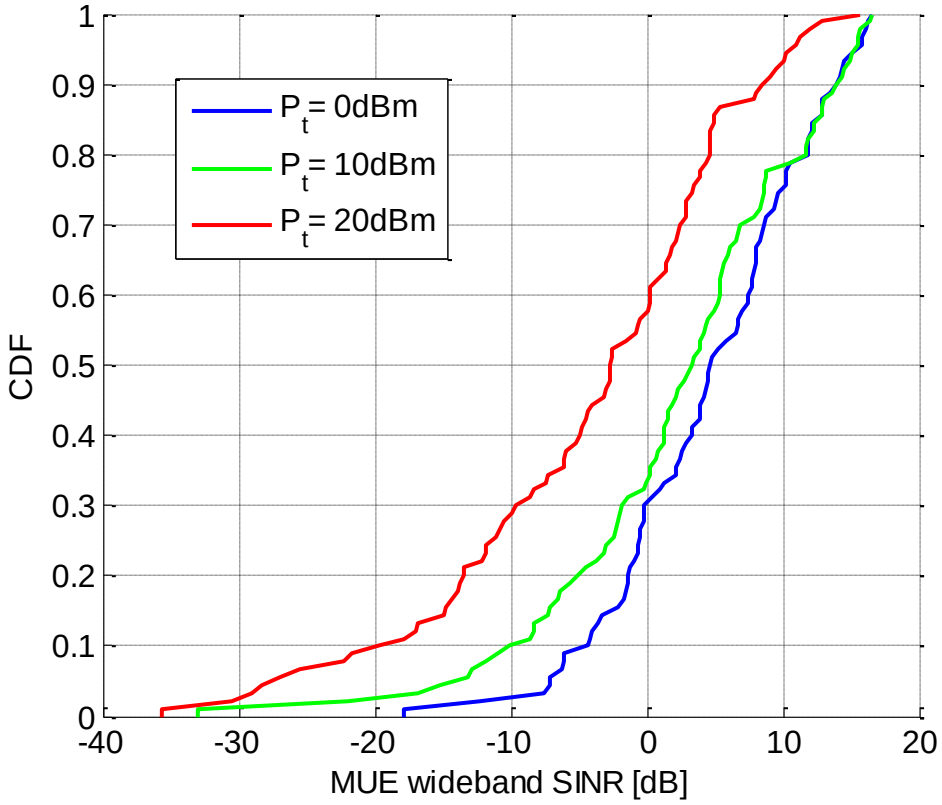

Figure 3.6: Varying FAP power control levels and effect on MUEs

3.4 Simulator platform for LTE femtocells

This research was conducted to design novel algorithms for cognitive femtocell networks. In order to achieve this and evaluate the reliability of these algorithms, MATLAB was used for all simulations as it provides the underlying platform for the system level simulations of LTE femtocells. Although a two-tier architecture was implemented in the simulation of femtocells and macrocells, there was no fixed simulation scenario as different scenarios were implemented to analyze the algorithms. These scenarios, as described in the proceeding chapters, include the use of open access or CSG in femtocells, densification of UEs as

deemed fit, adaptive power control levels for femtocells etc. The LTE Vienna simulator [124] was widely used in this research as it provides a platform for LTE networks. It will be important to note that the simulator was only used for its LTE capabilities. Simulation scenarios and all algorithms such as the novel scheduling algorithms and adaptive power control for femtocells were imported into the simulator. In the next section, the LTE Vienna simulator platform, its core building blocks and system parameters are discussed.

3.4.1 LTE Vienna system level simulator

The LTE Vienna simulator is a MATLAB-based system level simulation (SLS) environment for LTE. It enables reproducibility due to its open source availability and it is a suitable platform in comparison of novel algorithms.

3.4.1.1 Structure of the simulator

In SLS, the performance of a whole network can be analyzed. It supports the network implementation of a multitude of MBSs in a defined region of interest while supporting static or mobile UEs. Individual physical layer links can be simulated with the investigation of AMC feedback, MIMO gains, modelling of the channel code as well as retransmissions [125]-[129].

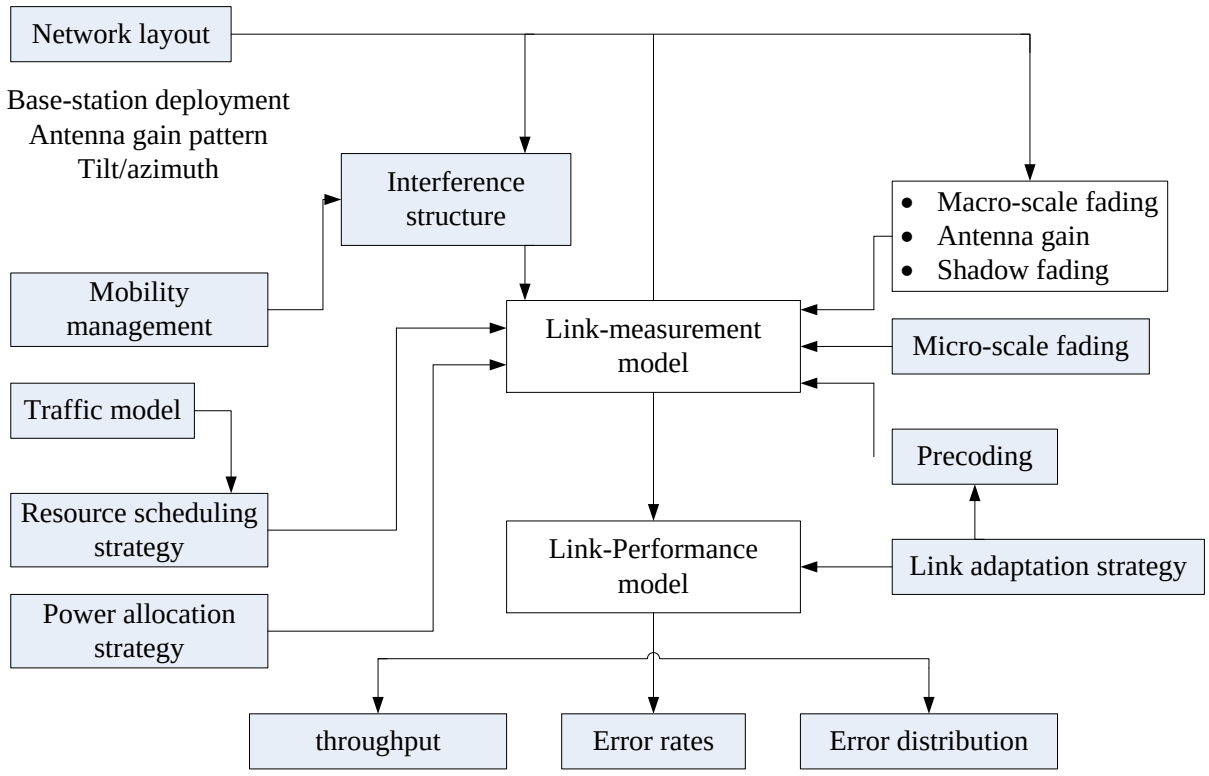

Figure 3.7 Schematic block diagram of the LTE Vienna system level simulator

From Figure 3.7, the simulator consists of two parts:

- **Link measurement model**: This reflects the quality of the link which is determined by UE measurement reports. This model is also responsible for link adaptation and resource allocation in the network. The quality of a link is largely measured by evaluating each SC. The UE computes the feedback based on the SINR, which is used for link adaptation at the MBS. SINR is evaluated based on the network layout based on macroscopic fading, pathloss, shadow fading [130], and microscopic fading [131].

- **Link performance model**: The link performance model builds upon the link measurement model and it is responsible for predicting the Block Error Ratio (BLER) of the link, which is based on transmission parameters such as modulation and coding and received SINR

3.4.1.2 Reduced complexity

One of the high points of the simulator is the ability to pre-calculate as many of the simulation parameters as possible. This offers repeatability by loading a pre-calculated scenario which is very useful when same scenarios have to be employed to compare different algorithms. This reduces computer overhead. Scenarios that can be pre-calculated include but are not limited to the generation of path loss maps and small-scale fading traces.

3.4.2 Validation of the simulator

The results of link level throughput from the simulator was compared with the minimum performance requirements stated by 3GPP in the technical specification TS 36.101 [65] with results showing up to 99% confidence intervals. Also the link and the system level simulators were cross validated by comparing their results against each other [124].

In the next chapter an adaptive power control algorithm in presented for blindly placed femtocells. It is presented as a solution to the power control problem discussed in section 3.3.4 (see Figure 3.5).

Chapter 4

Power control scheme for interference mitigation in blindly placed femtocells

Since FAPs are usually user deployed, blind placement of FAPs is inevitable leading to problems of power spillage causing severe co-tier and cross-tier interference and subsequent performance degradation. This chapter presents performance analysis of a coverage radius based power control scheme to circumvent the problems caused by blind placement of FAPs. The coverage radius based power control scheme does not require FAPs to be relocated to optimal positions for interference mitigation; rather a self-update algorithm is implemented by cognitive FAPs to reduce their cell radius by adaptive adjustment of power values for interference management. Using system level simulations, the performance of the scheme has been analysed for different scenarios and compared to existing schemes. The scheme provides improved interference mitigation and throughput results.

4.1 Introduction

A FAP is user deployed and is usually blindly placed in an indoor environment such as near the walls and windows. In the absence of any antennas' beam directivity (Section 2.1.3) the FAP power could spill out in the surrounding regions thereby causing considerable co-tier and cross-tier interference figure 4.1). Research work carried out in [132]-[134] investigates optimal positions to place a FAP in an indoor environment to improve the throughput and mean capacity. However, it might not always be possible and necessary to find the optimal positions and move a FAP to effectively mitigate the interference caused. Thus there is a serious need for the development of interference mitigation schemes for blindly placed LTE femtocells.

Coverage radius based power control scheme, which adaptively varies the pilot power of FAP based on its distance from the farthest served FUEs, is presented as a potential solution to this problem.

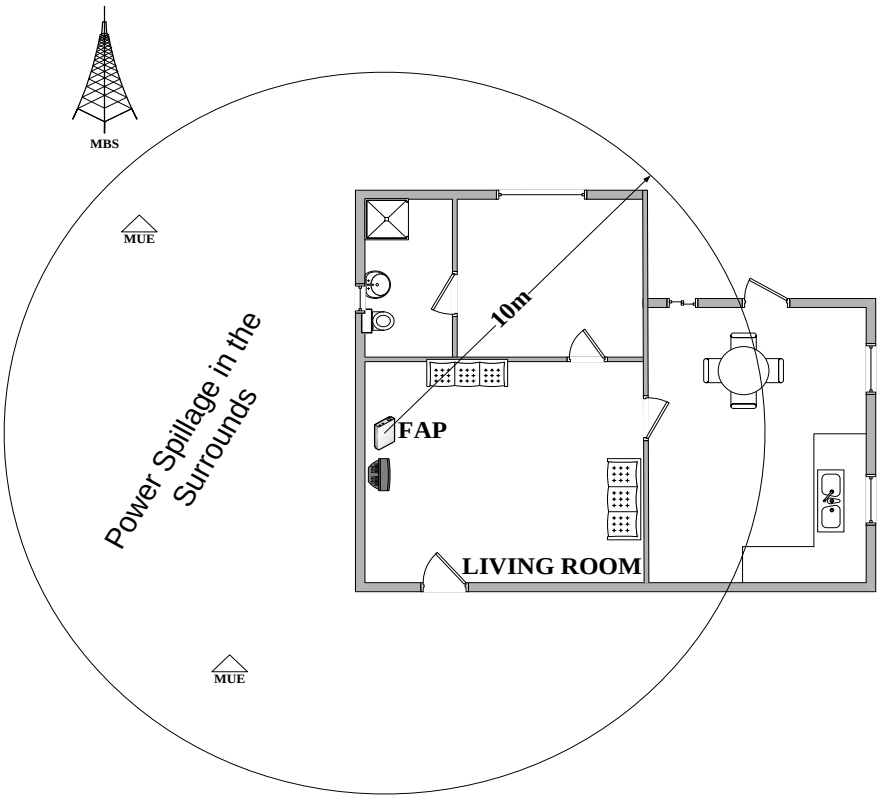

Figure 4.1 Blind placement of a FAP & Power Spillage

4.2 Coverage Radius based Power Control Scheme (PS)

The coverage radius based power control scheme (PS) is described below with the help of Equation 4.1 and illustrated in Figure 4.2.

$$P_t = min\left[P_m + G(\theta) - L_m(d) + L_f(r), P_{max}\right] \quad (4.1)$$

Where P_t is the FAP power value, P_m is the MBS power value, $G(\theta)$ is the MBS antenna gain in the direction of the FAP, $L_m(d)$ is the MBS path loss relative to a femtocell distance d, $L_f(r)$ is the FAP path loss relative to the target radius r, and P_{max} is an upper limit power value of P_t set at 20dBm which is the standard fixed transmit power of a femtocell when transmitting in the DL [10]. The varying value of r which is configured at each FAP is determined to be the distance between the FAP and its farthest served UE with constraints as described below.

4.2.1 PS Radius Limits Setting

Each FAP sets a coverage radius upper limit, R_u and lower limit R_l to be 10m and 3m respectively. The choice of $R_u = 10m$ and R_l= 3m is to provide adequate coverage radius in the UEs premises while keeping interference at a minimum. As already suggested in most of research works, FAPs are not always installed at the centre of premises rather blindly placed, therefore in reality even at a 10m radius, the pilot power of a CSG FAP could spill out of the premises and affect non subscribed users in the vicinity, such as MUEs.

4.2.2 Initial Coverage Radius

The initial coverage radius of FAP is set to be R_u assuming no FUEs are present. With the presence of FUEs, the FAP measures the distance between itself and the farthest FUE which is denoted as R_d. FAP employs received signal strength indication (RSSI) value of an FUE to

deduce distance (i.e. R_d) between itself and the FUE. In the event where only one FUE is served, R_d becomes the distance between the FAP and the said FUE.

4.2.3 PS Self-Update

Since FUEs are usually not static, in order to account for mobility of FUEs, the FAP puts a radius cap of *2m* to R_d to make the final radius $R_f = R_d + 2m$ thus ensuring the seamless coverage for mobile FUEs and further avoiding any handover to MBS. The FAP conducts a self–update per unit of time (for example 1*s* chosen in the simulations) to determine a new coverage radius. The choice of one second and threshold of 2m is based on the fact that the indoor user velocity is usually between 0-3.5 m/s [41].

4.2.4 PS Final Radius

The final radius R_f is always compared against R_u and R_l to maintain a coverage radius such that $R_l \leq R_f \leq R_u$. The proposed scheme can be represented with the help of an algorithm as follows:

Table 4.1: Coverage Radius Based Power Control Scheme

Initialization;
Set $\boldsymbol{R_u = 10m, R_l = 3m,}$
1: **if** ($\boldsymbol{FUE} > 1$)
2: **for** 1:n (n = number of all active FUEs) **do**
3: calculate each FUE: compare $\boldsymbol{R_u}$ and $\boldsymbol{R_l}$ to deduce $\boldsymbol{E = R_u : R_l}$
4: **sort** $\boldsymbol{E = \{1, 2, \ldots, K\}}$
5: **set** $\boldsymbol{R_d = \max\_value}$ from $\boldsymbol{E}$
6: **set** $\boldsymbol{R_f = R_d + 2m}$**:** final FAP coverage radius
7: **end if**
8: Continue loop next TTI = **1s**
9: **end**

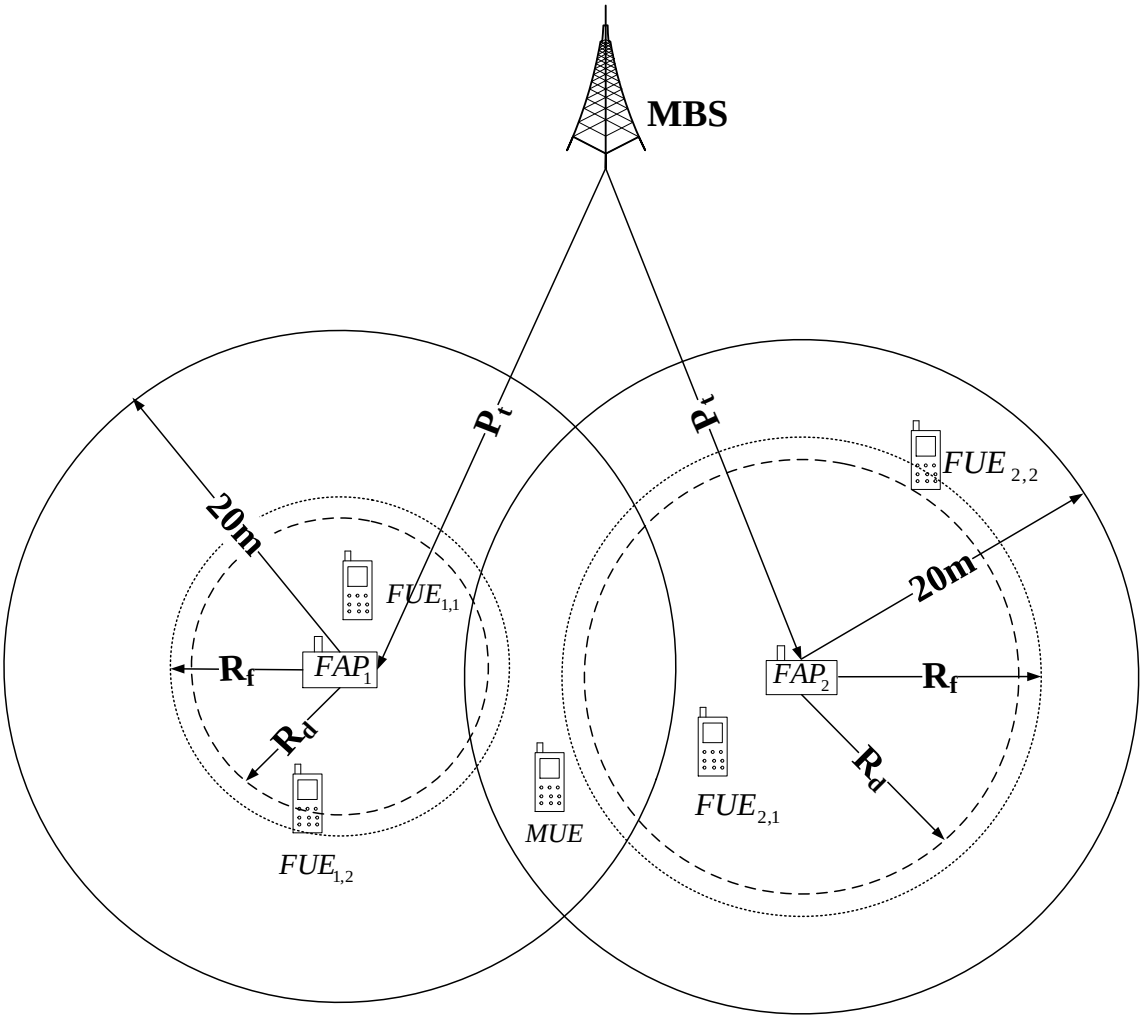

R_f = Final Radius

R_d = Distance from farthest FUE

Figure 4.2: Coverage Radius based Power Control Scheme (PS)

4.3 System model

This section describes the system model and simulation parameters based on 3GPP LTE specifications [135]. The main simulation parameters are given in Table 4.2. The considered network topology consists of two simulation scenarios; a single tri-sector and a densely deployed urban scenario which consists of 7 tri-sector hexagonal MBS cells with an inter-site distance of 500m. 10 FAPs are blindly distributed in each sector with four FUEs attached to

each FAP in a CSG fashion. Additionally, 30 MUEs are randomly deployed in each sector of the MBS to investigate effects of cross-tier interference.

Table 4.2: Simulation Parameters

Parameter	**Value**
Carrier Frequency	2.14 GHz
Bandwidth	20 MHz
MBS Inter-site Distance	500 m
MBS/FAP Tx Power	46 / Variable dBm
Scheduler	Proportional Fair
UE Receiver Noise Figure	9 dB
UE Thermal Noise	-174 dBm/Hz
Single cell	
No. of MBS/FAPs	1/30
MUEs	90
FUEs per FAP/Total FUEs	4/120
Multi-cell	
No. of MBS/FAPs	7/210
MUEs	630
FUEs per FAP/Total FUEs	4/840

To account for macrocell propagation model, the simulations employ the macroscopic path loss model as proposed in [136] in an urban environment and defined in Equation 4.2.

$$PL(dB) = 40 \cdot (1 - 4 \cdot 10^{-3} \times D_{hb}) \cdot \log_{10}(R) - 18 \cdot \log_{10}(D_{hb}) + 21 \cdot \log_{10}(f) + 80$$

(4.2)

Where R is the distance between base station and UE in km, D_{hb} is the height of the base station antenna above ground in metres and f, the carrier frequency in MHz. The path loss model implemented at the femtocell is the dual slope path loss for urban deployment while ignoring shadowing and penetration losses as defined in Equation 4.3.

$$PL(dB) = 38.45 + 20log_{10}(r) + 0.7d_{2D,indoor} \quad (4.3)$$

Where $d_{2D,indoor}$ in this context is the indoor distance between a FAP and its serving FUE.

The MBS antenna radiation pattern used is proposed in TS36.942 [23] and given as follows:

$$A(\theta) = -\min\left[12\left(\frac{\theta}{\theta_{3dB}}\right)^2, A_m\right] \quad (4.4)$$

Where θ_{3dB} = 70 degrees is the gain pattern angle and A_m = 20 dB is the side lobe gain.

4.4 Performance analysis

The performance analysis carried out is to investigate and compare the coverage radius based scheme with other power control schemes in both single and multi-cell scenarios. However, the main purpose is to investigate the coverage radius bounds and subsequently their impact on SINR for both these scenarios. Simulations have thus been performed for all the possible values of R_f between 10m – 3m for the coverage radius based scheme and compared with three existing power control schemes. The first is a baseline scheme where all FAPs are assigned a fixed value of 20dBm. It is important to note that this scheme is used for simulation and comparison analysis and not for implementation because a fixed maximum power is not an ideal solution for mitigating interference in femtocells. The second scheme assigns FAP power value based on the power it receives from its closest MBS while maintaining a target femtocell radius of 10m [23]. The third scheme is a distance based power control scheme proposed in [12] which intends to limit the impact a FAP has on the aggregate macrocell downlink throughput. In this distance based scheme, the MBS is divided into three regions. The power values assigned for FAPs in each region are defined in Equation 4.5.

$$P_{FAP}(d_{FAP}) = \begin{cases} 20dBm & 46m \leq d_{FAP} < 85m, \\ 10dBm & 85m \leq d_{FAP} < 156m \\ 0dBm & 156m \leq d_{FAP} < 289m \end{cases} \quad (4.5)$$

Where d_{FAP} below denotes the distance between a FAP and the closest MBS.

A graphical comparison of the schemes is presented in Figure 4.3 where sector 1 illustrates the distance based power control algorithm as defined in Equation 4.5. Sector 2 illustrates the

constant radius scheme and sector 3 illustrates the coverage radius based power control scheme (PS). The value of P_t in sectors 2 and 3 is as defined in Equation 4.1.

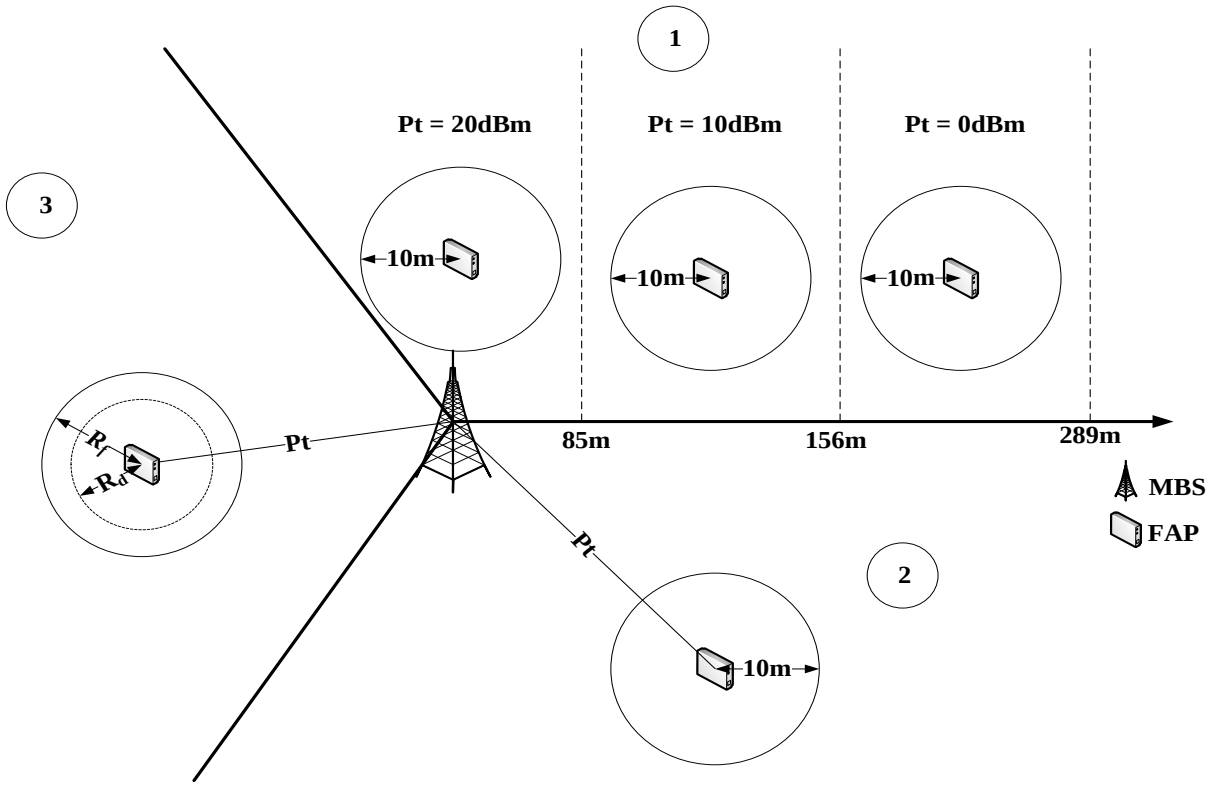

Figure 4.3: Comparison of PS with other schemes

The result of the fixed power value of 20dBm for all FAPs is denoted as 'FP' while the distance based power scheme is denoted as 'DB'. The constant radius power scheme is denoted as 'CR' and for the coverage radius based adaptive power control scheme (PS), the results are shown for the values of R_f at 7m, 6m and 5m denoted as PS-7 and PS-6 and PS-5 respectively. The results are from simulations performed for single cell and multi cell scenarios, where the single cell scenario is composed of a single tri-sector hexagonal MBS cell while the multi-cell scenario consists of 7 tri-sector hexagonal MBS cells with an inter-site distance of 500m. The single and multi-cell scenarios are chosen to investigate the effect of coverage radius bounds on the variations of SINR in each scenario as described below.

4.5 Results and Discussion

The results of the simulated scenarios are analysed in this section.

4.5.1 SINR Cross-Tier (Single Cell)

Figure 4.4 shows the cumulative distribution function (CDF) plot of SINR value for all the MUEs. The proposed scheme takes fully into consideration the cross-tier interference impact it has on MUEs. The transmit power value in proposed scheme is directly proportional to the coverage radius. Due to its low transmit power (P_t) value for smaller FAP coverage area, the scheme at PS-5 with a mean SINR value of 10.35 dB performs much better while compared to other schemes. With a slightly increased coverage area the mean SINR values of PS-6 and PS-7 are 8.75 and 6.13 dB respectively. On the other hand, due to maximumP_t in case of FP, MUEs experience heavy cross-tier interference with a low mean SINR value (-3.60 dB). The mean SINR values for DB and CR are 7.95dB and 2.26 dB respectively. As a whole, the scheme at PS-5 improves SINR by 13.90 dB compared to FP, 8.09 dB compared to CR and 2.04 dB compared to DB schemes.

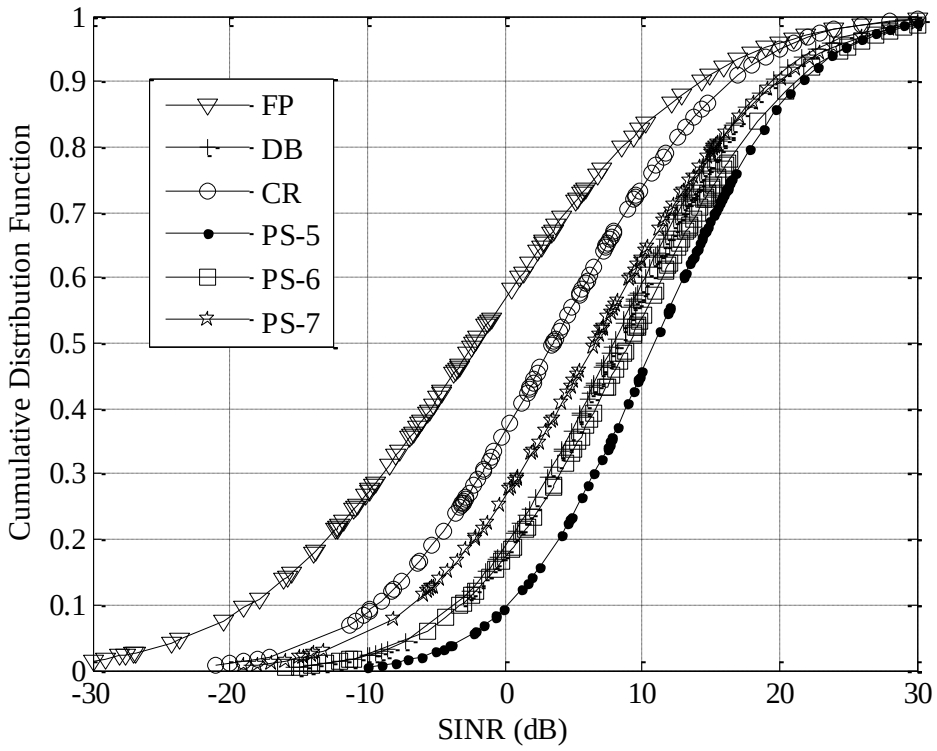

Figure 4.4: SINR cross-tier (Single Cell)

4.5.2 SINR Co-Tier (Single Cell)

Figure 4.5 shows the SINR results for all the FUEs. FP performs better compared to the proposed scheme because some of the femtocells in the simulated scenario are standalone with a maximum fixed value of P_t, thus resulting in a better co-tier SINR. This improvement is due to the fact that in FP, FAPs satisfy their serving FUEs, however completely disregarding neighbouring FAPs and MUEs (causing serious cross-tier interference as already shown in Figure 4.4).

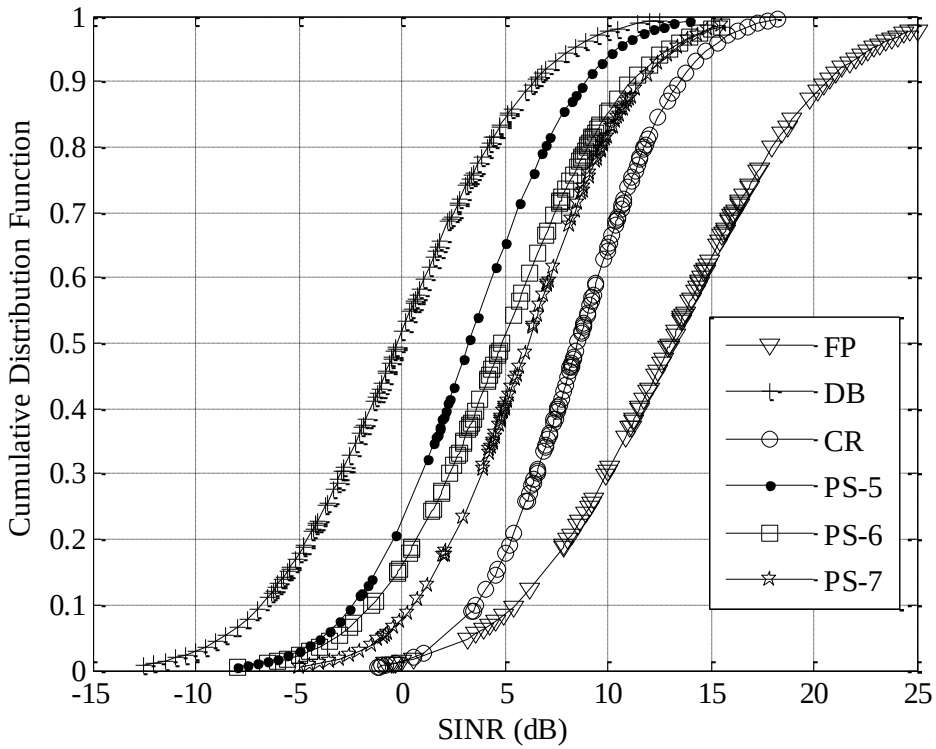

Figure 4.5: SINR co-tier (Single Cell)

The mean SINR values of DB, CR, PS-5, PS-6 and PS-7 are -0.16, 7.93, 3.45, 4.99 and 6.24 dB respectively. The slightly lower SINR values in the proposed scheme as compared to CR are attributed to lower values of P_t because of smaller coverage radius.

4.5.3 Downlink Throughput (Single Cell)

Figure 4.6 shows the CDF plot for downlink throughput over all FUEs. In accordance with SINR results, the baseline scenario FP performs better due to its high P_t value with mean throughput of 12.06Mbps. With mean throughput values of 6.72, 7.64 and 8.42 Mbps for PS-5, PS-6 and PS-7 respectively, the proposed scheme shows that a significantly high throughput can still be achieved with a varying coverage radius as compared to CR (8.64 Mbps) with fixed coverage radius. DB with a mean throughput value of 3.99 Mbps performs lower than the other schemes.

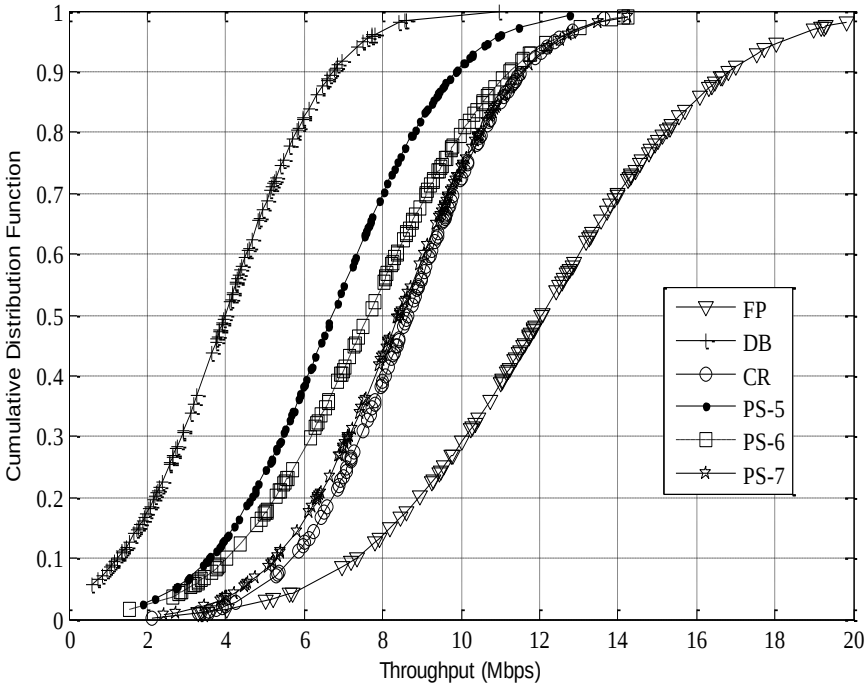

Figure 4.6: Downlink Throughput (Single Cell)

4.5.4 Co-tier and cross-tier SINR (Single Cell vs Multi Cell)

Figures 4.7 and 4.8 below shows how co-tier and cross-tier SINR vary for all the considered schemes while compared against single to multi-cell scenarios. Compared to single cell scenario, clearly for all the schemes both co-tier and cross-tier SINR values dropped in multi-cell scenario because of enhanced interference experienced by the cells due to increased number of blindly placed FAPs. In co-tier, with FP, due to its fixed power, each FAP transmits at a high power, P_t = 20dBm as well as a coverage radius of 20 dBm. The aim in FP is to satisfy its FUEs with no regard to neighbouring FAPs and MUEs hence the positive SINR results in co-tier. However, its performance degrades close-by MUEs hence the poor results in cross-tier SINR.

On the other hand, DB is set up to optimise its P_t with respect to the interference it causes on MUEs based on its location as reflected in figure 4.3. Therefore, it reduces its interference on MUEs which results in a higher cross-tier SINR. On the downside, it is inherent that

collocated femtocells who fall below 85m from the centre of the cell can cause interference to each other when transmitting at P_t = 20dBm hence the low co-tier SINR. In CR, a constant radius of 10m irrespective of P_t value is set up to satisfy FUEs by providing a seamless indoor coverage for FUEs hence the higher co-tier values. However, as cited earlier, a scheme which does not optimise its coverage radius in the presence of MUEs will always cause high interference which results in low SINR values.

The results of the coverage radius based power control scheme are presented for PS-5, PS-6 and PS-7 with the aim of finding the optimal scheme in both co-tier and cross-tier scenario. In both co-tier and cross-tier, the coverage radius is adaptable to restrict any spillage that might cause interference with considerations to both FUEs and MUEs unlike the aforementioned schemes. So at any moment, the coverage radius is limited to an indoor environment hence a better SINR in both co-tier and cross-tier scenarios.

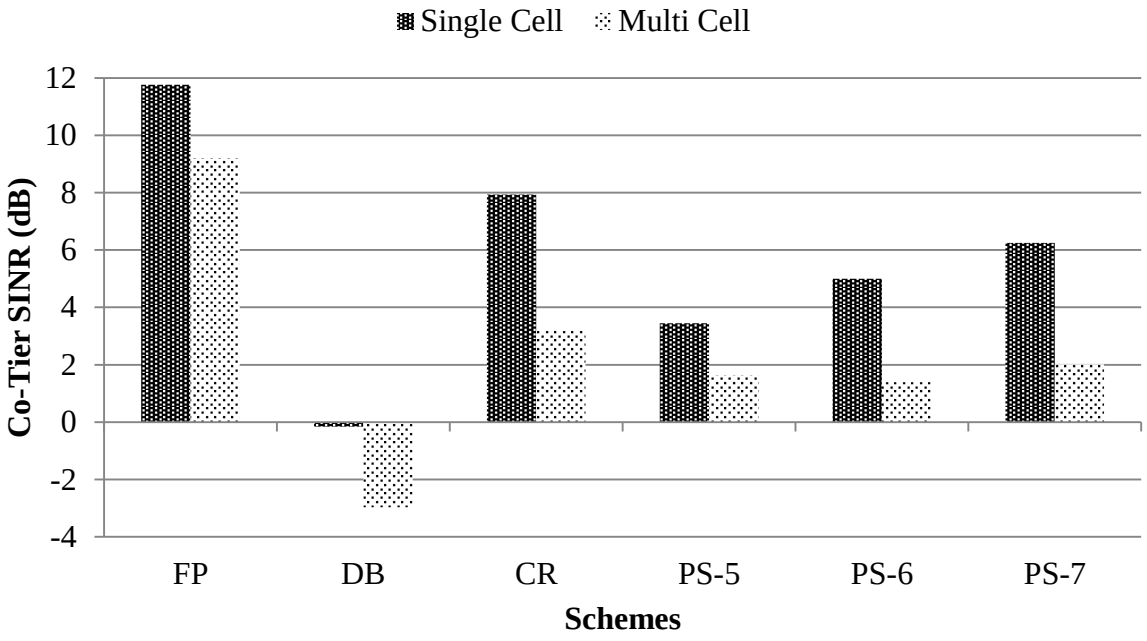

Figure 4.7: co-tier SINR comparison (Single vs Multi-Cell)

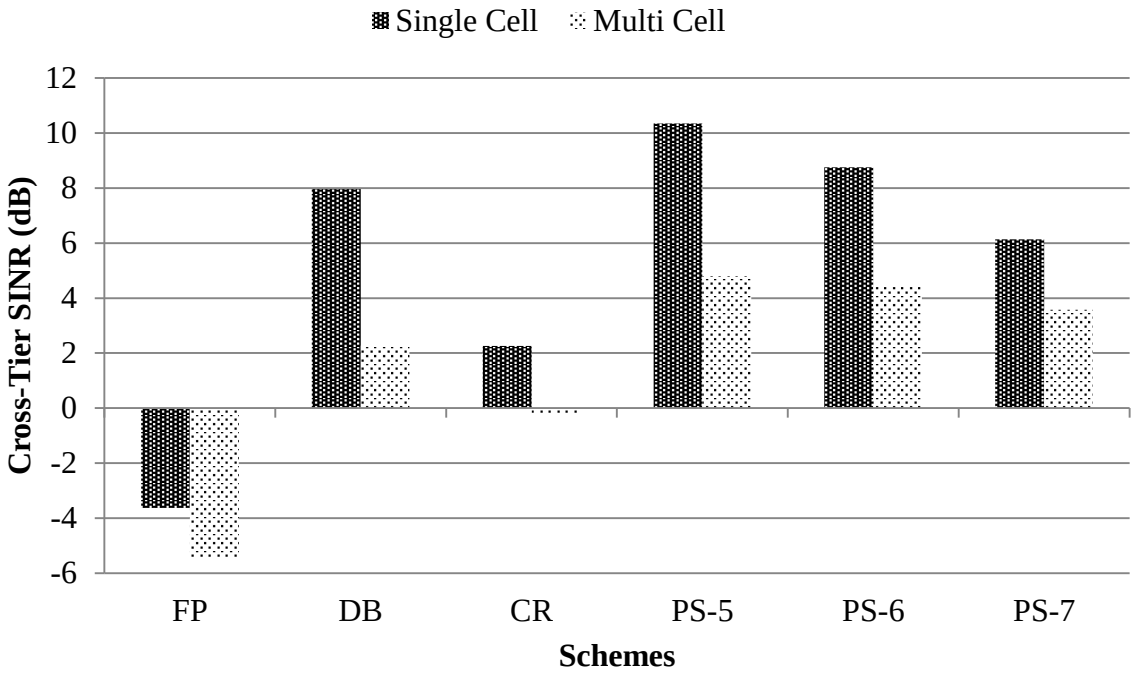

Figure 4.8: Cross-tier SINR comparison (Single vs Multi-Cell)

4.5.5 Droppage in SINR (Single Cell vs Multi Cell)

Figure 4.9 compares the four considered schemes for percentage drop in SINR values for single and multi-cell scenarios. Table 4.3 shows how SINR values have reacted to the change in scenario (single to multi cell).

Table 4.3: percentage Drop due to change in Scenario (Single to multi Cell)

Scheme	Co-Tier SINR (percentage)	Cross-Tier SINR (percentage)
FP	22	33
DB	95	71
CR	60	90
PS-5	53	54
PS-6	72	50
PS-7	68	42

Highlighted fields in Table 4.3 provide very important information about the schemes and how change of scenario has affected their SINR values. It might appear that compared to other schemes FP scheme suffered the lowest drop in its SINR values, however a careful consideration would reveal that irrespective of the scenarios, cross-tier SINR for FP has never

been of any importance because it has always stayed negative (-3.63 dB for single cell and-5.425 dB for multi cell, Figure 4.8). It further proves that a fixed power scheme such as FP is not at all a suitable scheme for cross-tier interference mitigation in densely deployed blindly placed femtocells.

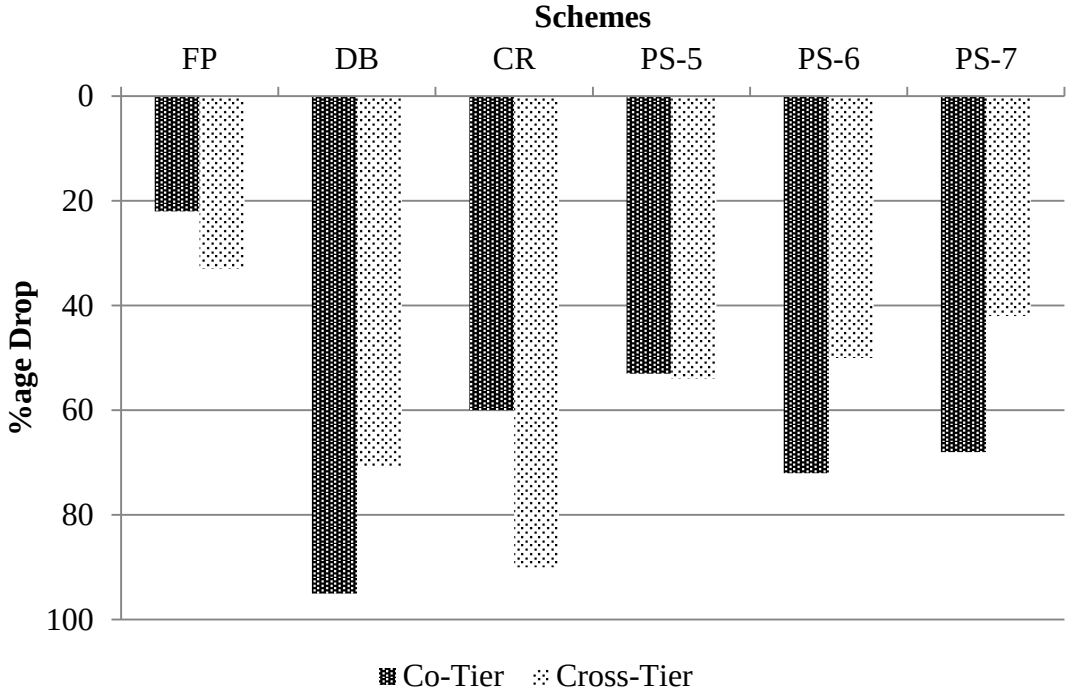

Figure 4.9: % Droppage in SINR (Single vs Multi Cell)

On the same lines, DB scheme behaved very poorly for co-tier SINR values (highlighted in Table 4.3, it suffered drop of 95 % with the change of scenario). co-tier SINR values for DB scheme stayed at -0.160 dB for single cell and -2.977 dB for multi cell scenarios (Figure 4.7). Lastly, even though CR scheme showed some promise in terms of co-tier SINR values, but it suffered a drop of 90% for its cross-tier SINR values. Despite the droppage due to change in scenario, the proposed scheme has always been promising both for co-tier and cross-tier SINR values. The bounds of coverage radius and its impact on SINR values for the PS are further described in section 4.5.6.

4.5.6 Coverage Radius bounds and impact on SINR (Single Cell vs Multi-cell)

Figure 4.10 plots the response of co-tier and cross-tier SINR values to the change in coverage radius and also the change in the scenario for the proposed scheme.

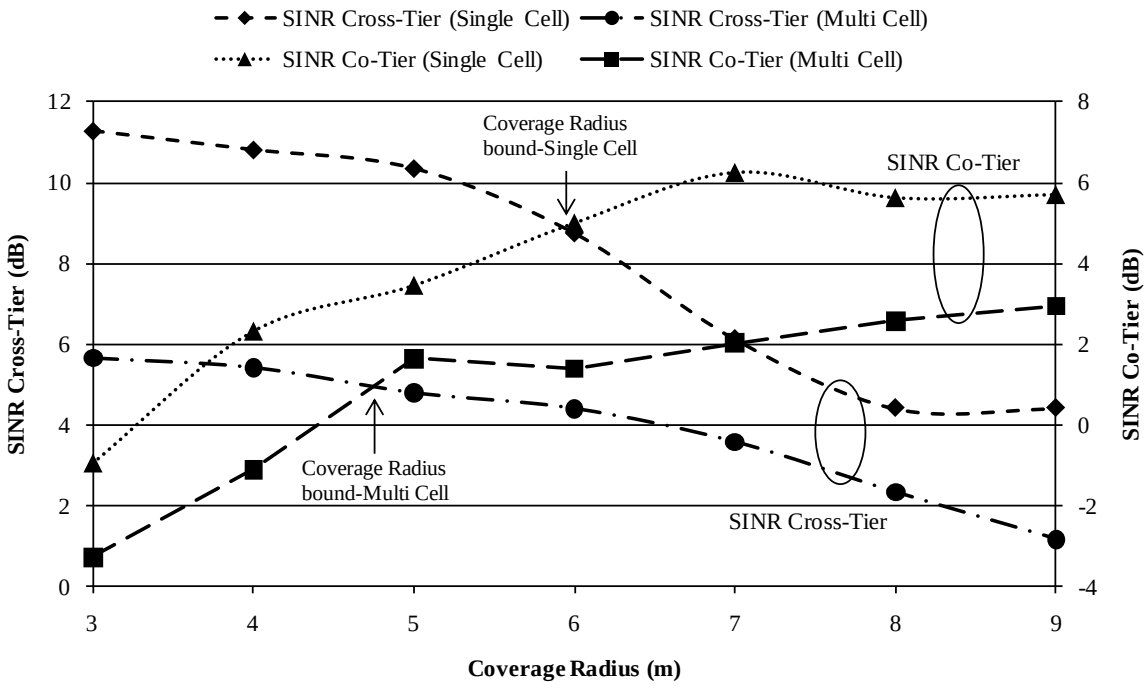

Figure 4.10: Coverage Radius bounds and Effect on SINR (Single vs Multi-cell)

Irrespective of the scenario (single or multi cell), lower coverage radius gave higher Cross-Tier SINR values whereas increase in coverage radius resulted into better co-tier SINR and vice versa. This further validates the results given in Figures 4.4, 4.5, 4.7 and 4.8 above. Higher cross-tier SINR values are obtained because of the fact that with reduced coverage radius more MUEs are left out thereby resulting into lesser interference and better cross tier SINR. On the other hand, since coverage radius is directly proportional to the transmit power, lower coverage radius resulted into lesser signal power per FUEs compared to increased interference due to densely deployed blindly placed femtocells thus resulting into reduced co-tier SINR. It is fair to conclude that in the interference mitigation scheme, for both scenarios

(single and multi-cell) lower coverage radius favours cross-tier SINR whereas higher coverage radius values favour co-tier SINR.

However, from the simulations it is shown that there are coverage radius bounds (i.e. ca. 6m for single cell and ca. 4.7 m for multi-cell), which resulted into balanced (optimum) value for both co-tier and cross-tier SINR values. These findings are very important in blindly placed densely deployed femtocells for the possible distribution and radial mobility of FUEs to avoid significant performance degradation.

4.6 Summary

Femtocells aim to improve poor indoor network coverage in cellular communication which has attracted network operators and stakeholders. Even though femtocells are discovering an important role, the issue of interference as a result of blindly placed FAPs needs to be addressed. In this chapter, a coverage radius based adaptive power control scheme to mitigate interference for blindly placed LTE femtocells is investigated. The proposed scheme does not require FAPs to be relocated on optimal locations for effective interference mitigation, rather it implements a self-update algorithm for FAPs to reduce their cell radius and adjust power values in an adaptive manner. The performance of the scheme was analysed using system level simulations for single and multi-cell scenarios. The results have shown that the proposed scheme has an improved value of cross-tier SINR, throughput and lower co-tier SINR while compared to baseline and existing adaptive interference mitigation schemes. Further the results have proven that irrespective of the scheme, the change of scenario from single to multi cell, affected and resulted in lower co-tier and cross-tier SINR values for multi cell compared to single cell values. It was also found that the adaptive power control scheme contributed towards coverage radius bounds which provide balanced co-tier and cross-tier SINR values. In terms of densely deployed blindly placed LTE femtocells, coverage radius

bounds is a very important finding because it can be helpful towards the effective distribution of FUEs to achieve balanced co-tier and cross-tier SINR values while maintaining other performance parameters too, e.g. throughput etc.

In the next chapter, a hybrid algorithm, which builds up upon this chapter is presented. It comprises a power control and a contention free resource allocation algorithm to mitigate interference in CFs.

Chapter 5

A hybrid UE admittance and contention free resource allocation for femtocells

Femtocells are designed to co-exist alongside macrocells providing spatial frequency reuse, higher spectrum efficiency and cover areas where macrocells cannot. This chapter proposes a joint threshold power based admittance and contention free resource allocation scheme for interference mitigation in cognitive femtocells. In the proposed scheme, a CF sets a threshold value on the mutual interference between itself and a close-by MUE. To mitigate cross-tier interference, a CF classifies MUEs which fall above this threshold value (high interference value) as Undesired MUEs (UMUEs). MUEs which fall below this threshold are classified as Desired MUEs (DMUEs). To mitigate co-tier interference, proposed scheme introduces a scheduling engine which employs matching policy attributes and assigns RBs of unique DMUEs to CFs to avoid any possible contention problems, thus providing improved co-tier interference. System level simulations have been performed to demonstrate working and effectiveness of proposed scheme.

5.1 Introduction

When it comes to frequency/spectrum allocation schemes, CFs perform the task of sensing spectrum holes of PUs, analyzing, deciding, and taking an action by assigning resources to secondary users (SUs) (see Section 1.4.1). However, the availability of a spectrum is not restricted to white spaces but the possibility of reusing the resources of PUs that have an insignificant interference to a SU. In this concept, a FAP is able to assign resources of less interfering MUEs (PUs) to its FUEs (SUs). This concept has been investigated in [104] where a FAP obtains the scheduling information in the uplink (UL) of far-away MUEs from the MBS through a backhaul or over the air.

A scheme which combines channel sensing and resource scheduling is proposed in [90, 104, 137, 138]. Femtocells in this scheme sense channel occupation, capitalizing on the strong uplink (UL) transmit power of a MUE as it tries to reach its serving MBS, to find available frequency channels. This is achieved by analyzing the energy in the sub-channels and subsequently assigning those with the lowest interference signature to its users. In [89] an algorithm is proposed to orthogonally assign MUE channels to FUEs. A channel is deemed available for communication if a FAP detects no busy tone at the expiration of the timer, otherwise it abandons and waits for the expiration of the next back off timer until each FAP is able to communicate on an available channel. In the scheme, the utility of each channel is calculated by each FAP and subsequently a back-off timer is set for each channel.

However, the aforementioned schemes largely target either co-tier or cross-tier interference mitigation, thereby failing to provide a complete solution. Thus in this section, a joint threshold power based admittance and matching policy based spectrum allocation scheme is proposed for co-tier and cross-tier interference mitigation in cognitive femtocells. The proposed scheme calculates the mutual interference between itself and a close-by MUE and

admits the closest MUEs (UMUEs) as one of its UEs to mitigate cross tier interference. Furthermore, this scheme employs a scheduling engine which engages a matching policy that orthogonally assigns the RBs of DMUEs resulting into significantly reduced co-tier interference. In other words, a CF interweaves into the transmission of the primary user (transmission is concurrent but interference is limited) and CFs can assign these RBs to their UEs due to frequency reuse with spatial separation policy.

5.2 UE admittance and contention free resource allocation scheme

In LTE standard, the reference signal received power (RSRP) for a downlink communication measures the average received signal strength of the serving MBS to initiate a handover (HO) of an MUE. The RSRP of the *l*th MBS to the *j*th MUE in the *k*th MBS can be expressed as

$$RSRP_{k,l}^{j} = P_{M,l} \cdot g_{l,k}^{j} \tag{5.1}$$

Where $P_{M,l}$ is the pilot signal of the neighbouring *l*th MBS and $g_{l,k}^{j}$ is the propagation loss from the *j*th MUE to the *k*th MBS. In others words, for HO to occur at the *j*th MUE,

$$P_{M,l} > P_{M,k} \tag{5.2}$$

where $P_{M,k}$ is the pilot signal of the serving MBS.

The proposed scheme can be best described with the help of a scenario as shown in Figure 5.1. Let us define T as the active number of MUEs all distributed in a group of collocated FAPs with coverage radius of R = 20m. The MUEs in the network are all experiencing low signal due to the long distance from the MBS. Further focusing on the zoomed section (Figure 5.1), consider $MUE_{3,2}$ (inset) which is in the coverage area of FAP_1 and FAP_3. Although it is experiencing a weak signal from the MBS, it is assumed that the condition for HO in Equation 5.2 is not met. This requires $MUE_{3,2}$ to transmit at a higher power to reach

the MBS and thereby it increases the interference level as a result of rise-over-thermal (RoT) noise at FAP_1 and FAP_3 [13].

The aggregate interference from of all the MUEs on the *n*th FAP can be expressed as:

$$p_m^i = G_n + \sum_{m=1}^{N_M} P_{M-} g_{m,f} \quad (5.3)$$

Where G_n is the noise level, p_M is the transmit power of each MUE as it tries to reach its serving MBS and $g_{m,f}$ is the propagation loss between a MUE and the FAP. The propagation loss is calculated using dual stripe propagation model [20] which models the scenario as two building blocks providing indoor to outdoor propagation as well as a collocated femtocell scenario. This provides a realistic and evaluation of practical femtocell deployment scenarios. It is expressed as:

$$g_{m,f} = 15.3 + 37.6 \times log_{10} D - L_f dB \quad (5.4)$$

Where L_f is the attenuation and D the distance between the MUE and FAP.

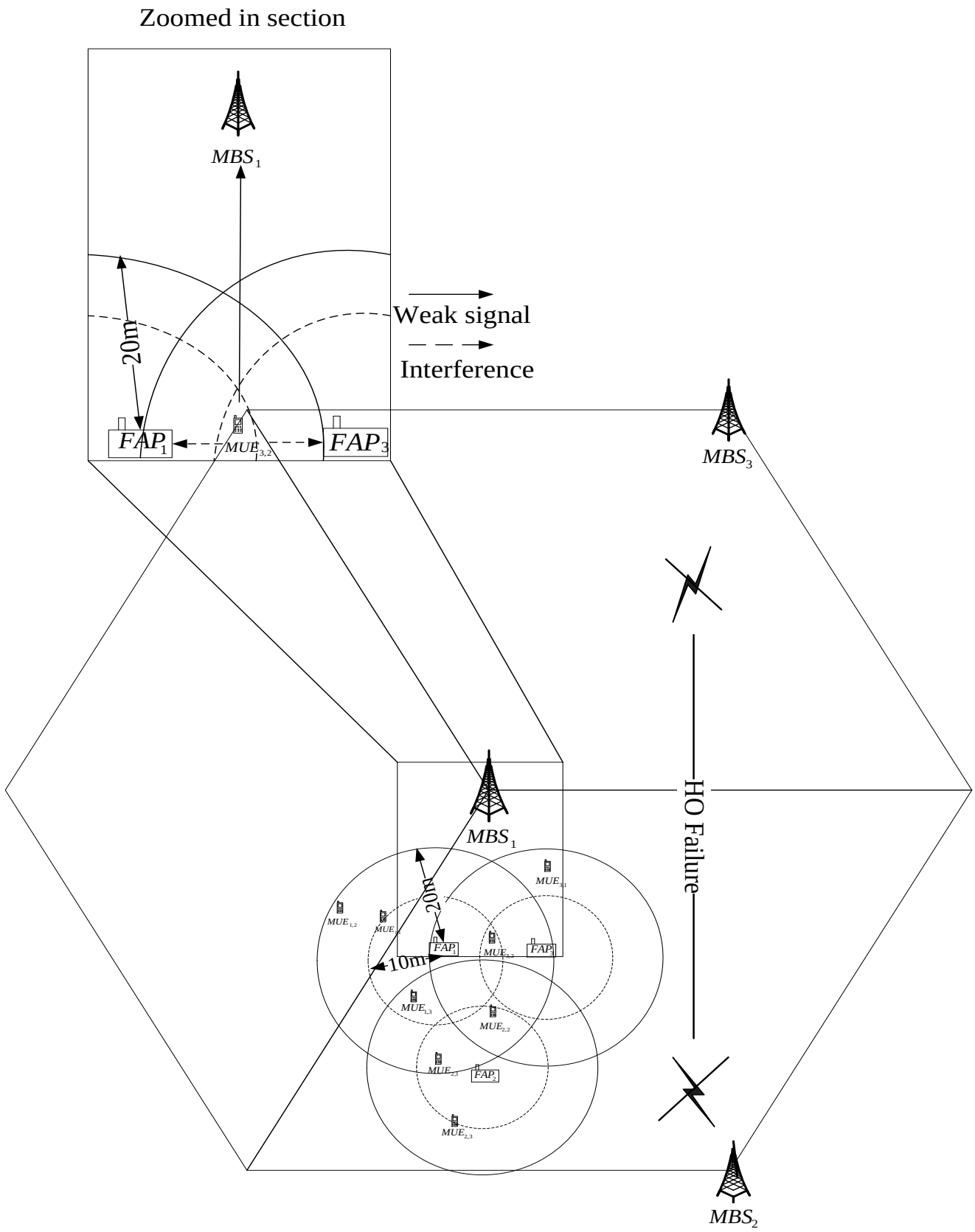

Figure 5.1: Proposed Scheme

5.2.1 Threshold Power based MUE admittance to FAP

In the proposed scheme, let p_q (deduced from Equation 5.3) be the interference power value a FAP can tolerate from a MUE which also translates as the threshold interference power or threshold boundary. This boundary is illustrated in Figure 5.1 by the inner dotted circle and is set based on the premise that the closer a MUE is to a FAP, the higher the mutual interference caused. Each FAP through sensing the communication between an MBS and MUE calculates p_m^i **(**Equation 5.3). Subsequently, for each MUE, a FAP compares the value of p_m^i against the threshold value p_q. In the scheme, the aim is for each FAP to admit a close by unsubscribed MUE as one of its FUE to mitigate the mutual interference. Let us denote all active MUEs in the coverage area of the i^{th} femtocell as $\mu_i = \{1, 2, \ldots N_i\}$. We further subdivide μ_i into;

$$\mu_i = \mu_i^u + \mu_i^D, \begin{cases} \mu_i^U = p_m^i > p_q \\ \mu_i^D = p_m^i < p_q \end{cases} \qquad (5)$$

Where μ_i^u is the list of MUEs that can be admitted to the FAP known as Undesirable MUEs (UMUEs) and μ_i^D is the list of MUEs that cause lesser interference to a FAP known as desirable MUEs (DMUEs). In other words, any MUEs that fall within the dotted region can cause significant interference to FAP and should be admitted to the FAP thus subsequently becoming FUEs. The pseudo code for MUEs admittance to FAP is provided in Table 5.1.

Table 5.1: MUE Admittance to FAP

Pseudo Code Algorithm 1:
1: **if** ($\boldsymbol{\mu_i}$ > 1)
2: **for** 1:n (n = number of all active MUEs) **do**
3: calculate $\boldsymbol{p_m^i}$(x)
4:compare $\boldsymbol{p_m}$ and $\boldsymbol{p_q}$
5: **if** $\boldsymbol{p_m^i}$ > $\boldsymbol{p_q}$**then**
6: $\boldsymbol{\mu_i} \in \boldsymbol{\mu_i^D}$ (MUE admitted to FAP)
7: **if** $\boldsymbol{p_m^i}$< $\boldsymbol{p_q}$**then**
8: $\boldsymbol{\mu_i} \in \boldsymbol{\mu_i^u}$
9: **end if**
10: **end if**
11: **end**

5.2.2 Matching policy based resource allocation

As part of proposed scheme, an algorithm is introduced which deals with the DMUEs (MUEs which fall outside the threshold boundary and cannot be admitted to the FAP) in μ_i^D. The algorithm introduces a method where a FAP properly utilizes the OFDMA sub-channels of the UMUEs to avoid the mutual interference caused.

Since the DMUEs in μ_i^D for each FAP are randomly distributed in the network, it is expected that some FAPs (especially in a collocated scenario) may have common elements of μ_i^D as shown in Figure 5.2. It describes a simple scenario with two femtocells. After sensing, each femtocell is able to deduce its list of μ_i^u and μ_i^Das shown in box A and B respectively. Since both femtocells are co-located with no coordination between them, FAP1 and FAP2 can have similar DMUEs such as $MUE_{2,1}$.

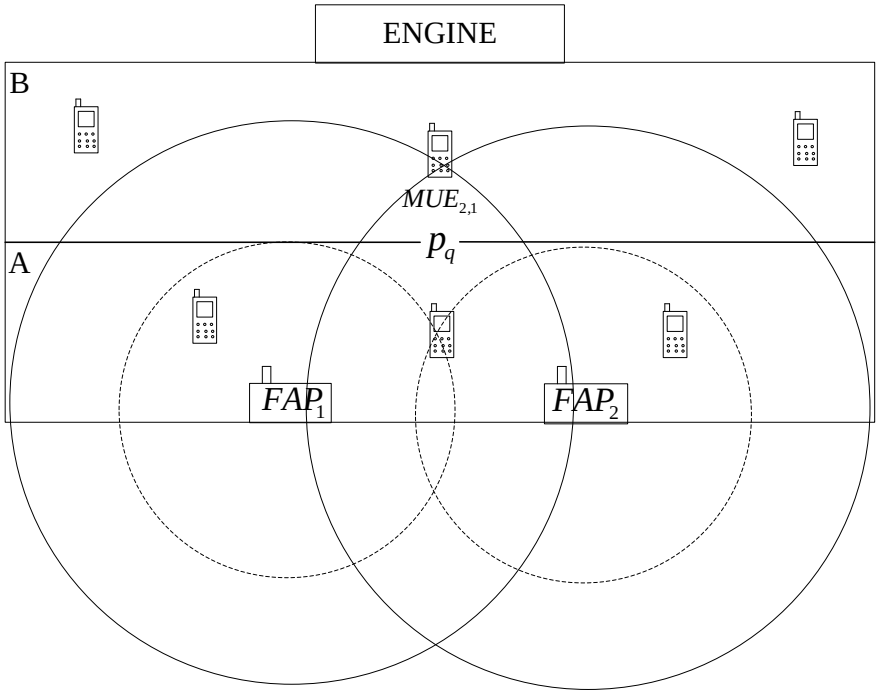

Figure 5.2: Femtocell Network- UMUEs and DMUEs

A matching policy to uniquely match DMUEs to each FAP to avoid any contention problems that may arise is introduced. The matching policy determines which FAP utilizes the OFDMA sub-channels of an UMUE from its list of μ_i^U to avoid co-tier interference. A cognitive enabled scheduling engine to create a matching policy is proposed working as follows;

Through sensing, the scheduling engine E, is aware of the locations of the FAPs ($\mathrm{FAP_{LOC}}$) and MUEs ($\mathrm{MUE_{LOC}}$) in the network (Figure 5.3). CR enables the femtocell to identify the transmission parameters of the elements in its environment and in this context it is the RB UMUEs.

Let $E = \{f_1, f_2, \ldots, f_n\}$

i. Each FAP in the network submits its list of μ_i^D to E. This list is continuously updated due to incoming and outgoing DMUEs in μ_i^D.

ii. E selects a DMUE iteratively and maps it against its list of FAP.

iii. Using a propagation model, the engine calculates the path loss $g_{f,m}^D$ between the μ_i^D and the mapped FAPs which is expressed as;

$$g_{f,m}^D = 38.46 + 20log_{10}\, DdB \quad (5.6)$$

Where D is the distance between the MUE and FAP in metres.

iv. A μ_i^D with the lowest path loss is assigned to a FAP and the process continues until all the μ_i^D in the list are uniquely assigned to each FAP in the network. This ensures that RBs of no two similar DMUEs are assigned to two different FAPs and thus subsequently provides contention free access thereby resulting into significantly reduced co-tier interference. Pseudo code for implementation of matching policy based scheduling algorithm is provided in Table 5.2.

Table 5.2: Matching Policy based Resource Allocation

Pseudo code for Algorithm 2:
Initialization;
$\boldsymbol{E = \{f_1, f_2, \ldots, f_n\}}$
1: Firstly $\boldsymbol{sort\ E}$
2: for $\boldsymbol{\mu_1^D \in f_i}$
3: calculate $\boldsymbol{p = \max\_value : \min\_value}$
4: $\boldsymbol{D_1 = \max\_value\{f_i\}}$
5: end
6: for $\boldsymbol{\mu_2^D \in f_i}$
7: calculate $\boldsymbol{p = \max\_value : \min\_value}$
8: $\boldsymbol{D_2 = \max\_value\{f_i\}}$
9: end
10: Continue loop until $\boldsymbol{\mu_i^D \in f_i = 0}$

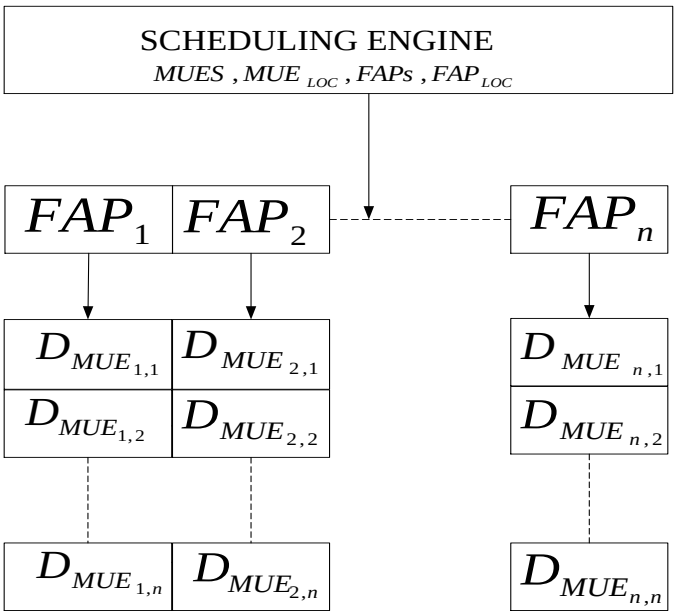

Figure 5.3: Matching policy based Scheduling Engine

5.3 System model

The system model comprises a tri-sector LTE MBS serving randomly distributed and mobile MUEs within its coverage area. ℓ LTE FAPs are randomly distributed within the MBS coverage area. The MBS and FAPs are deployed in a co-channel fashion sharing same resources which introduces a higher amount of interference on both parties. In order to facilitate allowance of UMUEs admittance by FAP, only one FUE is attached to each FAP. All active MUEs in the coverage area of the i^{th} femtocell are denoted as$\mu_i = \{1, 2, \ldots N_i\}$ and this number varies in all iterations in terms of the transmission time interval calculated per unit of time. We assume that each FAP has cognitive radio (CR) capability which makes it fully aware of its environment in a proactive manner to estimate and avoid/restrict the mutual interference in the co-channel network.

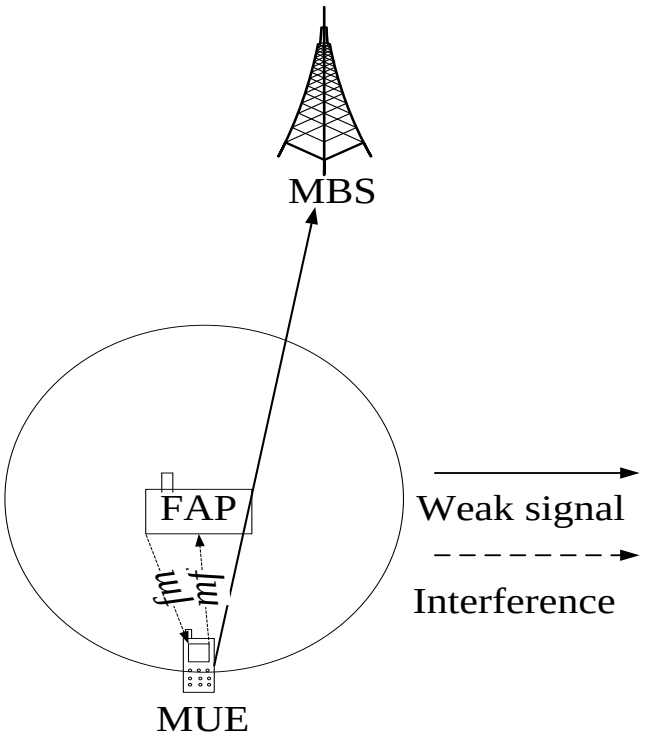

Figure 5.4: Mutual Interference between MUE and FAP

Figure 5.4 shows a simple system model to highlight the individual and aggregate interference from MUE to FAP and vice versa denoted by *mf* and *fm* respectively. An MUE experiences a weak signal from its serving MBS due to attenuation. As a result, it increases its transmit power value denoted, p_m as it tries to reach the MBS. If proper OFDMA sub-channels are not used, this could cause increased and severe uplink interference on a close by FAPs. This is because MUE could be transmitting at a high power in the same sub-channel as a FUE served by a close by FAP. As described in Section 5.2 above, to mitigate cross-tier interference, a threshold based power control scheme is presented where a FAP calculates *mf* and subsequently admits MUE (i.e. UMUE) as one of its FUEs. DMUEs which are not admitted to FAP are handled by matching policy based scheduling engine which uniquely matches RBs of DMUEs to each FAP to allow contention free access. The matching policy determines which FAP utilizes the OFDMA sub-channels of DMUEs to mitigate the ensuing co-tier interference.

The main simulation parameters based on 3GPP LTE specifications are given in Table 5.3. The network topology consists of a tri-sector MBS with 30 FAPs randomly distributed in each sector. A FAP usually accommodates 4 and up to 16 UEs for residential and commercial scenarios respectively [38]. In the simulations, a single FUE is attached to each FAP to facilitate admittance of UMUEs to FAP. 300 MUEs are randomly deployed to investigate effect of cross-tier interference. WINNERII+ channel modelling is used and traffic load is uniformly distributed among all the users.

Table 5.3: Simulation Parameters

Parameter	**Value**
Carrier Frequency	2.14 GHz
Bandwidth	20 MHz
No. of MBS/FAPs	3/30
MUEs	300
MBS Radius	500 m
MBS/FAP Tx Power	46 / 20 dBm
Scheduler	Proportional Fair
Fading Model	Claussen
Channel Modelling	WINNERII+
Mobility model	Random waypoint

5.4 Simulation results and analysis

In this context, the mutual interference caused on the MUEs and the FAPs is presented before a detailed performance analysis of the proposed scheme is provided.

5.4.1 Choice of MUE transmit power

Figure 5.5 plots the cumulative distribution function (CDF) of varying p_m values (15 dBm, 18 dBm, 20 dBm, 22 dBm, 24 dBm, 24 dBm, 26 dBm, 28 dBm and 30 dBm) and the *mf* interference caused on an arbitrary FAP.

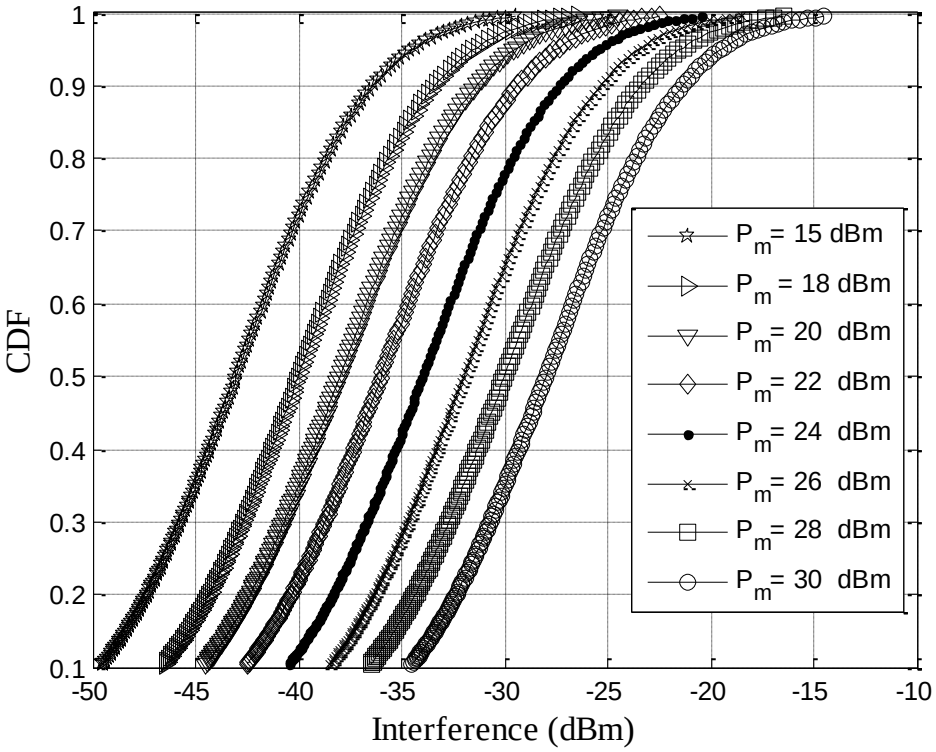

Figure 5.5: MUE transmit power vs Interference

Clearly there is a direct relationship between the MUE transmit power value P_m and interference *mf* caused on an FAP. As expected, a higher transmit power value causes greater interference. A graph like this is extremely useful in determining the interference caused on a FAP and subsequently in deciding about the maximum transmit power an MUE is allowed to transmit. Referring to scenario presented in Figure 5.1 above, since the assumption is that almost all the MUEs are experiencing poor reception from MBS, thus in the simulations the highest possible value of p_m, i.e. transmit power value for MUE (30 dBm) is used. This accordingly causes the highest level of cross-tier interference *mf* caused on an FAP and will be a good test for the proposed scheme to find out how efficiently it allows admittance of UMUEs to FAP to result in reduced cross-tier interference.

5.4.2 UMUE admittance and Cross-tier interference Mitigation

Figure 5.6 investigates the mutual interference caused between FAP and MUEs. MUE-FAP is the interference caused by an MUE on FAP and is calculated using Equation 5.3 with P_m = 30 dBm, whereas FAP-MUE highlights the interference level on an MUE caused by an FAP with a transmit power P_t = 20 dBm. P_m value of 30 dBm causes around -28 dBm of mean interference value on an FAP. These mean values vary depending on the number of MUEs and also with the value of P_m which is dependent on the signal attenuation.

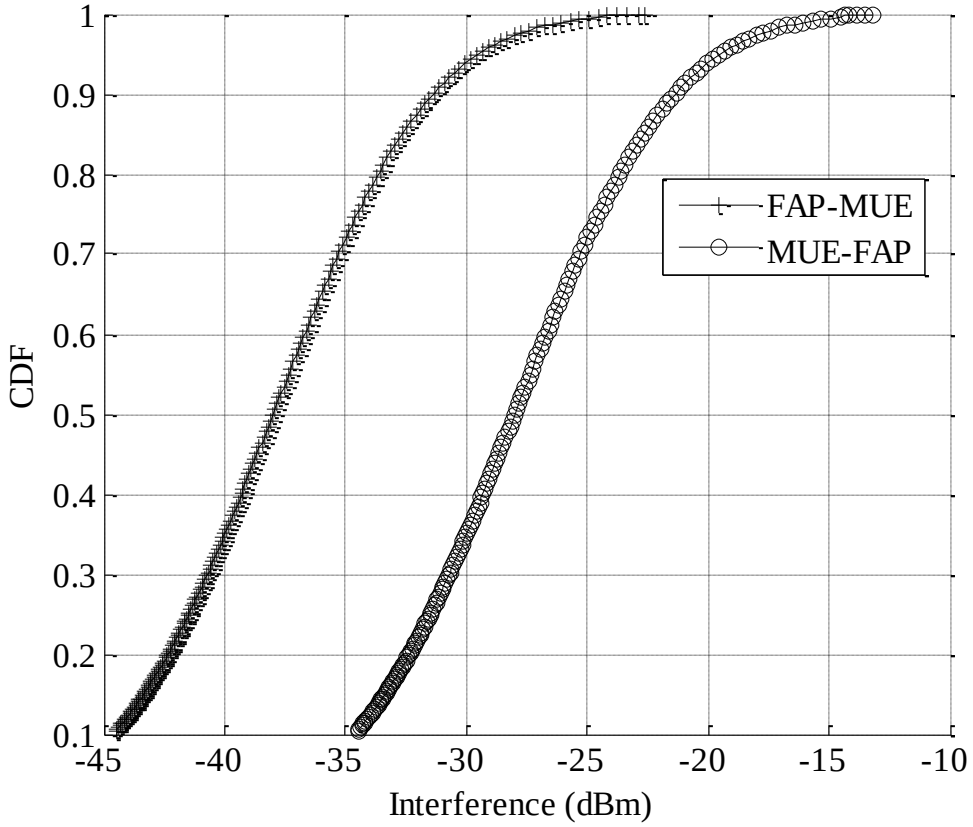

Figure 5.6: FAP-MUE mutual interference

Figure 5.7 depicts the core working of the proposed scheme. It plots the interference caused by MUEs (i.e. UMUEs) on FAPs and subsequent functionality of the proposed scheme to allow admittance to result in reduced cross-tier interference.

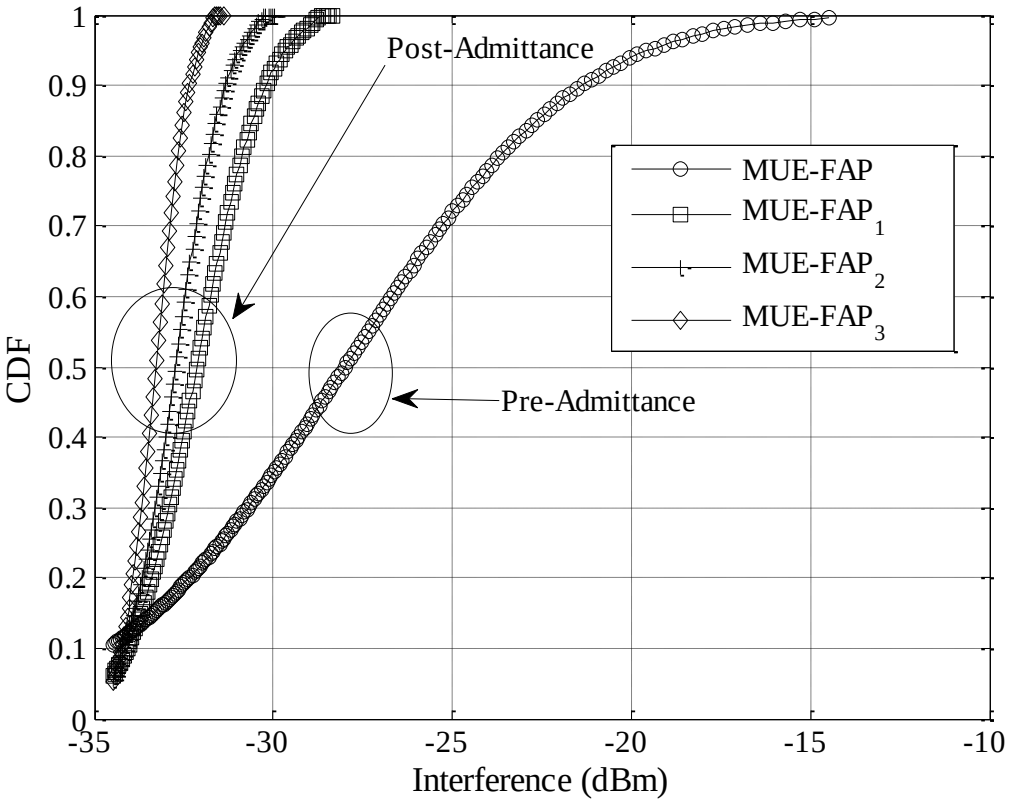

Figure 5.7: MUEs admittance for cross-tier interference mitigation

Figure 5.7 presents the results for pre and post admittance (once proposed scheme kicks in) stages. It depicts the results where cross-tier interference is mitigated due to the algorithm in a scenario where MUEs are randomly located within 3 collocated FAPs (FAP 1-3, Figure 5.1). We set the threshold value of P_q at -28.5 dBm where P_m = 30 dBm which is approximately equivalent to a femtocell radius value of 10m because of the high interference level between a FAP and MUE at distances 2m-10m. In line with Figures 5.5 and 5.6, the MUE-FAP (pre-admittance) curve highlights the interference due on any FAP by the MUEs before the algorithm kicks in with a mean value of -28 dBm. However, when Algorithm 1 is employed, the high interference causing MUEs being admitted to FAPs (FAP 1-3) thereby resulting in greatly reduced cross-tier interference as depicted by post admittance curves. The mean value of post admittance interference is around -34 dBm compared to -28 dBm pre-

admittance mean value. This is because each P_m value of MUE that exceeds P_q is admitted to the respective FAP and what is left is the lesser interference from the remaining UMUEs. Notably, the curves MUE-$FAP_{1,}$ MUE-FAP_2 and MUE-FAP_3 represent the interference values caused by remaining UMUES on FAPs 1, 2 and 3 respectively.

5.4.3 Matching policy based Co-tier Interference Mitigation

Algorithm 2 of the proposed scheme helps mitigate co-tier interference by employment of contention free resource blocks allocation. It eventually addresses DMUEs (i.e. MUEs which fall outside the threshold boundary and are not admitted to the FAP). The algorithm introduces a method where a FAP properly utilizes the OFDMA sub-channels of DMUEs to avoid the co-tier interference caused. Referring to Figure 5.1, emphasis is laid on two collocated FAPs, i.e. FAP_1 and $FAP_{2.}$ Figure 5.8 depicts the mutual interference of FAP_1 and FAP_2 on each other pre-algorithm and post-algorithm. In pre-algorithm, both FAPs vie for the same resources which results in a co-tier interference with a mean value of around -40 dBm. As the matching policy algorithm kicks in, this contention problem is resolved as these resources are appropriately matched to each FAP which reduces the co-tier interference by approximately 8dBm as depicted in the post-algorithm curve.

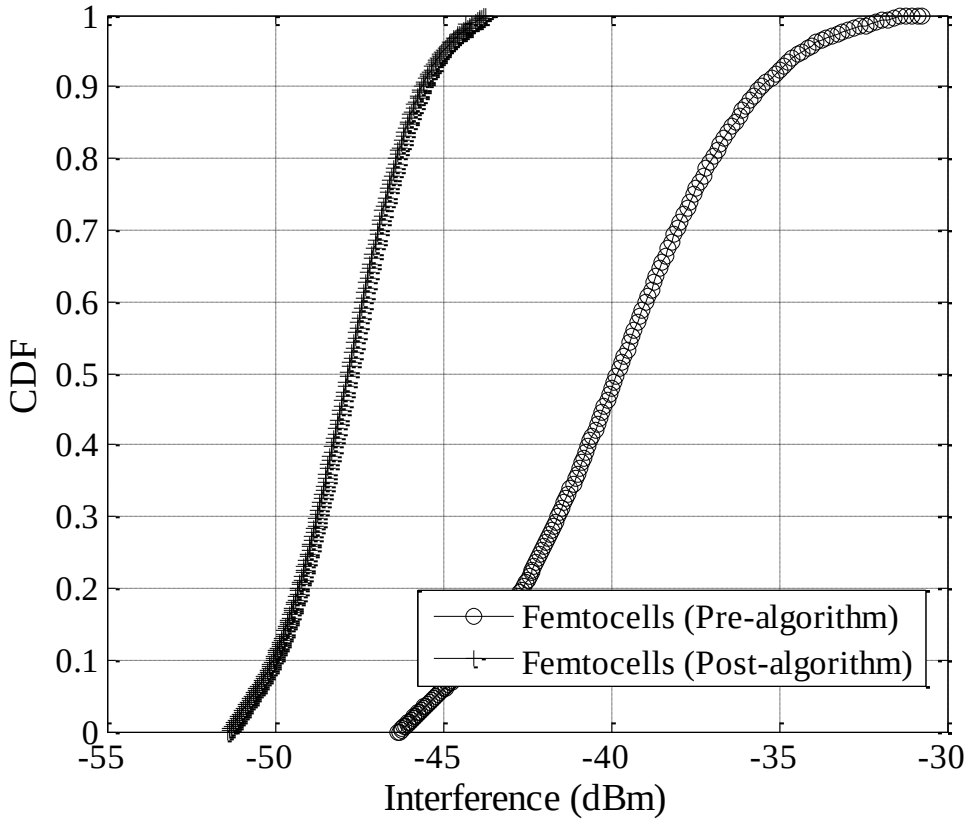

Figure 5.8: Matching policy based Co-Tier Interference Mitigation

5.4.4 Signal to Interference Ratio Comparison

Figure 5.9 compares the signal to interference ratio (SIR) between a random spectrum allocation (Random SA) and the proposed matching policy based spectrum allocation (Proposed SA). The random SA scheme is the situation where FAPs use the RBs of closely located MUEs in contrast to the matching policy based scheme.

Equation 5.7 represents the SIR of the kth UMUE when the nth FAP is using its resources (Random SA) and Equation 8 is the SIR value of the same kth UMUE when the nth FAP is using the resources of the jth DMUE (Proposed SA).

$$SIR_1 = \frac{p_{t\_MBS} - g_{k\_UMUE}^{MBS}}{I_{k\_UMUE}^{n\_FAP}} \quad (5.7)$$

$$SIR_2 = \frac{p_{t\_MBS} - g_{k\_UMUE}^{MBS}}{I_{j\_DMUE}^{n\_FAP}} \quad (5.8)$$

Where p_t^{MBS} is the transmit power of the MBS and $g_{k_UMUE}^{MBS}$is the channel power gain of the MBS on the k^{th} UMUE. $I_{k\_UMUE}^{n\_FAP}$ is the interference on the k^{th} UMUE by the n^{th} FAP and $I_{j\_DMUE}^{n\_FAP}$ is the interference on the j^{th} DMUE by the n^{th} FAP. $I_{k\_UMUE}^{n\_FAP}$ and $I_{j\_DMUE}^{n\_FAP}$ can be further decomposed as $p_t^{FAP} - g_{k\_UMUE}^{FAP}$ and $p_t^{FAP} - g_{j\_DMUE}^{FAP}$ respectively. p_t^{FAP} is the FAP transmit power and $g_{k\_UMUE}^{FAP}$ and $g_{j\_DMUE}^{FAP}$ are the channel power gains of the FAP on the k^{th} UMUE and the j^{th} DMUE respectively.

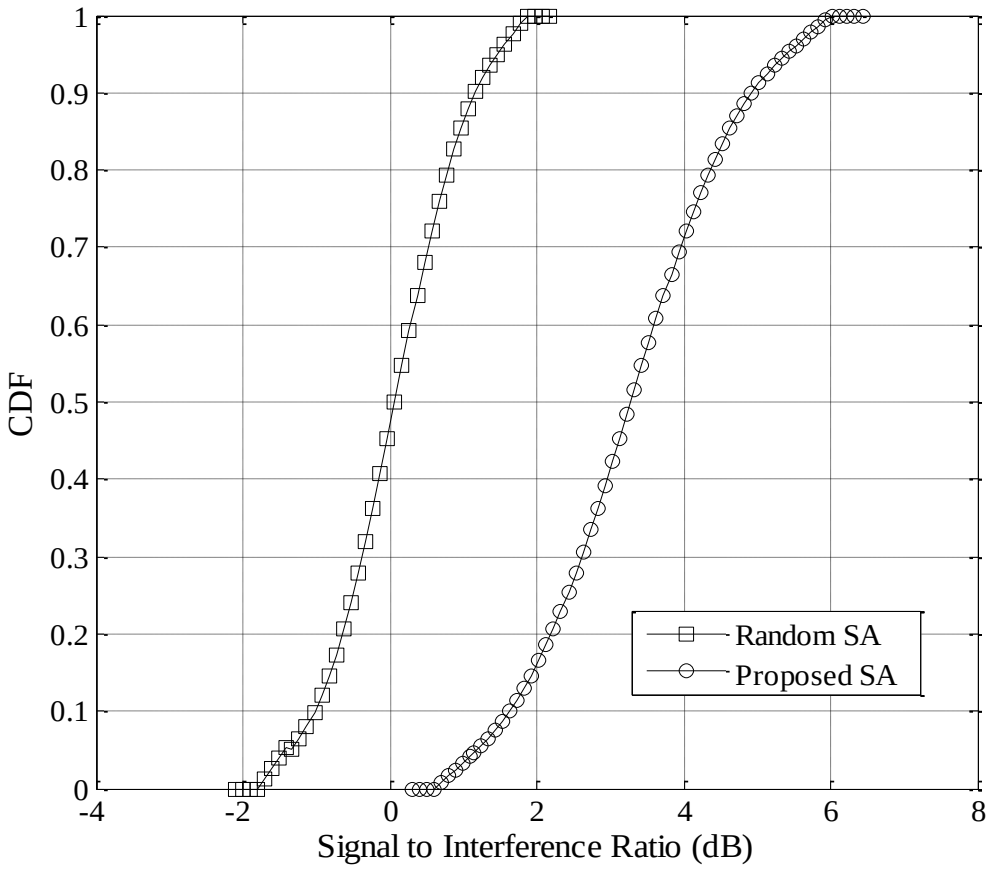

Figure 5.9: Signal to Interference Ratio Comparison

Thanks to the matching policy based spectrum allocation, clearly the proposed scheme results into significantly higher SIR value (3.3 dB) while compared to the random SA with a mean value of 0.1dB.

5.4.5 MUE Mobility Analysis

Referring to Figure 5.1, it is to be noted that based on direction of mobility and distance from serving FAPs, more and more UMUEs can be admitted to FAPs (Algorithm 1). Thus it is important to investigate the effect of MUEs mobility and show its impact on the functionality of the proposed scheme. The random waypoint model implemented describes the movement pattern of independent MUEs by simple terms and was first proposed in [139].

In the simulator, the implementation of this mobility model is as follows: as the simulation starts, each MUE randomly selects one location in the simulation field (which is defined as the region in the macrocell layer) as its destination. It then travels towards this destination with constant velocity chosen uniformly and randomly from [0, V_{max}], where the parameter V_{max} is the maximum allowable velocity for every mobile node [140]. The speed and direction of a node are chosen independently of other nodes. Upon reaching the destination, the node stops for a duration defined by the 'pause time' parameter denoted as T_{pause} . If T_{pause} = 0, this leads to continuous mobility. After this duration, it again chooses another random destination in the simulation field and moves towards it. The whole process is repeated again and again until the simulation ends.

Fig 5.10 investigates the interference intensity posed by mobile MUEs on a FAP as they move in and out of the r = 20m region (Figure 5.1). $UMUE_{static}$ and $DMUE_{static}$ represent the interference intensity values on a particular FAP due to static UMUEs and DMUEs respectively. The interference intensity caused by DMUEs is significantly lower because of the fact that they are located outside the interference region of an FAP. MUE_{mobile} represents

the mean interference intensity values on the same FAP when $UMUE_{static}$ is no more static, rather mobile and several UMUEs move in and out of the FAP interference region thereby increasing the chances of admittance and resulting into reduced interference (around 8 dBm lesser interference intensity compared to static UMUEs).

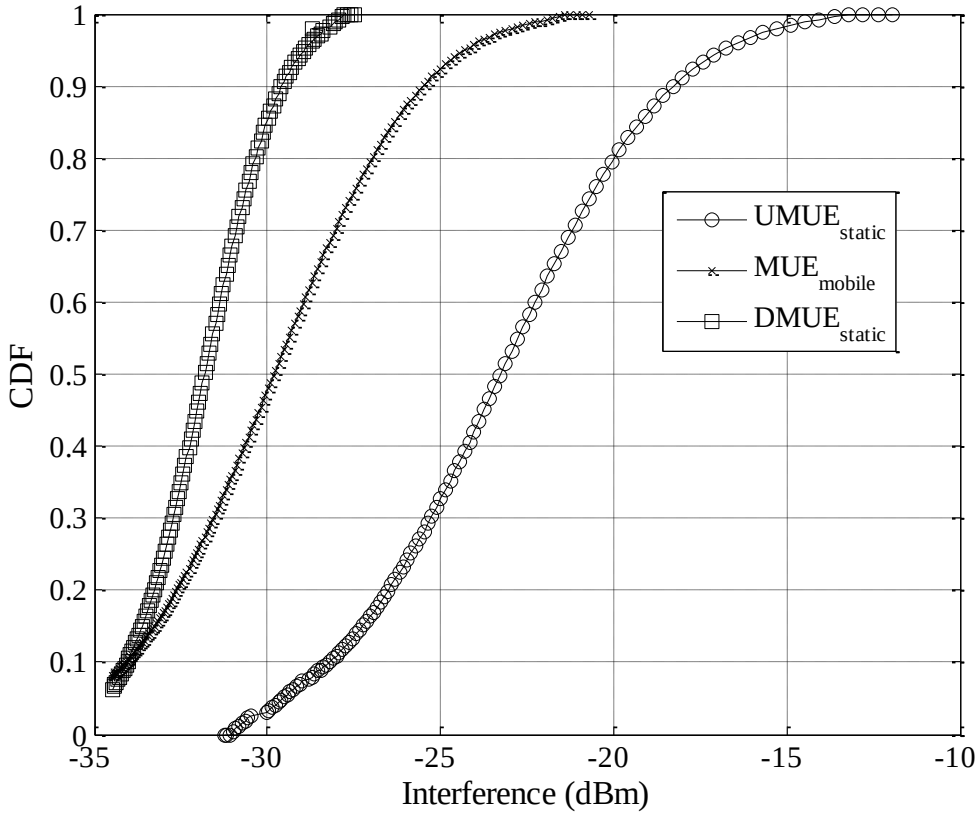

Figure 5.10: MUEs mobility analysis of Proposed Scheme

5.5 Summary

This chapter proposed a joint threshold power based macrocell user equipment admittance and contention free resource block allocation for effective interference mitigation in cognitive femtocells. Cross-tier interference in the proposed scheme is mitigated by allowing admittance by cognitive femtocells of MUEs which are far away from respective MBS and transmitting at higher power levels. Whereas a matching policy based resource allocation is

employed to intelligently allocate resources to the co-located FAPs to avoid any contention or collision thereby resulting in reduced co-tier interference. Performance analysis of the proposed scheme has also found that the scheme performs much better in relation to a random spectrum assignment scheme. The proposed scheme caters very well the mobility of the MUEs allowing more and more admittance thereby providing improved interference results.

In the next chapter, a novel hybrid algorithm scheduling algorithm where CFs assign the RBs of MUEs based on their traffic usage is presented.

Chapter 6

A service associated (SA) scheduling algorithm for cognitive femtocells

In this chapter, a novel effective scheduling algorithm is proposed to address the interference in a two-tier network system. This algorithm is based on the premise that MUEs transmit with different traffic loads and it is highly likely for its assigned resource units or resource blocks (RBs) being either empty or with a low interference. In the SA algorithm, cognitive FAPs (CFs) assign the RBs of macrocell user equipments (MUEs) with a low data traffic load which experience a low interference temperature to its FUEs. Specifically, it focuses on mitigating the downlink FAP interference to nearby macrocell MUE as well as mitigating the uplink interference from MUE towards FAP. Since the proposed interference mitigation scheme requires non-existence of macro-femto backhaul coordination and no modifications, it is promising for applications in the LTE-advanced (LTE-A) cellular systems that employ heterogeneous networks. The performance of the service associated (SA) scheme is presented and the results show an improved SINR, throughput and spectral efficiency as compared to two existing state of the art scheduling algorithms.

6.1 Introduction

Emerging wireless networks support the simultaneous mix of traffic models which demand more flexible and efficient use of the scarce spectral resource. The usage of these traffic models differs per user at different times. Simulations with a mix of realistic traffic models such as Voice over Internet Protocol (VoIP), Hypertext Transfer protocol (HTTP), video, File Transfer Protocol (FTP) and gaming can be mimicked with specifications as defined in [141] to analyse spectral use in a wireless network (Figure 6.1). MUEs usually transmit with varying traffic loads and at times it is highly likely for their assigned resource blocks (RBs) being empty. A scheduling algorithm where CFs assign the RBs of MUEs with a low data traffic load which experience a low interference temperature to its FUEs is presented. Figure 6.1 depicts 10 MUEs, each assigned 4 RBs by the MBS, transmitting using different traffic applications. It is highly unlikely in most cases for each MUE to fully utilize its assigned resource units or 4 RBs as shown in Figure 6.1 with some utilizing 3 RBs or just 1 RB.

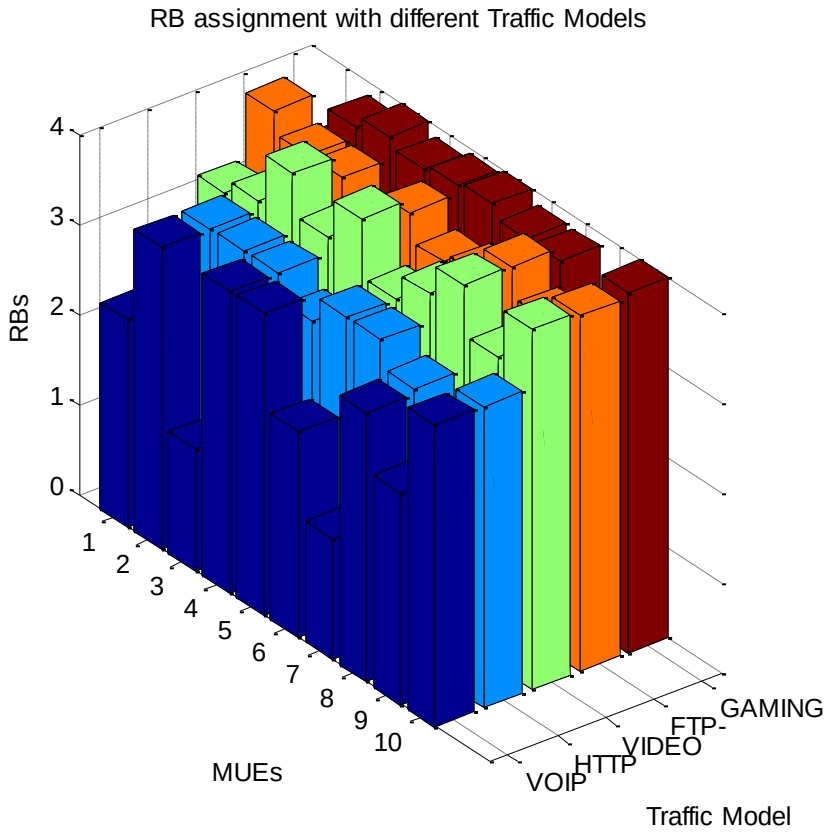

Figure 6.1: Macrocell scenario with varying RB usage/Traffic model

Contrary to exclusive RB allocation considered in previous works, the scheme opportunistically controls the number of RBs shared with other cells in a statistical sense to maximize FUE and MUE SINR. The adaptive resource block sharing is based on not instantaneous but statistical interference levels among cells to satisfy practical implementation constraints. The gains of the adaptive resource block sharing based on statistical interference levels among cells are demonstrated. The proposed scheme achieves higher average FUE SINR than conventional resource scheduling schemes.

6.2 Traffic aware matching Policy based Interference mitigation

The scheme could be best described with the help of Figure 6.2. The MBS periodically broadcasts the traffic load $n(t)$ of all its MUEs via signalling interface. CF is able to retrieve

traffic load data of MUEs up to a distance of 40m. The choice of sensing up to 40m is to enable a FAP sense and retrieve as much empty RBs from MUEs as possible at a distance slightly above its coverage radius which is pegged at 20m. On the other hand, exceeding a 40m will introduce sensing overhead which will be detrimental to the algorithm since it is a time dependent opportunistic approach of using resources. Also it is fair to assume this radius in a densely deployed femtocell. The proposed algorithms both for cross-tier and co-tier interference mitigation are explained in the following sections.

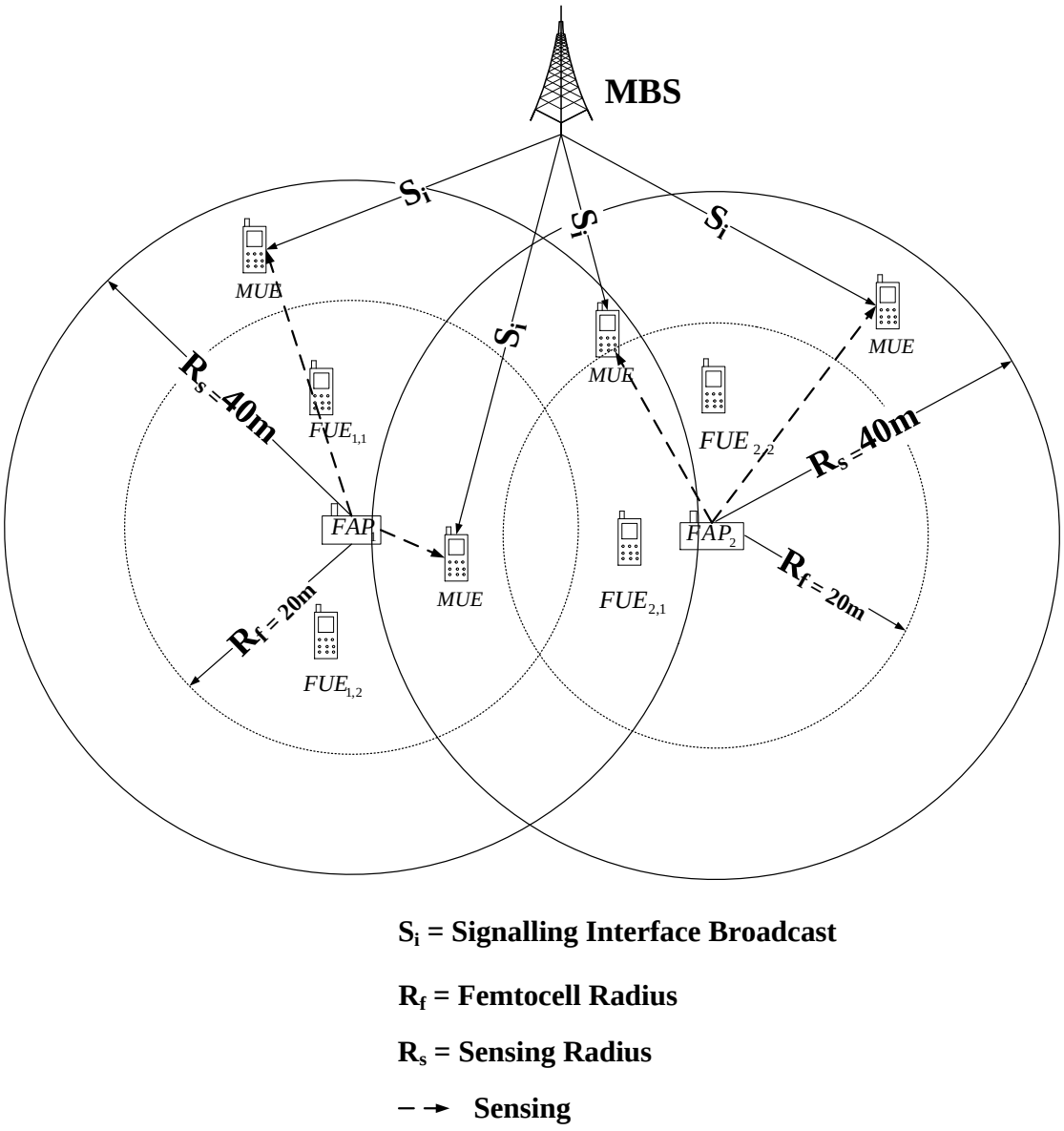

Figure 6.2: A collocated femtocell scenario with MBS signalling interface

6.2.1: SA Cross-Tier Interference Mitigation

RB retrieving strategy: During each scheduling interval, the MUEs are scheduled with RBs from the set:

$$A = m_i : 1 \leq i \leq n(t) \tag{6.1}$$

where mi denotes ith 180kHz sub-band over the system bandwidth and $n(t)$ represents the instantaneous traffic load generated from MUEs at time τ.

Let $\tau =$ TTI = 1ms

In SA algorithm, a CF schedules a FUE on the RB of a MUE with the least traffic load or minimum performance metric for each RB from its throughput analysis and can be expressed as in [21]:

$$k_{i,j}(\tau) = \arg min \left({}^{R_{i,j,k}(\tau)} \Big/ _{R_{k,i}(\tau)} \right) \tag{6.2}$$

Where $k_{i,j}(\tau)$ is the chosen UE in component carrier (CC) i and in RB j at a specific ime τ, $R_{i,j,k}(\tau)$ is the throughput, and $R_{k,i}(\tau)$ is the average last throughput of user k [142]. Therefore, the average throughput of each UE is updated for each j according to:

$$R_{k,i}(\tau + 1) = \begin{cases} R_{k,i}(\tau)\left(1 - \frac{1}{t_c}\right) + \frac{1}{t_c} R_{i,j,k}(\tau), & k = k_{i,j}(\tau) \\ R_{k,i}(\tau)\left(1 - \frac{1}{t_c}\right), & k \neq k_{i,j}(\tau) \end{cases} \tag{6.3}$$

where t_c is the time constant [22]. In SA, each CF retrieves this traffic load $R_{k,i}(\tau + 1)$ via the broadcast signalling interface and makes a table known as the traffic load map of all the MUEs within the distance as shown in Table 6.1.

Table 6.1: Dynamic Traffic Load Map

RB			

	TTI_1	TTI_2	TTI_3
RB_1	1	1	0
RB_2	0	1	0
RB_3	0	1	1
RB_4	0	1	1
.		.	.
.		.	.
.		.	.
RB_n	1	0	1

In Table 6.1, at every TTI the traffic load of all the RBs attached to all the MUEs is retrieved and interpreted as:

1 = high data traffic

0 = Low data traffic

Therefore, assume for every femtocell i, $(i \in \{1,2, \ldots . F\})$, we have an $N \times 1$ vector f_i ,

Where each element $f_i^w \in \{0, 1\}$ denotes whether a FAP will use the RB w when it is 0 or not when it is 1.

6.2.2: SA Co-Tier Interference Mitigation

Co-tier interference mitigation focuses on the effective usage of retrieved RBs which is denoted as available RBs among FAPs. In the solution, an RB is assigned to a FUE by its FAP for its sole use at every TTI (Table 6.2).

Table 6.2: RBs assignment to FUEs/TTI

RB	RB_1	RB_2	RB_3	RB_4	RB_5	RB_6	RB_7	RB_8	RB_9	RB_{10}
TTI	1	0	0	0	1	1	1	0	0	1

In SA, each FAP will maintain a table similar to Table 6.2, although it will be an extensive table highlighting all the TTIs (say up to $TT1_{10}$). Importantly, the RBs that will be available

to share will be ones with low data traffic, such as RB_2, RB_3, RB_4, RB_8 and RB_9. For instance, if we have 50 RBs available and 10 collocated CFs, the RBs are shared equally which will be 5 RBs/CF. The basis for an outright sharing formula is because, through cognition, retrieved RBs of MUEs can be used by FUEs while keeping interference at its barest minimum. Also, the number of RBs will always be more than FUEs since a CF (in this scenario a home CF) will only accommodate 4 FUEs.

Assume for every femtocell, f_n ,

$$f_n = \alpha_n + \beta_n \tag{6.4}$$

$$\alpha_n = \{RB_{n,1,} RB_{n,2,} \dots RB_{n,n}\} \tag{6.5}$$

$$\beta_n = \{RB_{n,1,} RB_{n,2,} \dots RB_{n,n}\} \tag{6.6}$$

Where α_n and β_n are the list of occupied RBs and available RBs respectively in the n^{th} FAP. After sensing, each CF is able to deduce its list of α_n and β_n. Since femtocells may be collocated with no coordination between them, they can have similar α_n and β_n. In order to resolve contention among available RBs, a matching policy is introduced to uniquely match retrieved (available) RBs to each CF. The matching policy determines which CF utilizes a particular RB from its list of β_n to avoid co-tier interference. To implement the matching policy in every CF_i, we also have a $N \times 1$ vector p_i where each of the elements p_i^w represents the transmit power of a RBw and similarly $N \times 1$ vector q_i where each of the elements q_i^w represents the transmit power in the MBS.

In the proposed SA, a cognitive enabled scheduling engine to create a matching policy is introduced as follows:

Through sensing, the scheduling engine E, is aware of the locations of the FAPs (FAP_{LOC}) and MUEs (MUE_{LOC}) of the retrieved RBs in the network. CR enables the femtocell to

identify the SINR of the FUE in FAPi on the RBw. To derive the SINR, Let the following channel gain variables be introduced as:

Channel gain L from:

FAPj to FAPi: $L_{j,i}^{w}$; FAPi to FUEi: $L_{i,i}^{w}$; MBS to FAPi: $L_{b,i}^{w}$; FAPi to MBS: $L_{i,b}^{w}$ and MBS to MUE: $L_{b,b}^{w}$

Therefore the SINR as perceived by a FUE on an available RBw in β_n is given by:

$$SINR_i^w = \frac{f_i^w p_i^w L_{i,i}^w}{f_i^w q^w L_{b,i}^w + \sum_{j=1, j\neq 1}^{F} f_i^w f_j^w p_j^w L_{j,i}^w + N} \quad (6.7)$$

Where N is the Gaussian noise.

Co-tier interference mitigation is further explained as follows.

Let $E = \{1,2,\ldots,K\}$

i. Each FAP in the network submits its list of β_n to E. This list is periodically updated due to the availability of retrieved RBs in β_n.
ii. E selects a RB from β_n iteratively and maps it against its list of FAP.
iii. E calculates the $SINR_i^w$ of an FUE on an available RBw in β_n as in Equation 6.7
iv. A RB with the highest $SINR_i^w$ is assigned to a FAP and the process continues until all the RBs in β_n (which is denoted in the algorithm as $N_{RB}w\_left$) are uniquely assigned to each FAP in the network as shown in Figure 6.3 and the algorithm pseudo code given below in Table 6.3.

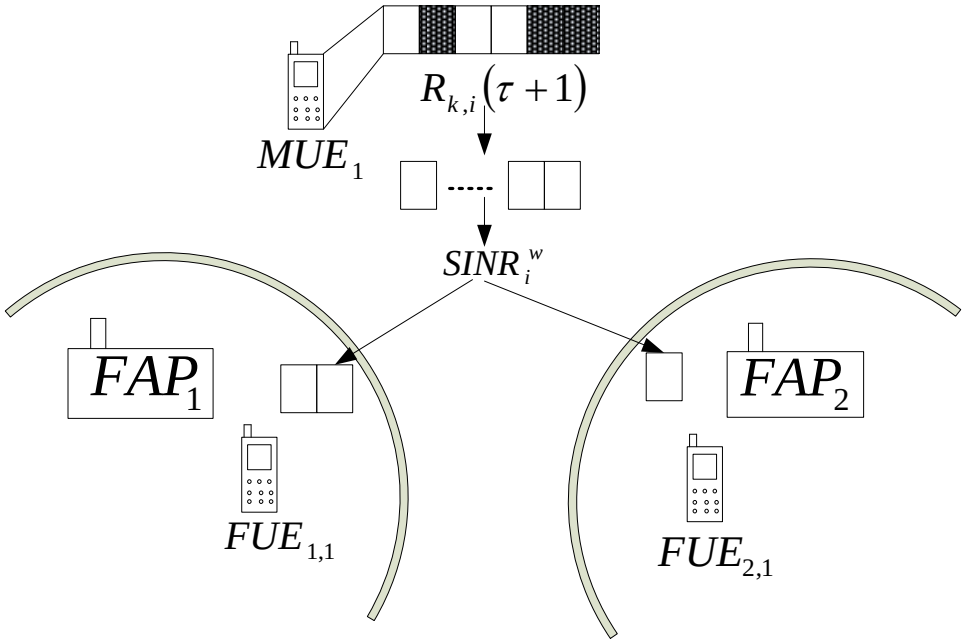

Figure 6.3: Matching policy based scheduling for co-tier interference mitigation

Table 6.3: Co-tier interference Mitigation- RBs Matching policy
Initialization;
$\boldsymbol{E = \{1, 2, \ldots, K\}}$
1: for $\boldsymbol{RBw\ 1 : N_{RB}w}$
2: calculate $\boldsymbol{RBw_1, SINR_i^w = \max\_value : \min\_value}$
3: set $\boldsymbol{RBw_1 = \max\_value\{f_i\}}$
4: for $\boldsymbol{RBw_2}$
4: calculate $\boldsymbol{SINR_i^w = \max\_value : \min\_value}$
6: set $\boldsymbol{RBw_2 = \max\_value\{f_i\}}$
7:Continue loop until $\boldsymbol{N_{RB}w\_left = \text{zero}}$
8:end

6.3 System model

Consider an OFDMA system where the femtocell and macrocell are deployed in a co-channel fashion. The MBS is in the centre of the network and serves the randomly distributed MUEs within its coverage area. Since there is more activity of MUEs in the downlink (DL) and less activity in the UL, more focus is paid on downlink interference in the system model. N_{FAP} femtocells are randomly located within the coverage area of the MBS and the number of MUEs within the coverage area of j^{th} femtocell is denoted as $j = \{1, 2, \ldots, N_{FAP}\}$. In the

system model MUEs locations are assumed to change per TTI. The CFs in the network operates as a CSG which means MUEs outside its coverage area are not allowed to avail services from it. The simulation parameters are based on 3GPP LTE specifications and given in Table 6.4. The considered network topology consists of a MBS with 30 CFs randomly distributed with four FUEs attached to each CF in a CSG fashion.

Table 6.4: System Parameters

Parameter		Value
Macrocell		
Cell layout		Dense-urban 3-sector MBS
Carrier Frequency		2.14 GHz
Bandwidth		20 MHz
Antenna configuration		SISO(for both BS and UE)
Transmit power		46 dBm (MBS)
Inter-site distance		500m
Total number of MBS/MUE		1/60
Channel model		Winner+
Traffic model	VOIP, HTTP, video, FTP, gaming	% of users = [30,20,20,10,20] (as defined in 3GPP RAN R1-070674) [1]
Log-normal shadowing		8dB
Mobility Model		Random walking Model
TTI		1ms
Path loss: MUE to macro MBS	Outdoor MUE	$PL(dB) = 15.3 + 37.6 \log_{10} R$
	Indoor MUE	$PL(dB) = 15.3 + 37.6 \log_{10} R +$ 10
Femtocell		
Transmit power		20 dBm
Total number of FAP/FUE		30/120
Penetration loss		10dB indoor
Path loss: FUE to FAP	Dual-stripe model	$PL(dB) = 127 + 30 \log_{10} {}^{R}/_{1000}$

6.4 Fading Modelling

To highlight the performance of the algorithm two types of fading namely Claussen fading and multi-path fading are incorporated in the simulations. The choice of these two fading

models is to present the effect of two different levels of destructive interference on the radio channel.

6.4.1 Claussen fading

Claussen fading model, is incorporated in the system level simulation which makes it possible to generate and save the environment maps of path loss and shadowing of all potential locations as introduced in [143]. This significantly reduces the computational complexity of deriving the shadow fading correlations from conventional means such as based on mobile velocity of UEs [144]. In modelling claussen fading in the simulations, the fading values are derived based only on the correlation with respect to the neighbouring values in the map as illustrated in Figure 6.4. Each of the fading values denoted S_1, S_2, and S_3 is calculated with the correlation matrix R and L from [142].

$$R = \begin{bmatrix} 1 & r(x) \\ r(x) & 1 \end{bmatrix} \quad \text{and} \quad L = \begin{bmatrix} 1 & 0 \\ r(x) & \sqrt{1 - r^2(x)} \end{bmatrix} \tag{6.9}$$

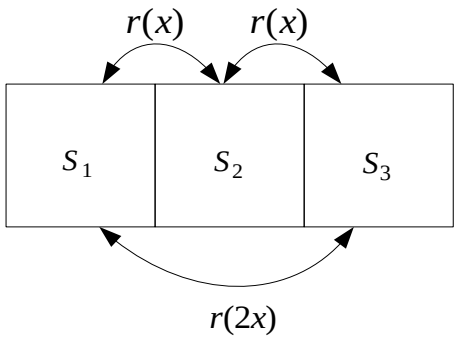

Figure 6.4: Claussen Fading

$$S_1 = a_1 \tag{6.10}$$

$$S_2 = r(x)S_1 + \sqrt{1 - r^2(x)}a_2 \tag{6.11}$$

$$S_3 = r(x)S_2 + \sqrt{1 - r^2(x)}a_3 \tag{6.12}$$

S_3 can also be written as:

$$r^2(x)a_1 + r(x)\sqrt{1-r^2(x)}a_2 + \sqrt{1-r^2(x)}a_3$$

Where, a_1, a_2, and a_3 are generated in dB as distributed random variables with standard deviation.

The Mutual Information Effective SINR metric (MIESM) [26] is adopted for the simulation. To achieve this, the average Mutual Information (MI) on all RBs over all UEs is deduced. Subsequently, the effective SINR, $y_{eff(dB)}$), per RB in every TTI is calculated.

The system level spectral efficiency per RB per TTI can be expressed as:

$$R_{sys} = \propto log_2\left(1 + 10^{\frac{y_{eff(dB)}}{10}}\right) \quad (6.13)$$

6.4.2 Multi-path fading

In cellular communication, the RF signal propagates from the transmitter to the receiver via multiple-paths due to the obstructions and reflectors existing in the wireless channel. These multi paths are caused by diffraction, reflection, and scattering from buildings, structures, and other obstacles existing in the environment.

When a MUE is considerably far from the MBS or a FUE is in a different location from its serving FAP, the line of sight (LOS) signal is not achievable and reception occurs mainly from the indirect signal paths. These multiple paths have various propagation lengths, and thus will cause phase and amplitude fluctuations and the received signal time will be delayed. Therefore, the main effect of multipath propagation can be described in terms of fading and delay spread.

The multi-path fading implemented in the simulation is the Rayleigh fading [145]. It is modelled as follows;

The transmitted signal $s(t)$ is assumed to be from an unmodulated carrier and it takes the form:

$$s(t) = \cos(2\pi \mathrm{f_c t}) \tag{6.14}$$

where $\mathrm{f_c}$ is carrier frequency of the radio signal.

The transmitted signal is modeled to be propagated over N reflected and scattered paths. The received signal is calculated as the sum of these N components with random amplitude and phase for each component. The received signal $r(t)$ can be written as:

$$r(t) = \sum_{i=1}^{N} a_i \cos(2\pi \mathrm{f_c t} + \varphi_\mathrm{i}) \tag{6.15}$$

where a_i is a random variable equivalent to the amplitude of the i^{th} signal component, and φ_i is also a uniformly distributed random variable equivalent to the phase angle of the i^{th} signal component.

6.5 Simulation results

In this section, the effectiveness of the scheduling algorithm for interference mitigation in a two-tier CF network is evaluated and compared with best Channel Quality Indicator (CQI) [146] and Proportional Fair (PF) schedulers [147]. Also, the effect on throughput and spectral efficiency are investigated through simulations. The cross tier analysis is divided in two so as to look at the scheduling algorithms in varying channel conditions with a fading and no fading cross-tier analysis. Further analysis is conducted with the increment of MUEs in the network to reflect how it affects the algorithms in both channel conditions while keeping the FUEs constant.

6.5.1 Cross-Tier Interference Mitigation (No Fading):

Figure 6.5 presents comparative analysis of the average UEs wideband SINR. Clearly SA results into higher values of SINR (c.a. 22.5 dB) compared to best CQI (c.a. 19 dB) and PF (c.a. 18 dB). The reasons behind this achievement are laid out as follows. In a two-tier co-channel network where FAPs are generally randomly deployed with no coordination, RBs which are used by MUEs are reused by FUEs which introduces mutual interference on both parties. In best CQI, RBs are assigned to the MUEs with the best radio link conditions; an MUE which is not close to its serving MBS can suffer greatly in the presence of collocated FAPs. These FAPs which are uncoordinated vie to reuse same RBs as of this MUE even though they may have a higher channel gain over the RB. This increases the interference due on that particular MUE resulting into reduced SINR (as shown in Figure 6.5). In SA, scheduling is coordinated to avoid a situation like this by only reusing RBs available and unused by an MUE. On the other hand, best CQI performs slightly better than PF because scheduling is primarily based on fairness in PF, with lesser emphasis on interference mitigation.

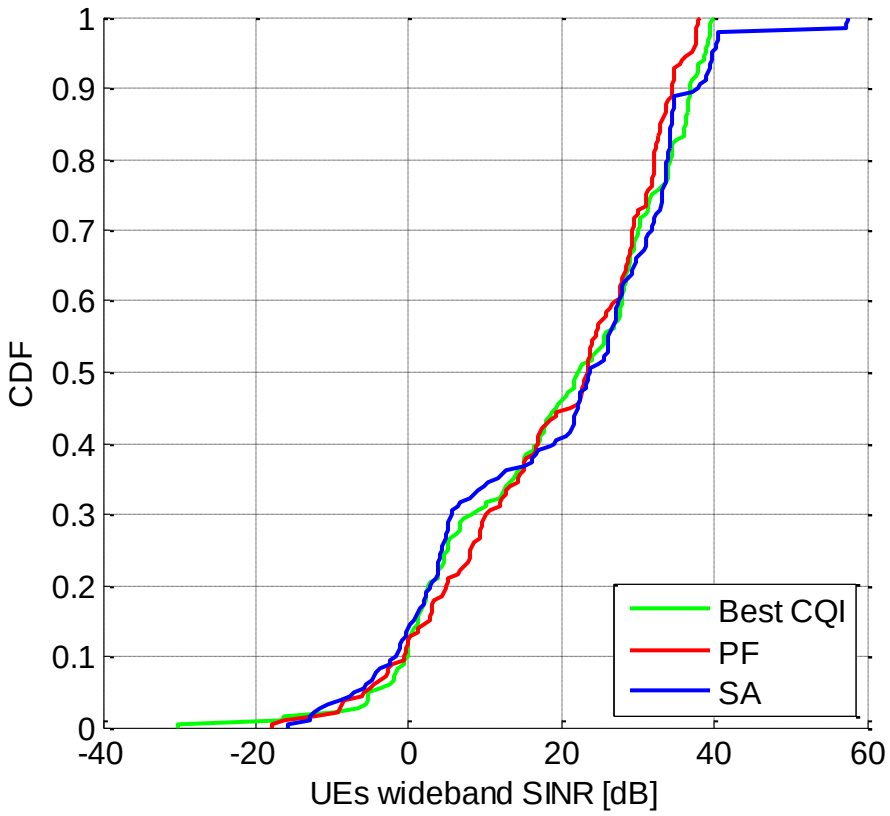

Figure 6.5: Average UEs wideband SINR (No Fading)

Figure 6.6 shows the average throughput gap of the UEs of SA against best CQI and Proportional fair (PF) schedulers. The UEs were randomly distributed scattered around from the cell centre to the cell edge to reflect diversity in deployment and channel conditions. In line with the results of SINR, SA scheduler achieves better throughput, around 37 Mbps, compared to 25 Mbps and 21 Mbps for best CQI and PF schedulers respectively. The SA scheduler benefits from the CFs diversity where available and unused RBs are allocated to FUEs while fulfilling a coordinated strategy. Thus irrespective of the channel conditions, the UEs are able to achieve higher and considerate throughput levels. On the other hand, although best CQI uses a channel indicator coefficient to allocate RBs, however higher interference values accordingly result into lesser throughput for CQI as compared to SA. PF scheduler respects fairness among UEs thereby resulting into reduced average system throughput.

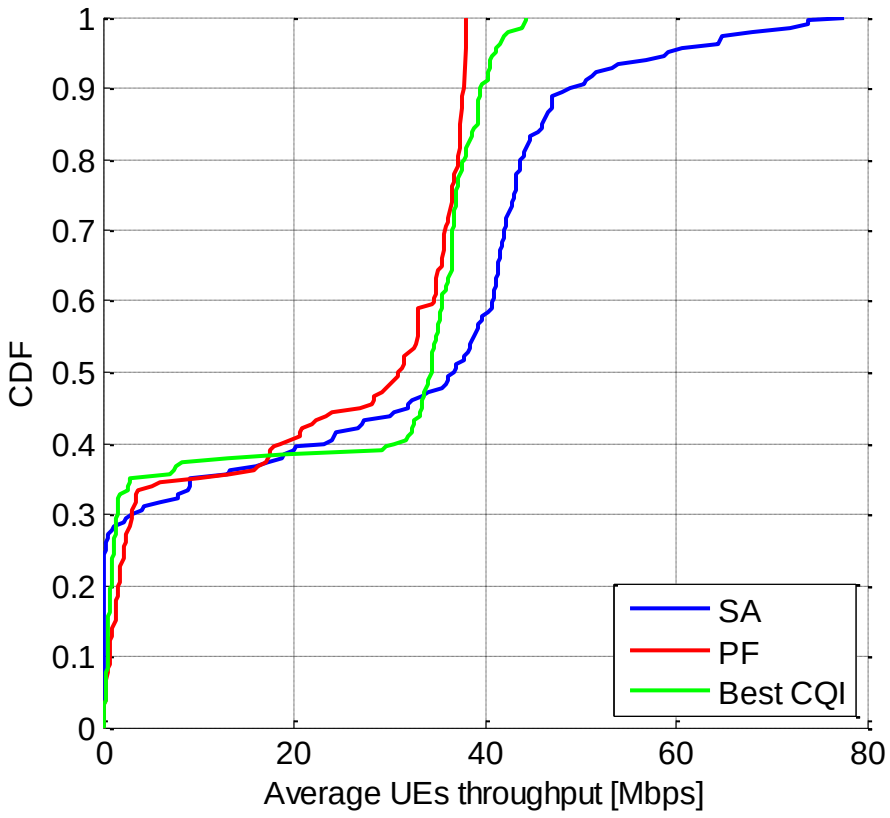

Figure 6.6: Average UEs throughput (No Fading)

Figure 6.7 presents comparative analysis of the average spectral efficiency. In line with the results of SINR and throughput, SA has a spectral efficiency of 10 bits/cu compared to best CQI (8 bits/cu) and PF (around 7 bits/cu). The reason SA performs better over both other schedulers can be described by looking into parameters α_n and β_n. In SA scheme, it is considered that the RBs in α_n are always fully utilized by MUEs. The RBs in β_n on the other hand are shared between the CFs in the network. Home based CFs are incorporated in the simulation which accommodates up to 4 FUEs. With a total of 120 CFs in tri-sector network, the RBs were shared equally among the 30 CFs in the network resulting into higher spectral efficiency. Using enterprise FAPs which accommodate up to 16 FUEs per FAP, it is assumed that the spectrum efficiency will be even higher. Best CQI has slightly higher spectral efficiency compared to PF, as it increases cell capacity and in turn spectral efficiency at the expense of fairness.

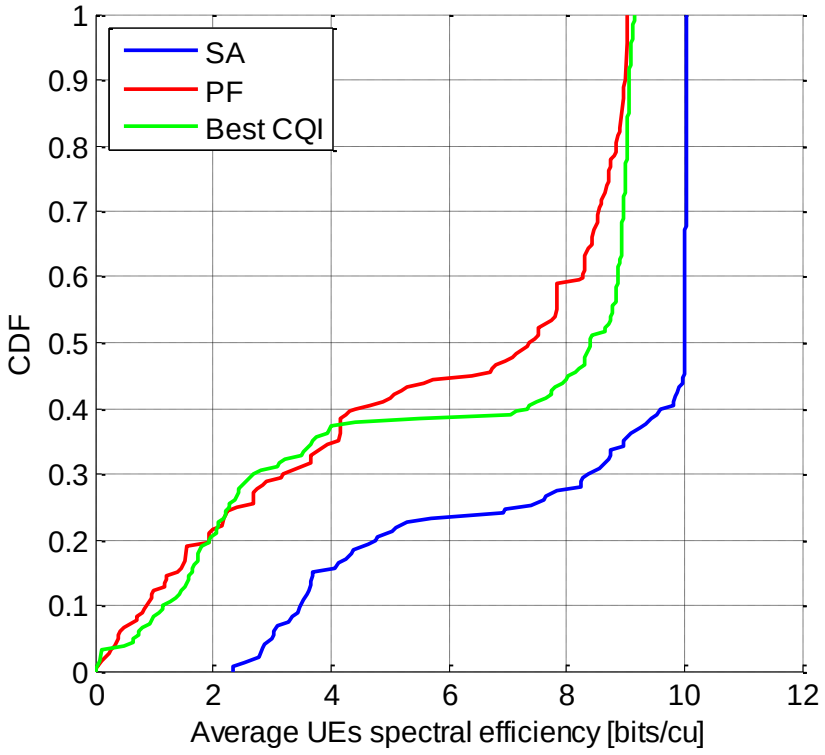

Figure 6.7: Average UEs spectral efficiency (No Fading)

Figure 6.8 and Figure 6.9 conclude the non-fading analysis, where the SINR and throughput values are computed and compared for the three schemes by varying number of MUEs, i.e. lighter to denser deployment analysis. As shown in Figure 6.10, compared to SINR value of 22dB (for 20 MUEs), SINR drops to 17dB (30 MUEs) and 13 dB (50 MUEs) for SA scheme due to the added strain on the network. It only reflects a reduced SINR which is proportional to increased interference from augmented number of MUEs. However, SA mirrors better SINR compared to best CQI and PF schedulers. In line with the SINR results, Figure 6.10 shows how UEs average throughput change for all the compared schemes with varying number of MUEs. Clearly SA provides encouraging results compared to the best CQI and PF schedulers when more MUEs are formed part of the network.

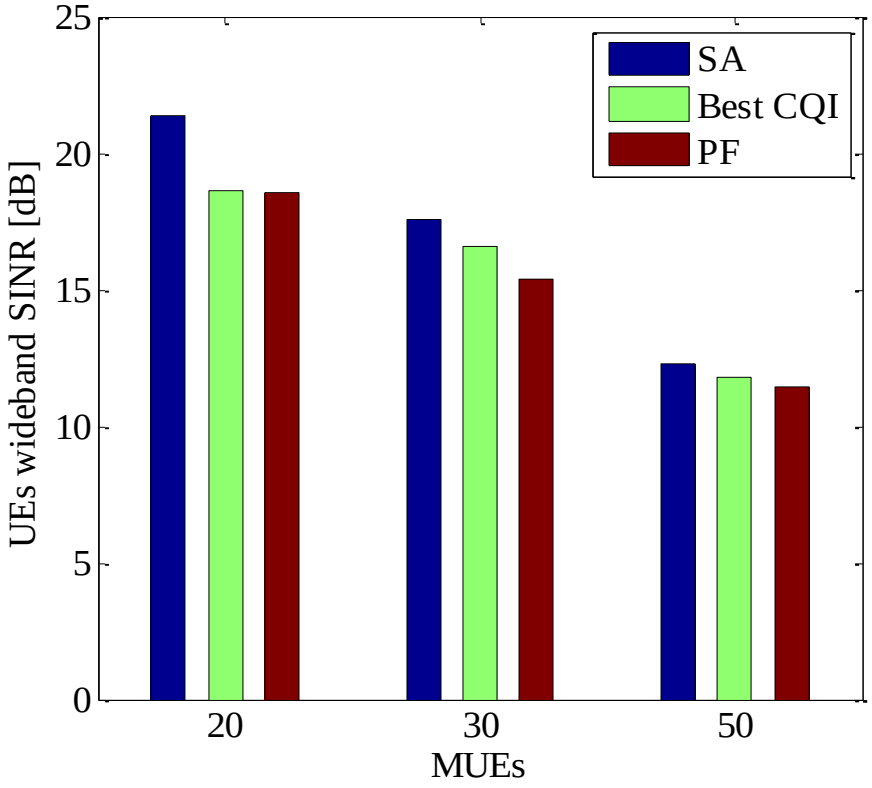

Figure 6.8: UEs Wideband SINR with varying number of MUEs (No Fading)

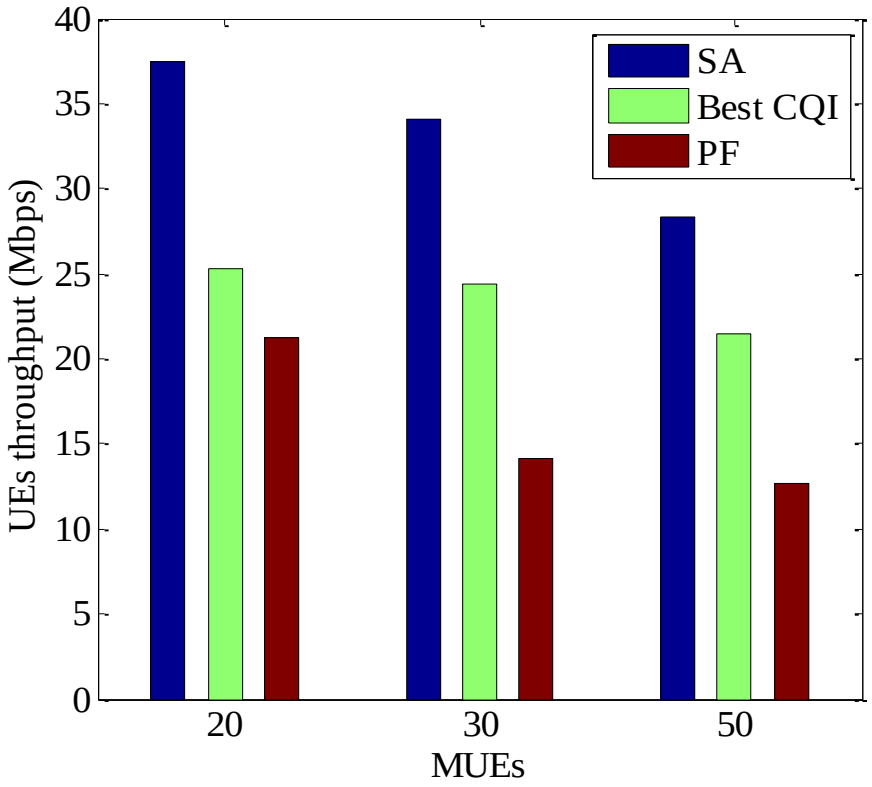

Figure 6.9: UEs Throughput with varying number of MUEs (No Fading)

6.5.2 Cross-Tier Interference Mitigation (With Fading):

Simulations were performed with the same system parameters in the presence of claussen and rayleigh fading. For clarity, straight line plots with subscript “c” represent claussen fading while dotted line plots with subscript “r” represent rayleigh fading. Figure 6.10 shows the average UEs wideband SINR. In claussen fading, 50 percent of the UEs in SA have an SINR of 19.5 dB. It is evident that fading has somehow affected SA more compared to best CQI (c.a. 19 dB) and PF (c.a. 18 dB). Even though SA is somehow independent of channel conditions, however, compared to no fading, SA has slightly reduced SINR value in the presence of fading as there are now lesser RBs available to be utilised due to employment of channel conditions.

However, in the presence of rayleigh fading, the average received power of each UE is lower due to obstacles which increases the outage probability. This outage probability increases further as a result of doppler effect which is directly proportional to UE mobility (speed). The average SINR in best CQI and PF are similar with 50 percent of the UEs at 9.8 dB. Since SA opportunistically utilizes the resources of MUEs, it is capable of re-using the resources of MUEs who suffer less degradation hence a much better average SINR of 18.5 dB.

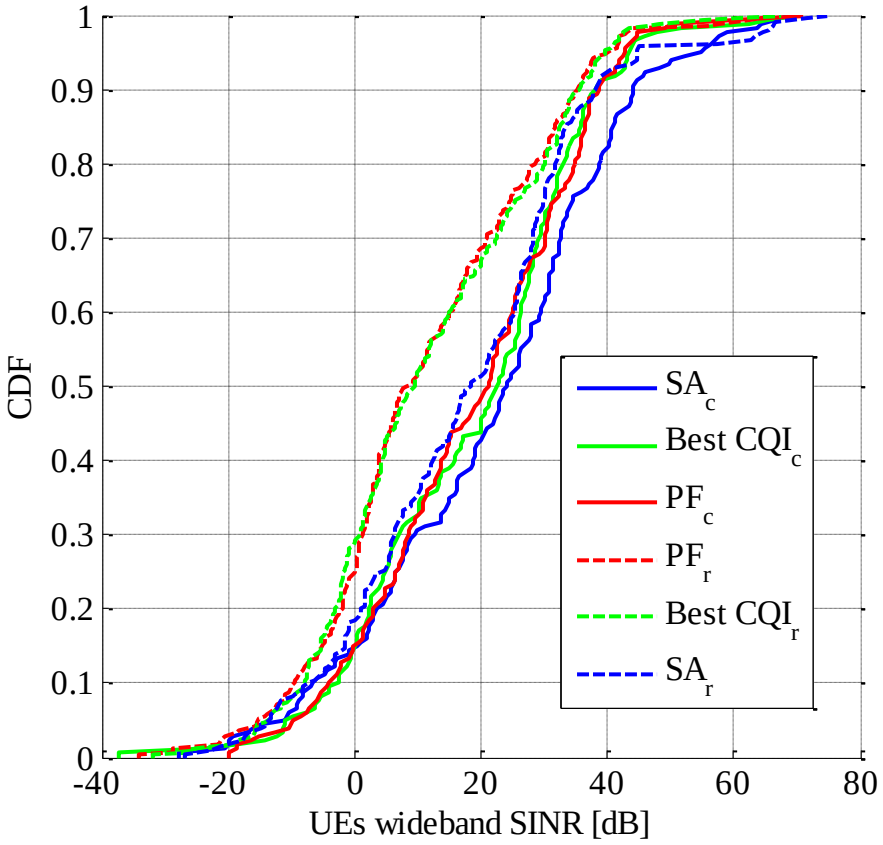

Figure 6.10: Average UEs wideband SINR (With Fading)

Figure 6.11 shows the variation of the throughout for both claussen and rayleigh fading. SA experiences lesser throughput (33 Mbps, Figure 6.11) in claussen fading, compared to no fading. The throughput for CQI is not affected much by the channel conditions because of the fact that CQI takes into account channel conditions. PF again performs poorer in fading conditions (17 Mpbs) because of its preference to fairness. The combined propagation in Rayleigh fading, on the other hand, yields lower channel capacity, which affect all schemes. The transmitted packets experience fading and the receiver may not detect the faded packets even without collision.

With an average throughput of 15 Mbps PF performs poorly because in the presence of interference from other packets in multi-path fading, it does not offer service differentiation even for traffic with different QoS requirements. Best CQI on the other hand offers service

differentiation as it assigns the best links during channel degradation to the users with the best channel quality thereby experiencing an average throughput of 22 Mbps. SA, with an average throughput of 24 Mbps performs better than both PF and SA because it capitalises on schemes like SA where it is able to utilise resources of the UEs with the best links.

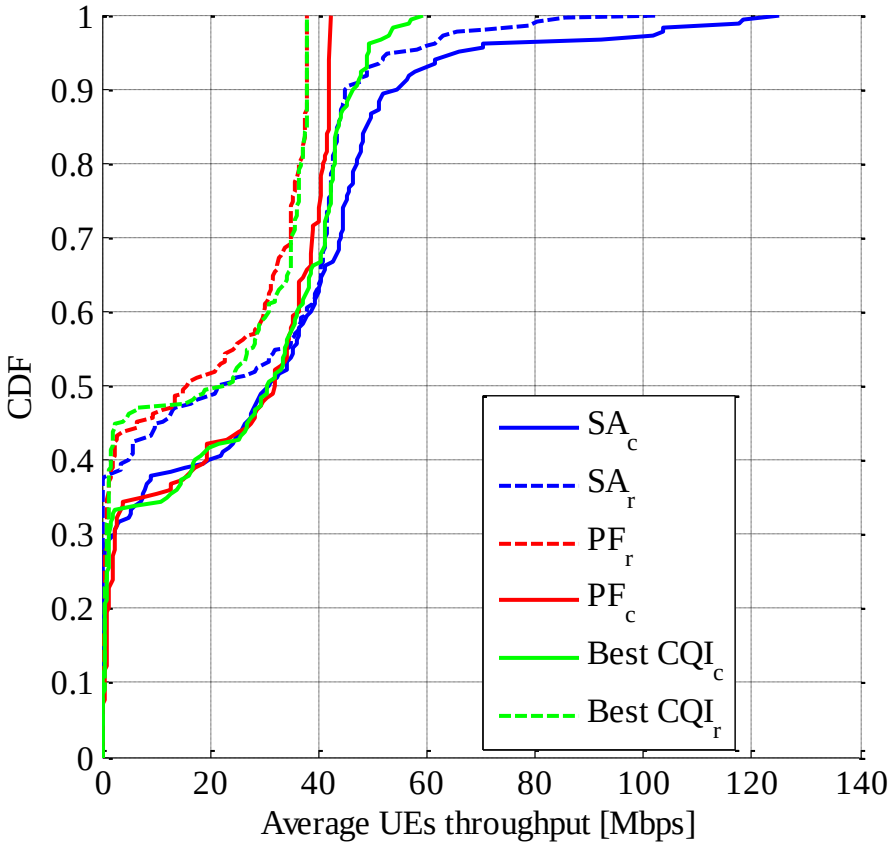

Figure 6.11: Average UEs throughput (With Fading)

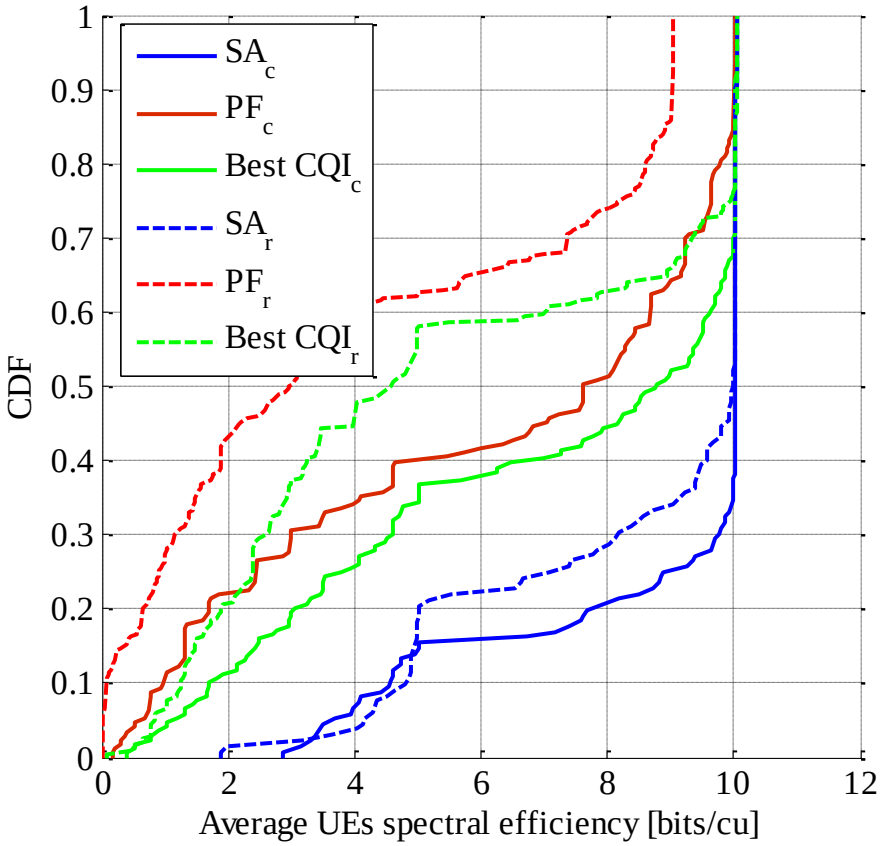

Figure 6.12: Average UEs spectral efficiency (With Fading)

In figure 6.12, the spectral efficiency was simulated for each scheme. Compared to no fading results, the average spectral efficiency for best CQI and PF under claussen fading change significantly with best CQI at 6.779 bits/cu compared to PF at 5.588. In the presence of further degradation from rayleigh fading, spectral efficiency is reduced significantly for best CQI and PF with 50 percent of the users utilising 4.6 bits/cu and 3.2 bits/cu respectively. This is because the multi-path channel has the effect of spreading or broadening the transmitted pulse thereby reducing channel availability.

However, the effect of claussen and rayleigh in SA is not noticeable as 50 percent of the users still have an efficiency of 10 bits/cu. This is simply because in SA, unlike in PF and best CQI, SA has the capability to utilise as many available and non-degraded resource units.

Figure 6.13 and 6.14 presents claussen fading analysis and provides SINR and throughput values against MUEs. Even though SA still provides competitive and slightly better values over the compared schemes, however it is clear that the presented scheme has been affected more in the presence of fading compared to best CQI and PF. The main reasons are the fact that lesser RBs are available for assignment by SA in fading conditions compared to no fading conditions resulting in to slightly reduced SINR and throughput values. The added strain on the network applies equally both for claussen fading and no fading conditions and accordingly reflected in the results.

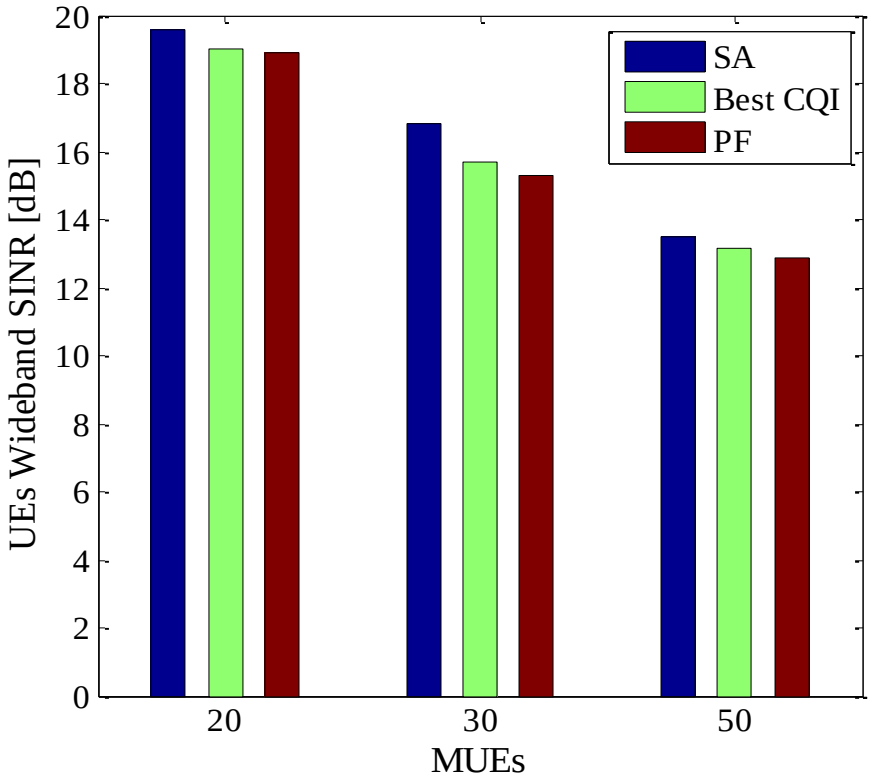

Figure 6.13: UEs Wideband SINR with varying MUEs (With Fading)

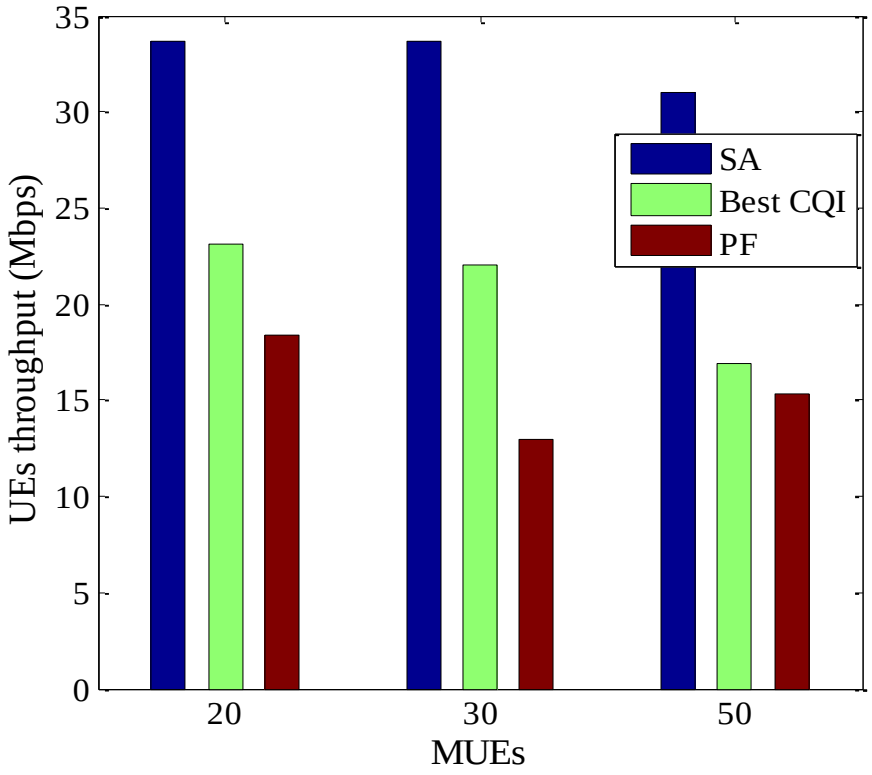

Figure 6.14: UEs throughput with varying MUEs (With Fading)

6.5.3 Co-tier Interference Mitigation

The effect of the matching policy algorithm (Section 6.2) for co-tier interference mitigation is evaluated and the results are presented in Figures 6.15, 6.16, and 6.17 for SINR, throughput and spectral efficiency respectively. To analyse the co-tier environment, the simulation is streamlined to include only collocated CFs and FUEs to reflect higher interference temperature. The performance of the presented algorithm in Section 6.2.2, denoted by matching policy 'MP' with a conventional scheduling denoted as 'NO MP' is investigated and compared. Unlike 'MP' which is presented in Section 6.2.2, 'NO MP' represents a scenario where no coordination exists between FAPs and all FAPs vie for same resources simultaneously.

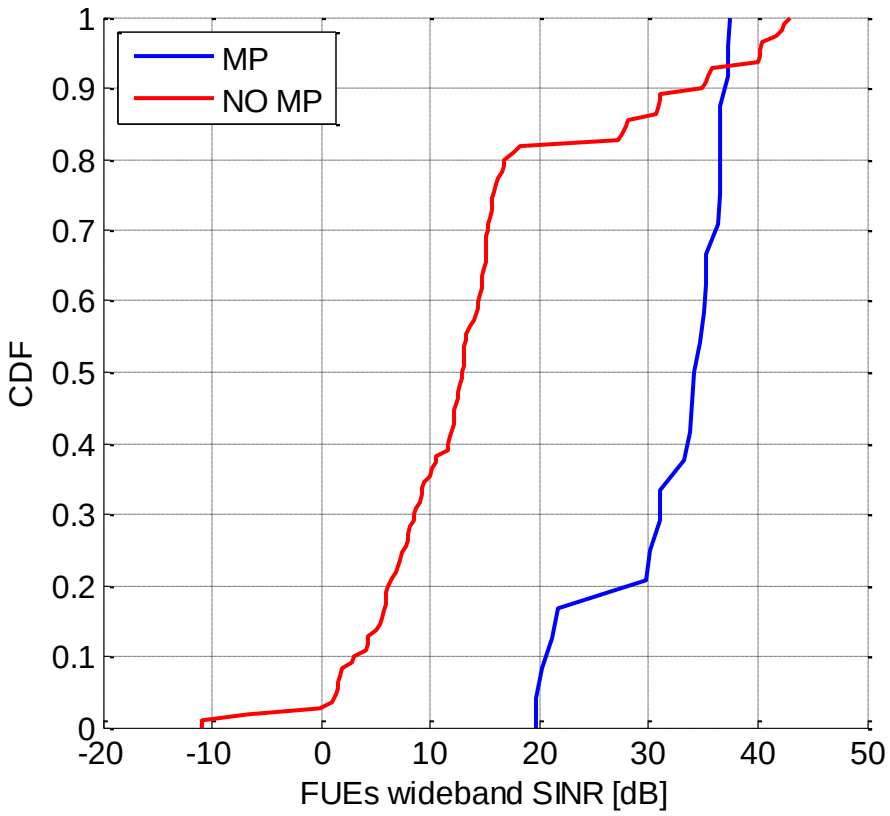

Figure 6.15: FUEs wideband SINR

Figure 6.15 represents the average SINR values of all the FUEs in the collocated scenario when RBs are shared among the CFs as deduced in Equation 6.7 and represented in Figure 6.3. The surge in SINR values in MP reflects the contention free access to the RBs as opposed to NO MP and this directly affects the throughput value in Figure 6.16 and spectral efficiency in Figure 6.17.

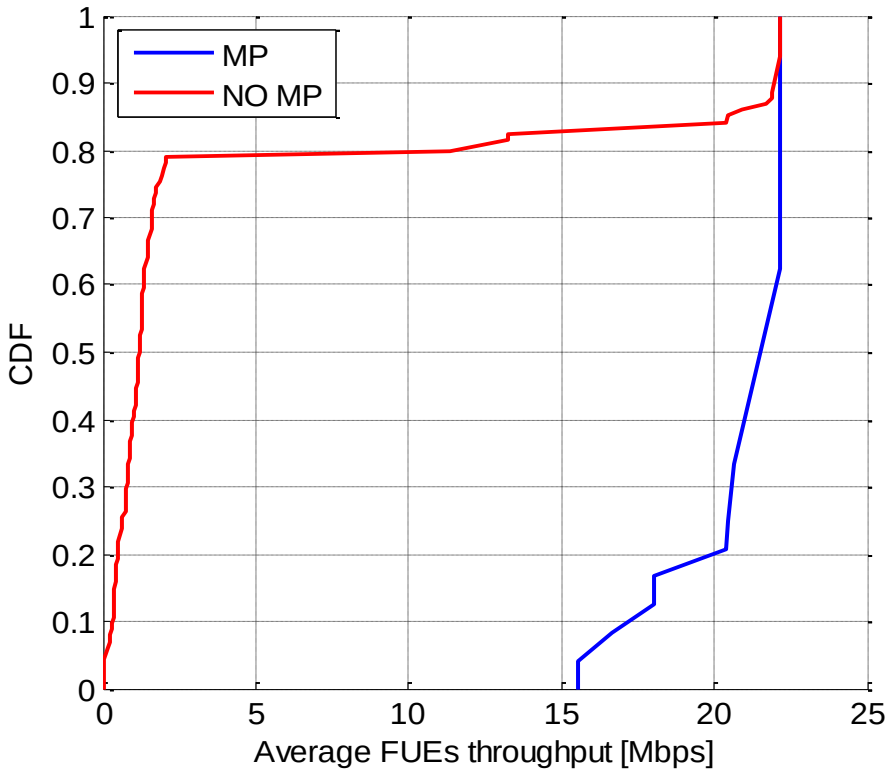

Figure 6.16: Average FUEs throughput

As reflected in Figures 6.15, 6.16 and 6.17, clearly MP algorithm helps mitigate co-tier interference significantly thereby resulting into hugely improved statistics in a collocated scenario. To have an overall view, the mean values of SINR, throughput and spectral efficiency with MP and NO MP are presented in Table 6.5.

Table 6.5: Co-tier Interference Mitigation

	SINR (dB)	Throughput (Mbps)	Spectral Efficiency (bits/cu)
MP	31.77	18.97	4.515
NO MP	14.46	3.04	0.2833

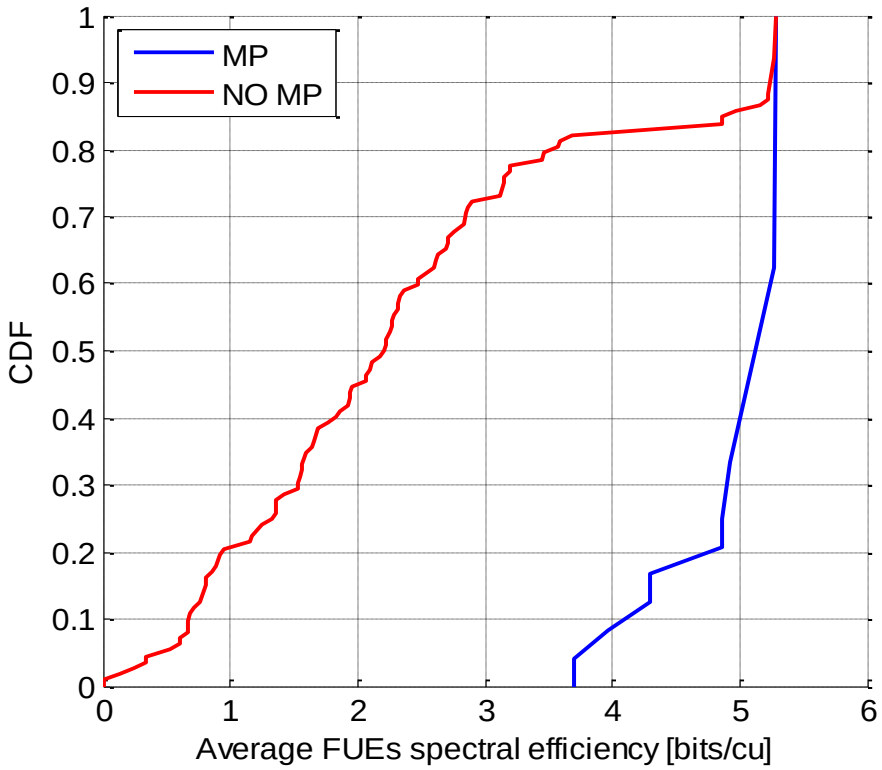

Figure 6.17: Average FUEs spectral efficiency

6.6 Summary

A multiuser channel provides multiuser diversity because of the statistical independence of the individual users' fading processes. Exploiting this diversity by scheduling users on favourable resources is one of the major opportunities to reduce interference and increase the system capacity. Network providers face the problem of delivering services to users with strongly varying channel quality. In two tier networks, where uncoordinated FAPs are overlaid in the MBS network, interference is eminent. In some cases, system capacity needs to be traded off against user satisfaction, requiring some fairness metric to be considered in the resource allocation process. In this chapter a scheduling algorithm to mitigate both cross-tier and co-tier interference in two-tier networks was presented. Cross-tier interference is mitigated by employing cognitive FAPs (CFs) which assign the RBs of MUEs with a low data traffic load to its FUEs based on the interweave concept in spectrum assignment.

Whereas the co-tier interference is mitigated by resolving the contention for the same RBs by employment of matching policy among the coordinating CFs. Performance analysis of the proposed scheme is done by system level simulations and results obtained are compared with best CQI and PF schemes. Simulations are performed both for no fading and fading channel conditions represented by claussen fading. It is found that the proposed scheduling scheme outperforms other schemes in no fading conditions; however it provides competitive results when fading conditions are considered. The concept of matching policy successfully mitigates the effect of co-tier interference in collocated femtocells by providing improved SINR, throughput and spectral efficiency results, thereby proving the effectiveness of scheme. Since the proposed interference mitigation scheme does not require major modifications and existence of macro-femto backhaul coordination, thus it is promising for applications in the LTE-advanced (LTE-A) cellular systems that employ heterogeneous networks.

Chapter 7

Conclusion and future work

7.1 Conclusion

Even though femtocells are discovering an important role in cellular mobile communication, the issue of interference when deployed in a co-channel fashion with the macrocell needs to be addressed. The integration of CR in femtocells introduces the ability of femtocells to dynamically adapt to varying network conditions through learning and reasoning. This network intelligence by cognitive femtocells have the capability of retrieving operating parameters which can be manipulated to mitigate the inherent mutual interference between femtocells and macrocells to enhance network performance.

This research introduced new practical approaches to mitigate interference of cognitive femtocells in two-tier networks by means of novel algorithms and system level simulations in LTE networks. In order to achieve this, we presented a structural analysis of different interference mitigation schemes existing in literature today which are specific to our field of concern, cognitive femtocells. In this analysis, we classified the schemes into categories based on their characteristic interference mitigating feature such as power control, resource/spectrum allocation as well as antenna schemes. Also, hybrid schemes were introduced as a mix of two of more of the aforementioned categories. Subsequently, we

introduced our contributions in a progressive manner that comprised of a power control scheme, a resource allocation/scheduling scheme and a hybrid scheme consisting of power control and resource allocation features. In addition, simulations and analysis for the two-tier network scenario was not static but diverse to include different scenarios (changing number of FAPs and MUEs/FUEs) and OSG and CSG access modes for femtocells. Also, the analysis was conducted to include the mutual interference between femtocells and macrocells (co-tier and cross-tier).

According to our results, the adaptive power control scheme and resource allocation/scheduling algorithms proposed in this thesis improves the SINR in the two tier architecture in LTE networks. This is validated by performing comparison with traditional interference mitigation schemes.

7.2 Future work

From the practical interference mitigation approaches presented in this research, further improvements can be implemented as specified below:

In chapter 4, with respect to the power control scheme, cognition in the network is restricted to the femtocells thereby creating a centralised network architecture. However, a distributed architecture where the FUEs are also capable of cognition will introduce some flexibility in the scheme and reduce the constant overhead of FAPs measuring FUE locations.

With regard to chapter 5 and the UEs admittance and contention free resource allocation scheme, future work can attempt to develop a different approach to the second part of the algorithm where the matching policy to mitigate co-tier interference is based on channel conditions of the femtocells such as path loss used in this scheme. Greedy algorithms can be introduced to reflect a better sharing formula not based on channel conditions.

In chapter 6 with regard to the service associated scheduling for femtocells, where the cognitive femtocell utilize RBs of MUEs based on their traffic use, future work will attempt to add another criteria to make it a two layer feature. This added parameter which can be sensed alongside the traffic load parameter can avoid the likelihood of a missed detection.

From above, it can be seen that the importance of CR in femtocells cannot be overemphasised. CR provides a wide range of channel statistics which are suitable for interference mitigation schemes in femtocells. The idea of an efficient CR interference mitigation scheme is how these individual channel statistics are utilized taking into consideration a number of parameters such as the air interface technology, density of the femtocells and the femtocells deployment (e.g. co-channel/dedicated, open access, CSG or hybrid). Although cognitive femtocells can retrieve operating parameters, there are few open research issues and challenges which need to be addressed to effectively mitigate interference.

- **Intelligent / Efficient Spectrum Sensing Schemes**: The implementation or improvement of the aforementioned CR enabled mitigation schemes depends entirely on how efficient spectrum sensing is conducted to retrieve channel statistics utilizing some of the standard spectrum sensing techniques. Although spectrum sensing techniques can be conducted by FAPs either on a channel by channel basis (single channel sensing) across the whole spectrum or over a group of channels (group channel sensing) simultaneously, there are issues that arise with both types of sensing techniques and needs to be addressed. Single channel sensing introduces accuracy in sensing as each individual channel is sensed thoroughly but introduces sensing overhead and delays. Channel degradation is also imminent when a group of FAPs sense each individual channel concurrently. Group channel sensing on the other hand is less accurate as available channels might be confused with interference channels.

Thus in practice, an intelligent and efficient spectrum sensing mechanism is of paramount importance in CR enabled interference mitigation schemes.

- **Primary / Secondary User Issue**: Most spectrum schemes reflect a scenario where the MBS and MUEs are the licensed users and regarded as the PUs and the FAPs and FUEs as SUs. This approach sounds fair enough for SUs who opportunistically access resources of the PUs with priorities given to PUs. However, in reality, FAPs and FUEs require and utilise high data and traffic since they are mainly used indoors as compared with MUEs. Therefore, more priorities should be dedicated to SUs with constraints not to affect MBS and MUE transmission. This is an important research issue to be looked in as it may reshape the way how concept of PU and SU is addressed in CR enabled interference mitigation schemes.
- **Energy Saving**: Cognition in CR enabled interference mitigation schemes is usually performed by the FAP and sometimes assisted by a cognitive enabled FUEs which can help to improve the interference mitigation technique and the overall capacity of the network. However, this puts a strain on the cognitive FUE with its limited energy capacity and makes it susceptible to battery drain. This is an important research challenge as efficient energy saving schemes need to be employed to cater for this added strain on cognitive FUEs.
- **Security**: An open access mode significantly reduces interference in femtocells, but unlike CSG it also introduces an increased threat to the privacy of the owner as well the network itself. The ability of any UE to gain access into a FAP makes it vulnerable as a hacker with malicious intent can ultimately take control of it to access the restricted information, such as private key and authentication procedure with the core network. Although a secure gateway provides security between the femtocell and the core network, an open access makes it exposed to advanced hacking techniques

which could disrupt the entire network. Therefore adequate security measures are required in open access mode to protect the subscriber and network operator and some issues such as criteria for joining the FAP should be addressed.

- **Pilot power / Coverage Radius Issue:** Most power control schemes utilize an adaptive power control mode where the pilot power levels of an FAP is controlled effectively to adjust coverage radius not only to mitigate interference but to reduce the need for handover of close by UEs in open access mode. Power control schemes which are based on pilot power of an FAP become less significant in densely deployed femtocells if a FUE is located close to a neighbouring co-located FAP. This may result into lower co-tier SINR values and it leads to an important research issue to be further investigated.
- **Signalling Overhead:** Femtocells employing CR to mitigate interference would need sophisticated cognition schemes. There will be lots of information sensing and gathering involved and some signalling channels would be needed to achieve the required coordination among nodes. This is an important research area to be investigated as signalling overhead can result into increased delays, energy consumption reduced bandwidth and sometimes total loss of quality of service.

References

[1] A.F. Molisch, *Wireless Communications*, 2nd Edition, Wiley-IEEE, February 2011.

[2] Ericsson. 2010, *Mobile data traffic surpasses voice*, 23 March. Stockholm, Sweden.

[3] Cisco, "Cisco visual networking index: Global mobile data traffic forecast update, 20102015," Whitepaper, Feb. 2011.

[4] S. Landström, A. Furuskär, K. Johansson, L. Falconetti and F. Kronestedt "Heterogeneous Networks (HetNets) – an approach to increasing cellular capacity and coverage," Feb 11, 2011.

[5] Cellular Asset, "Femtocells – Benefits, Challenges and Deployment Scenarios" [Online]. Available: http://www.cellularasset.com

[6] V. Chandrasekhar, J. Andrews and A. Gatherer, "Femtocell networks: a survey," *Communications Magazine, IEEE*, vol.46, no.9, September 2008, pp.59-67.

[7] H. Osman, H. Zhu, T. Alade and J. Wang, "Downlink Transmission of Distributed Antenna Systems in High Building Environments," *Communications (ICC), 2011 IEEE International Conference on*, 5-9 June 2011, pp.1-5.

[8] L. Gatzoulis, A. Aragon, G. Povey, S. R. Saunders, "Performance Analysis of In-building FDD Deployment Measured Data," *in Proc. 4th IEEE Intl. Conf. on 3G Mobile Communicaton Techn.*, June 2003, pp. 167-172.

[9] K. J. Grandell, "Indoor Antennas for WCDMA Systems," *in Proc. Of 11th IEEE Intl. Conf. on Antennas and Propagation*, 2001, Vol. 1, pp.208-211.

[10] M. S. Alouini and A. J. Goldsmith, "Area Spectral Efficiency of Cellular Mobile Radio Systems," *IEEE Trans. Vehic. Tech.*, vol. 48, no. 4, July 1999, pp. 1047–66.

[11] 3GPP TS 32.591: "Telecommunications management; Home eNode B (HeNB) Operations, Administration, Maintenance and Provisioning (OAM&P); Concepts and requirements for Type 1 interface HeNB to HeNB Management System".

[12] Small Cell Forum, "*Interference Management in OFDMA Femtocells*", Small Cell Forum, Mar. 2010.

[13] J. Zhang and G. Roche, *Femtocells: Technologies and Deployment*, Wiley, 2010.

[14] F. Liu, E. Bala, E. Erkip and R. Yang; , "A framework for femtocells to access both licensed and unlicensed bands," *International Symposium on Modelling and Optimization in Mobile, Ad Hoc and Wireless Networks (WiOpt)*, 9-13 May 2011, pp.407-411.

[15] J.G Andrews, H. Claussen, M. Dohler, S. Rangan, and M.C Reed, "Femtocells: Past, Present, and Future," *IEEE Journal on Selected Areas in Communications*, vol.30, no.3, April 2012, pp.497-508.

[16] 3GPP TR 25 967: "FDD Home Node B (HNB) RF Requirements".

[17] S.F. Hasan, N.H. Siddique and S. Chakraborty, "Femtocell versus WiFi - A survey and comparison of architecture and performance," *1st International Conference on Wireless Communication, Vehicular Technology, Information Theory and Aerospace & Electronic Systems Technology*, May 2009, pp.916-920.

[18] H.A. Mahmoud and I. Guvenc, "A comparative study of different deployment modes for femtocell networks," *IEEE 20th International Symposium on Personal, Indoor and Mobile Radio Communications,* Sept. 2009, pp.1-5, 13-16.

[19] N. Saquib, E. Hossain, Long Bao Le and Dong In Kim, "Interference management in OFDMA femtocell networks: issues and approaches," *Wireless Communications, IEEE,* vol. 19, no. 3, June 2012, pp. 86-95.

[20] T. Zahir, K. Arshad, A. Nakata and K. Moessner, "Interference Management in Femtocells," *Communications Surveys & Tutorials, IEEE* , February 2013, vol. 15, no. 1, pp. 293-311.

[21] Y. Bai, J. Zhou and L. Chen, "Hybrid Spectrum Usage for Overlaying LTE Macrocell and Femtocell," *IEEE Global Telecommunications Conference, GLOBECOM,* Nov. 2009, pp.1-6.

[22] D. L. Perez, A. Valcarce, G. D. L. Roche, E. Liu, and J. Zhang, "Access methods to WiMAX femtocells: A downlink system-level case study," in *Proc. IEEE Int. Conf. Commun. Syst. (ICCS)*, Guangzhou, China, Nov. 2008, pp. 1657–1662.

[23] H. Claussen, "Performance of macro- and co-channel femtocells in a hierarchical cell structure," in *Proc. IEEE Int. Symp. Personal, Indoor, Mobile Radio Commun. (PIMRC)*, Athens, Greece, Sep. 2007, pp. 1–5.

[24] L. T. W. Ho and H. Claussen, "Effects of user-deployed, co-channel femtocells on the call drop probability in a residential scenario," in *Proc. IEEE Int. Symp. Personal, Indoor, Mobile Radio Commun. (PIMRC)*, Athens, Greece, Sep. 2007, pp. 1–5.

[25] V. Chandrasekhar and J. G. Andrews, “Uplink capacity and interference avoidance for two-tier cellular networks,” in *Proc. IEEE Global Telecommunication Conference, November 2007*, pp 3322 – 3326.

[26] G. de la Roche, A. Valcarce, D. Lopez-Perez, and J. Zhang, “Access control mechanisms for femtocells,” *IEEE Communication Magazine*, vol. 48, no.1, Jan. 2010, pp. 33–39.

[27] J. Chen, P. Rauber, D. Singh, C. Sundarraman, P. Tinnakornsrisuphap and M.Yavuz “Femtocells – Architecture & Network Aspects”, 2007. [Online]. Available: http://www.qualcomm.com/media/documents/files/femtocells-architecture-network-aspects.pdf.

[28] V.U. Sankar and V. Sharma, "Subchannel Allocation and Power Control in Femtocells to Provide Quality of Service," *National Conference on Communications (NCC),* 3-5 Feb. 2012, pp.1-5.

[29] A. Goldsmith, S.A. Jafar, I. Maric and S. Srinivasa, "Breaking Spectrum Gridlock With Cognitive Radios: An Information Theoretic Perspective," *Proceedings of the IEEE*, vol.97, no.5, May 2009, pp.894-914. 46

[30] J. Mitola III and G. Q. Maguire Jr., “Cognitive radio: making software radios more personal,” *IEEE Personal Communications*, vol. 6, no. 4, 1999, pp. 13–18.

[31] FCC, Unlicensed Operation in the TV Broadcast Bands, *ET Docket No. 04-186*, (2006).

[32] S.Y. Lien, Y. Lin and K. Chen “Cognitive and Game-Theoretical Radio Resource Management for Autonomous Femtocells with QoS Guarantees” *IEEE Transactions on Wireless Communications*, Vol. 10, no. 7 pp. 2196 – 2206.

[33] F. Akyildiz, W. Lee, M. C. Vuran and S. Mohanty "NeXt generation/dynamic spectrum access/cognitive radio wireless networks: A survey" *The International Journal of Computer and Telecommunications Networking*, Vol. 50, no. 13, 15 Sept. 2006, pp. 2127-2159.

[34] J. Palicot, J. Mitola, Z. Lei, and F. K. Jondral **"**Special Issue on 10 years of Cognitive Radio: State of the Art and Perspectives**"** *EURASIP Journal on Wireless Communications and Networking*, 2012.

[35] A. Jovicic and P. Viswanath, "Cognitive Radio: An Information-Theoretic Perspective," *IEEE Transactions onInformation Theory*, vol.55, no.9, Sept. 2009, pp.3945-3958.

[36] K. A. Yau, F. G. Tan, P. Komisarczuk and P.D. Teal, "Exploring new and emerging applications of Cognitive Radio systems: Preliminary insights and framework," *IEEE Colloquium on Humanities, Science and Engineering (CHUSER)*, Dec. 2011, pp.153-157.

[37] B. Wang and K.J.R Liu, "Advances in cognitive radio networks: A survey," *Selected Topics in Signal Processing, IEEE Journal of*, vol.5, no.1, Feb. 2011, pp.5-23.

[38] G. Gur, S. Bayhan, and F. Alagoz, "Cognitive femtocell networks: an overlay architecture for localized dynamic spectrum access [dynamic spectrum management]," *IEEE Wireless Communications*, vol. 17, no. 4, August 2010, pp. 62–70.

[39] Q. Li, Z. Feng, W. Li, Y. Liu and P. Zhang "Joint access and power control in cognitive femtocell networks," *International Conference on Wireless Communications and Signal Processing (WCSP)*, Nov. 2011, pp.1-5.

[40] H.O. Kpojime and G.A. Safdar "Interference Mitigation in Cognitive-Radio-Based Femtocells," in *Communications Surveys & Tutorials, IEEE* , vol.17, no.3, 2015 pp.1511-1534.

[41] H.O. Kpojime and G.A. Safdar., "Efficacy of coverage radius-based power control scheme for interference mitigation in femtocells," in *Electronics Letters , IET*, vol.50, no.8, April 10 2014, pp.639-641.

[42] H.O. Kpojime and G.A. Safdar " Coverage Radius Bounds and Impact on SINR in Blindly Placed LTE Femtocells," in *International Journal of Wireless Information Networks* , vol.22, no.3, Sept. 2015, pp.262-271.

[43] I. Guvenc, M. Jeong and F. Watanabe, "A Hybrid Frequency Assignment for Femtocells and Coverage Area Analysis for Co-Channel Operation", *IEEE Communication Letters*, Vol. 12, Issue 12, Dec. 2008, pp. 880-882.

[44] V. Chandrasekhar and J. Andrews, "Spectrum allocation in tiered cellular networks," *IEEE Transactions on Communications,* vol.57, no.10, pp.3059-3068, October 2009.

[45] C. Xu, M. Sheng, X. Wang, C-X. Wang and J. Li, "Distributed Subchannel Allocation for Interference Mitigation in OFDMA Femtocells: A Utility-Based Learning Approach," in *Vehicular Technology, IEEE Transactions on* , vol.64, no.6, June 2015, pp.2463-2475.

[46] A. Mutairi and S. Roy, "An OFDM-Aware Reservation Random Access Protocol for Interference Mitigation in OFDMA Femtocells," in *Communications, IEEE Transactions on* , vol.63, no.1, Jan. 2015, pp.301-310.

[47] D. Chen, T. Jiang and Z. Zhang, "Frequency Partitioning Methods to Mitigate Cross-Tier Interference in Two-Tier Femtocell Networks," in *Vehicular Technology, IEEE Transactions on* , vol.64, no.5, May 2015, pp.1793-1805.

[48] H. Zhang, C. Jiang, N.C. Beaulieu, X. Chu, X. Wen and M. Tao, "Resource Allocation in Spectrum-Sharing OFDMA Femtocells With Heterogeneous Services," in *Communications, IEEE Transactions on* , vol.62, no.7, July 2014, pp.2366-2377.

[49] A. Abdelnasser, E. Hossain and I. K. Dong, "Clustering and Resource Allocation for Dense Femtocells in a Two-Tier Cellular OFDMA Network," in *Wireless Communications, IEEE Transactions on* , vol.13, no.3, March 2014, pp.1628-1641.

[50] P. Liu, J. Li, H. Li, K. Wang and Y. Meng, "Two-Dimensional Resource Pattern Optimization for Interference Avoidance in Heterogeneous Networks," in *Vehicular Technology, IEEE Transactions on* , vol.64, no.8, Aug. 2015, pp.3536-3546.

[51] D. Lopez-Perez, C. Xiaoli, A.V. Vasilakos and H. Claussen, "Power Minimization Based Resource Allocation for Interference Mitigation in OFDMA Femtocell Networks," in *Selected Areas in Communications, IEEE Journal on* , vol.32, no.2, February 2014, pp.333-344.

[52] H. Kalbkhani, V. Solouk and M.G.Shayesteh, "Resource allocation in integrated femto–macrocell networks based on location awareness," in *Communications, IET* , vol.9, no.7, July 2015, pp.917-932.

[53] D. Chen, T. Jiang and Z. Zhang, "Frequency Partitioning Methods to Mitigate Cross-Tier Interference in Two-Tier Femtocell Networks," in *Vehicular Technology, IEEE Transactions on* , vol.64, no.5, May 2015, pp.1793-1805.

[54] D. Kim, E. H. Shin and M. S. Jin, "Hierarchical Power Control With Interference Allowance for Uplink Transmission in Two-Tier Heterogeneous Networks," in *Wireless Communications, IEEE Transactions on* , vol.14, no.2, Feb. 2015, pp.616-627.

[55] H. Li and K. Wang, "Weighted Bandwidth–Power Product Optimization in Downlink Femtocell Networks," in *Communications Letters, IEEE* , vol.19, no.9, Sept. 2015, pp.1588-1591.

[56] T. M. Ho, N.H. Tran, C.T. Do, S.M. Ahsan Kazmi, E-N. Huh and C. S.Hong, "Power Control for Interference Management and QoS Guarantee in Heterogeneous Networks," in*Communications Letters, IEEE* , vol.19, no.8, Aug. 2015, pp.1402-1405.

[57] D. Roche, G. Ladányi, D. López-Pérez, D.C. Chong and J. Zhang; , "Self-organization for LTE enterprise femtocells," *IEEE GLOBECOM Workshops (GC Wkshps)*, Dec. 2010, pp.674-678.

[58] L. Mohjazi, M. Al-Qutayri, H. Barada and Kin Poon, "Femtocell coverage optimization using genetic algorithm," *Technical Symposium at ITUTelecom World (ITU WT)*, 24-27 Oct. 2011, pp.159-164.

[59] H. Wang and Z. Ding, "Power Control and Resource Allocation for Outage Balancing in Femtocell Networks," in *Wireless Communications, IEEE Transactions on* , vol.14, no.4, April 2015, pp.2043-2057.

[60] B. Choi, E.S. Cho, M.Y. Chung, K. Cheon and A. Park, "A femtocell power control scheme to mitigate interference using listening TDD frame," *Information Networking (ICOIN), 2011 International Conference on,* Jan. 2011, pp.241-244.

[61] S. Khan and S.A. Mahmud, "Power Optimization Technique in Interference-Limited Femtocells in LTE and LTE Advanced Based Femtocell Networks," in *Computer and Information Technology; Ubiquitous Computing and Communications; Dependable, Autonomic and Secure Computing; Pervasive Intelligence and Computing (CIT/IUCC/DASC/PICOM), 2015 IEEE International Conference on* , 26-28 Oct. 2015, pp.749-754.

[62] H. Wang and Z. Ding, "Macrocell-Queue-Stabilization-Based Power Control of Femtocell Networks," *Wireless Communications, IEEE Transactions on* , vol.13, no.9, Sept. 2014, pp.5223-5236.

[63] H. Wang , C. Zhu and Z. Ding, "Femtocell Power Control for Interference Management Based on Macro-Layer Feedback," *Vehicular Technology, IEEE Transactions on* , vol.PP, no.99, August, 2015, pp.1-1.

[64] J. Wang, L. Wang, Q. Wu, P. Yang, Y. Xu and J. Wang, "Less Is More: Creating Spectrum Reuse Opportunities via Power Control for OFDMA Femtocell Networks," in *Systems Journal, IEEE* , vol.PP, no.99, March, 2015. pp.1-12.

[65] F. Fu, Z. Lu, X. Wen, W. Jing, Z. Zhang, Z. Li, "Exact potential game based power control with QoS provisioning in two-tier femtocell networks," in *Wireless Personal Multimedia Communications (WPMC), 2014 International Symposium on* , Sept. 2014, pp.180-185.

[66] H. Wang and Z. Ding, "Power Control and Resource Allocation for Outage Balancing in Femtocell Networks," in *Wireless Communications, IEEE Transactions on* , vol.14, no.4, April 2015, pp.2043-2057.

[67] S-H. Chen and T-C. Hou, "Dynamic channel allocation and power control for OFDMA femtocell networks," in *Wireless Communications and Networking Conference (WCNC), 2014 IEEE* , April 2014, pp.1721-1726.

[68] F. Wang and W. Wang, "Analytical modeling of uplink power control in two-tier femtocell networks," in *Wireless Telecommunications Symposium (WTS), 2015* , April 2015, pp.1-6.

[69] H. Wang, R. Song and S-H Leung, "Analysis of Uplink Intercarrier Interference in OFDMA Femtocell Networks," in *Vehicular Technology, IEEE Transactions on* , vol.64, no.3, March 2015, pp.998-1013.

[70] G. Zhang, T. Liang, W. Heng, C. Meng and J. Hu, "Downlink cross-tier interference pricing and power control in OFDMA HetNets," in *Networks and Communications (EuCNC), 2015 European Conference on* , June 2015, pp.244-248.

[71] S. Park, W. Seo, S. Choi, and D. Hong, "A beamforming codebook restriction for cross-tier interference coordination in two-tier femtocell networks," *Vehicular Technology, IEEE Transactions on*, vol. 60, no. 4, May 2011, pp. 1651–1663.

[72] T. Lv, H. Gao and S.Yang, "Secrecy Transmit Beamforming for Heterogeneous Networks," in *Selected Areas in Communications, IEEE Journal on* , vol.33, no.6, June 2015, pp.1154-1170.

[73] V. Chandrasekhar, M. Kountouris and J.G Andrews, "Coverage in multi-antenna two-tier networks," *IEEE Transactions on Wireless Communications*, vol.8, no.10, Oct. 2009, pp.5314-5327.

[74] M.R. Sanatkar and B. Natarajan, "Power selection for maximizing SINR in femtocells with sectorized antennas," *IEEE Consumer Communications and Networking Conference (CCNC)*, Jan. 2012, pp.690-692.

[75] D.H.N. Nguyen, B. L. Long and L. Tho, "Multiuser Admission Control and Beamforming Optimization Algorithms for MISO Heterogeneous Networks," in *Access, IEEE* , vol.3, June 2015, pp.759-773.

[76] D.H.N. Nguyen, B. L. Long and L. Tho, "Joint multiuser downlink beamforming and admission control in heterogeneous networks," in *Global Communications Conference (GLOBECOM), 2014 IEEE* , Dec. 2014, pp.3653-3658.

[77] O. Soykin, A. Kolobov, V. Ssorin, A. Artemenko and R. Maslennikov, "Planar MIMO antenna system with polarization diversity for 2.5–2.7 GHz LTE indoor FemtoCells," in *Antennas and Propagation (EuCAP), 2015 9th European Conference on* , April 2015, pp.1-5.

[78] M. Ndong and T. Fujii, "Joint femtocell clustering and cross-tier interference mitigation with distributed antenna system in small cell networks," in *Communication Systems, Networks & Digital Signal Processing (CSNDSP), 2014 9th International Symposium on* , July 2014, pp.652-657.

[79] A. Adhikary, V. Ntranos and G. Caire, "Cognitive femtocells: Breaking the spatial reuse barrier of cellular systems," *Information Theory and Applications Workshop (ITA)*, 6-11 Feb. 2011, pp.1-10.

[80] J.E. Hakegard, A. Lie and T.A. Myrvoll, “Power control in HetNets and cognitive networks”, *Communications and Information Technologies (ISCIT), 2012 International Symposium on*, 2-5 Oct. 2012, pp. 568-573.

[81] F.H. Khan and Y. Choi, "Towards introducing self-configurability in cognitive femtocell networks," *9th Annual IEEE Communications Society Conference on Sensor, Mesh and Ad Hoc Communications and Networks (SECON)*, 18-21 June 2012, pp.37-39.

[82] H. Saad, A. Mohamed and T. ElBatt, "Distributed Cooperative Q-Learning for Power Allocation in Cognitive Femtocell Networks," *Vehicular Technology Conference (VTC Fall), 2012 IEEE*, 3-6 Sept. 2012, pp. 1-5.

[83] S.E. Nai and T.Q.S. Quek, "Coexistence in two-tier femtocell networks: Cognition and optimization," *International Conference on Computing, Networking and Communications (ICNC)*, Jan. 2 2012, pp.655-659.

[84] D. Sun, X. Zhu, Z. Zeng and S. Wan, "Downlink power control in cognitive femtocell networks," *International Conference on Wireless Communications and Signal Processing (WCSP)*, Nov. 2011, pp.1-5.

[85] P. Hu, J. Ye, F. Zhang, S. Deng, C. Wang and W. Wang, "Downlink Resource Management Based on Cross-Cognition and Graph Coloring in Cognitive Radio Femtocell Networks," *Vehicular Technology Conference (VTC Fall), 2012 IEEE*, Sept. 2012, pp. 1-5.

[86] D. Oh, H. Lee, and Y. Lee, "Cognitive radio based femtocell resource allocation," *International Conference on Information and Communication Technology Convergence (ICTC)*, Nov. 2010, pp.274-279.

[87] Y. Saleem, A. Bashir, E. Ahmed, J. Qadir and A. Baig, "Spectrum-aware dynamic channel assignment in cognitive radio networks," *Emerging Technologies (ICET), 2012 International Conference on*, Oct. 2012, pp. 1-6.

[88] S. Bose and B. Natarajan, "Reliable spectrum sensing for resource allocation of cognitive radio based WiMAX femtocells," *IEEEConsumer Communications and Networking Conference (CCNC),* Jan. 2012, pp.889-893.

[89] Li Huang, Guangxi Zhu and Xiaojiang Du, "Cognitive femtocell networks: an opportunistic spectrum access for future indoor wireless coverage," *Wireless Communications, IEEE,* vol. 20, no. 2, Apr. 2013, pp. 44-51.

[90] L. Li, C. Xu and M. Tao, "Resource Allocation in Open Access OFDMA Femtocell Networks," *Wireless Communications Letters, IEEE*, vol. 1, no. 6, Dec. 2012, pp. 625-628.

[91] Xiao Yu Wang, Pin-Han Ho and Kwang-Cheng Chen, "Interference Analysis and Mitigation for Cognitive-Empowered Femtocells Through Stochastic Dual Control," *Wireless Communications, IEEE Transactions on*, vol. 11, no. 6, June 2012, pp. 2065-2075.

[92] S. Cheng, W.C. Ao and K. Chen, "Efficiency of a Cognitive Radio Link with Opportunistic Interference Mitigation," *Wireless Communications, IEEE Transactions on*, vol. 10, no. 6, June 2011, pp. 1715-1720.

[93] K.A. Meerja, P.H. Ho and B. Wu, "A Novel Approach for Co-Channel Interference Mitigation in Femtocell Networks," *IEEE Global Telecommunications Conference (GLOBECOM 2011),* Dec. 2011, pp.1-6.

[94] A. Attar, V. Krishnamurthy and O.N. Gharehshiran, "Interference management using cognitive base-stations for UMTS LTE," *Communications Magazine, IEEE*, vol. 49, no. 8, Aug. 2011, pp. 152-159.

[95] L. Zhang, L. Yang and T. Yang, "Cognitive Interference Management for LTE-A Femtocells with Distributed Carrier Selection," *IEEE 72ndVehicular Technology Conference Fall (VTC 2010-Fall),* 6-9 Sept. 2010, pp.1-5.

[96] S. Kaimaletu, R. Krishnan, S. Kalyani, N. Akhtar and B. Ramamurthi, "Cognitive Interference Management in Heterogeneous Femto-Macro Cell Networks," *IEEE International Conference onCommunications (ICC),* June 2011, pp.1-6.

[97] S. Cheng, W.C. Ao, F. Tseng and K. Chen, "Design and Analysis of Downlink Spectrum Sharing in Two-Tier Cognitive Femto Networks," *Vehicular Technology, IEEE Transactions on,* vol. 61, no. 5, June 2012, pp. 2194-2207.

[98] Y.S. Soh, T.Q.S. Quek, M. Kountouris and G. Caire, "Cognitive Hybrid Division Duplex for Two-Tier Femtocell Networks," *Wireless Communications, IEEE Transactions on,* vol. 12, no. 10, Oct. 2013, pp. 4852-4865.

[99] 3GPP RAN1, "RAN1-090133 Huawei Beamforming enhancement in LTE-Advanced," Jan. 2009.

[100] J.W. Huang and V. Krishnamurthy, "Cognitive Base Stations in LTE/3GPP Femtocells: A Correlated Equilibrium Game-Theoretic Approach," *IEEE Transactions on Communications,* vol.59, no.12, Dec. 2011, pp. 3485-3493. 104

[101] R.J. Aumann, "Correlated equilibrium as an expression of Bayesian Rationality," *Econometrica,* vol.55, Jan 1987, no.1, pp. 1-18.

[102] M. Bennis and S.M. Perlaza, "Decentralized Cross-Tier Interference Mitigation in Cognitive Femtocell Networks," *IEEE International Conference onCommunications (ICC),* June 2011, pp.1-5.

[103] S. Leveil, Le Martret, J. Christophe, H. Anouar, K. Arshad, T. Zahir, J. Bito, U. Celentano, G. Mange, J. Rico, A. Medela, "Resource management of centrally

controlled cognitive radio networks," *Future Network & Mobile Summit (FutureNetw),* July 2012, pp.1-9.

[104] M.E. Sahin, I. Guvenc, M. Jeong and H. Arslan, "Handling CCI and ICI in OFDMA femtocell networks through frequency scheduling," *Consumer Electronics, IEEE Transactions on* , vol.55, no.4, Nov. 2009, pp.1936-1944.

[105] Y. Ma, T. Lv, J. Zhang, H. Gao and Y. Lu, "Cognitive interference mitigation in heterogeneous femto-macro cell networks," *Personal Indoor and Mobile Radio Communications (PIMRC), 2012 IEEE 23rd International Symposium on*, Sept. 2012, pp. 2131-2136.

[106] E. Mugume, W. Prawatmuang and D.K.C. So, "Cooperative spectrum sensing for green cognitive femtocell network," *Personal Indoor and Mobile Radio Communications (PIMRC), 2013 IEEE 24th International Symposium on*, Sept. 2013, pp. 2368-2372.

[107] L. Yizhe, F. Zhiyong, Z. Qixun, T. Li, and T. Fang, "Cognitive optimization scheme of coverage for femtocell using multi-element antenna," *IEEE 72nd VTC*, Sept 2010, pp. 1–5.

[108] M. Z. Shakir, R. Atat and M. Alouini, "On the interference suppression capabilities of cognitive enabled femto cellular networks," *International Conference on Communications and Information Technology (ICCIT),* June 2012, pp.402-407.

[109] Z. Zhao, M. Schellmann, H. Boulaaba and E. Schulz, "Interference study for cognitive LTE-femtocell in TV white spaces," *Telecom World (ITU WT), 2011 Technical Symposium at ITU,* Oct. 2011, pp.153-158.

[110] F. Peng, Y. Gao, Y. Chen, K.K. Chai and L. Cuthbert, "Using TV White Space for interference mitigation in LTE Femtocell Networks," *IET International*

Conference on Communication Technology and Application (ICCTA 2011), Oct. 2011, pp. 5-9.

[111] G. Zhao, C. Yang, G.Y. Li and G. Sun, "Fractional Frequency Donation for Cognitive Interference Management among Femtocells," *Global Telecommunications Conference (GLOBECOM 2011), 2011 IEEE,* Dec. 2011, pp.1-6.

[112] G.W.O da Costa, A.F. Cattoni, V.A. Roig and P.E. Mogensen, "Interference mitigation in cognitive femtocells," *Proc. IEEE GLOBECOM Workshops,* Dec. 2010, pp.721 -725.

[113] Y. Li, M. Macuha, E.S. Sousa, T. Sato and M. Nanri, "Cognitive interference management in 3G femtocells," *20th International Symposium onPersonal Indoor and Mobile Radio Communications (PIMRC),* Sept. 2009, pp.1118-1122.

[114] Y. Li and E.S. Sousa, "Cognitive uplink interference management in 4G cellular femtocells," *IEEE 21st International Symposium on Personal Indoor and Mobile Radio Communications (PIMRC),* Sept. 2010, pp.1567-1571.

[115] X. Tao, Z. Zhao, R. Li, J. Palicot and H. Zhang, "Downlink interference minimization in cognitive LTE-femtocell networks," *Communications in China (ICCC), 2013 IEEE/CIC International Conference on,* Aug. 2013, pp. 124-129.

[116] C.C. Chai, "Distributed subcarrier and power allocation for OFDMA-based cognitive femtocell radio uplink," *Personal Indoor and Mobile Radio Communications (PIMRC), 2013 IEEE 24th International Symposium on*, Sept. 2013, pp. 2876-2880.

[117] Technical Specification Group RAN, E-UTRA; LTE physical layer – general description. 3GPP, Tech. Rep. TS 36.201 Version 8.3.0, March 2009.

[118] A. Valcarce, G. De La Roche, A. Juttner, D. L opez- erez, and J. Zhang, "Applying FDTD to the coverage prediction of WiMAX femtocells", *EURASIP Journal on Wireless Communications and Networking*, Feb. 2009.

[119] "Radio Resource Management", Aricent White Paper, January 2008.

[120] J Kim, A Ashikhmin, A van Wijngaarden, E Soljanin, N Gopalakrishnan, "On efficient link error prediction based on convex metrics", *in Proc. IEEE 60th Vehicular Technology Conference (VTC2004-Fall)*, Sept. 2004, pp.4190–4194.

[121] S Tsai, A Soong, "Effective-SNR mapping for modeling frame error rates in multiple-state channels", 3GPP2, Tech. Rep. 3GPP2-C30-20030429-010 Apr. 2003.

[122] L Wan, S Tsai, M Almgren, "A fading-insensitive performance metric for a unified link quality model", *in Proc. IEEE Wireless Communications and Networking Conference (WCNC2006,*. Apr. 2006, pp. 2110–2114.

[123] 3GPP, "Simulation assumptions and parameters for FDD HeNB RF requirements," R4-092042, TSG-RAN WG4, Meeting 51, 2009.

[124] S. Caban, C. Mehlführer, M. Rupp, and M. Wrulich, (2011) LTE Link- and System-Level Simulation, in Evaluation of HSDPA and LTE: From Testbed Measurements to System Level Performance, John Wiley & Sons, Chichester, UK.

[125] S. Schwarz, C. Mehlfuhrer and M. Rupp, "Calculation of the spatial preprocessing and link adaption feedback for 3GPP UMTS/LTE", in *Wireless Advanced (WiAD), 2010 6th Conference on* , June 2010, pp.1-6.

[126] M. Šimko, C. Mehlführer, M. Wrulich and M. Rupp, "Doubly dispersive channel estimation with scalable complexity", *in Proc. International ITG Workshop on Smart Antennas (WSA 2010)*, Feb. 2010, pp. 251–256.

[127] Q. Wang, C. Mehlführer and M. Rupp, "Carrier frequency synchronization in the downlink of 3GPP LTE", *in Proc. 21st Annual IEEE International Symposium on Personal, Indoor and Mobile Radio Communications (PIMRC 2010)*, Sept. 2010.

[128] J.C. Ikuno, C. Mehlführer and M. Rupp, "A novel link error prediction model for OFDM systems with HARQ", in *Communications (ICC), 2011 IEEE International Conference on* , June 2011, pp.1-5.

[129] P. Wu and N. Jindal, "Performance of hybrid-ARQ in block-fading channels: A fixed outage probability analysis", *IEEE Transactions on Communications*, vol. 58, no. 4, Apr. 2010, pp.1129–1141.

[130] Technical Specification Group RAN, E-UTRA; LTE RF system scenarios. 3GPP, Tech. Rep. TS 36.942 (2008).

[131] T. Zemen and C. Mecklenbräuker, "Time-variant channel estimation using discrete prolate spheroidal sequences", *in IEEE Trans. Signal Process*. vol. 53, no. 9, Sept. 2005, 3597–3607.

[132] J. Liu, Q. Chen and H.D. Sherali, "Algorithm design for femtocell base station placement in commercial building environments," *INFOCOM, 2012 Proceedings IEEE*, 25-30 March 2012, pp. 2951-2955.

[133] S. Wang, W. Guo and T. O'Farrell, "Optimising Femtocell Placement in an Interference Limited Network: Theory and Simulation," *Vehicular Technology Conference (VTC Fall), 2012 IEEE*, 3-6 Sept. 2012, pp. 1-6.

[134] W. Guo and S. Wang, "Interference-Aware Self-Deploying Femto-Cell," *Wireless Communications Letters, IEEE*, vol. 1, no. 6, Dec. 2012, pp. 609-612. 20

[135] Technical Specification Group RAN, "E-UTRA; LTE RF system scenarios," 3GPP, Tech. Rep. TS 36.942, 2008-2009.

[136] ETSI TR 136 942 V10.3.0 “LTE; Evolved Universal Terrestrial Radio Access (E-UTRA); Radio Frequency (RF) system scenarios” July 2012.

[137] W. Wang, G. Yu and A. Huang, "Cognitive radio enhanced interference coordination for femtocell networks," *IEEE Communications Magazine*, vol.51, no.6, June 2013, pp.37 – 43.

[138] C-W. Chang "An Interference-Avoidance Code Assignment Strategy for the Hierarchical Two-Dimensional-Spread MC-DS-CDMA System: A Prototype of Cognitive Radio Femtocell System," *IEEE Transactions on Vehicular Technology*, vol.61, no.1, Jan. 2012 pp.166 – 184.

[139] J. Broch, D. A. Maltz, D. B. Johnson, Y.-C. Hu and J. Jetcheva, “A performance comparison of multi-hop wireless ad hoc network routing protocols”, *in Proceedings of the Fourth Annual ACM/IEEE International Conference on Mobile Computing and Networking(Mobicom98)*, ACM, October 1998.

[140] L. Breslau, D. Estrin, K. Fall, S. Floyd, J. Heidemann, A. Helmy, P. Huang, S. McCanne, K. Varadhan, Y. Xu, and H. Yu, Advances in network simulation, in IEEE Computer, vol. 33, no. 5, May 2000, pp. 59--67.

[141] 3GPP RAN WG1 TSGR1-48, “LTE physical layer framework for performance verification”, February 2007.

[142] W. Yuanye, K.I. Pedersen, T.B. Sorensen, P.E. Mogensen, "Carrier load balancing and packet scheduling for multi-carrier systems," *Wireless Communications, IEEE Transactions on* , vol.9, no.5, pp.1780,1789, May 2010

[143] H. Claussen, "Efficient modelling of channel maps with correlated shadow fading in mobile radio systems," *IEEE 16th International Symposium on Personal, Indoor and Mobile Radio Communications, PIMRC*, Sept. 2005, pp.512-516.

[144] M. Gudmundson, "Correlation model for shadow fading in mobile radio systems," *Electronic Letter*, vol. 27. no. 2. Nov. 1991, pp. 2145-2146.

[145] B. Sklar, "Rayleigh Fading Channels in Mobile Digital Communication Systems - Part I: Characterization", *IEEE Communications Magazine*, July 1997, pp. 90-100.

[146] E. Dahlman, S. Parkvall, J. Skold and P. Beming, "3G Evolution HSPA and LTE for Mobile Broadband", *Elsevier*, 2008.

[147] A. Matthew, "Instability of the Proportional Fair Scheduling Algorithm for HDR", *IEEE Transactions on Wireless Communications*, Vol.3, No. 5, Sept 2004, pp. 1422–1426.